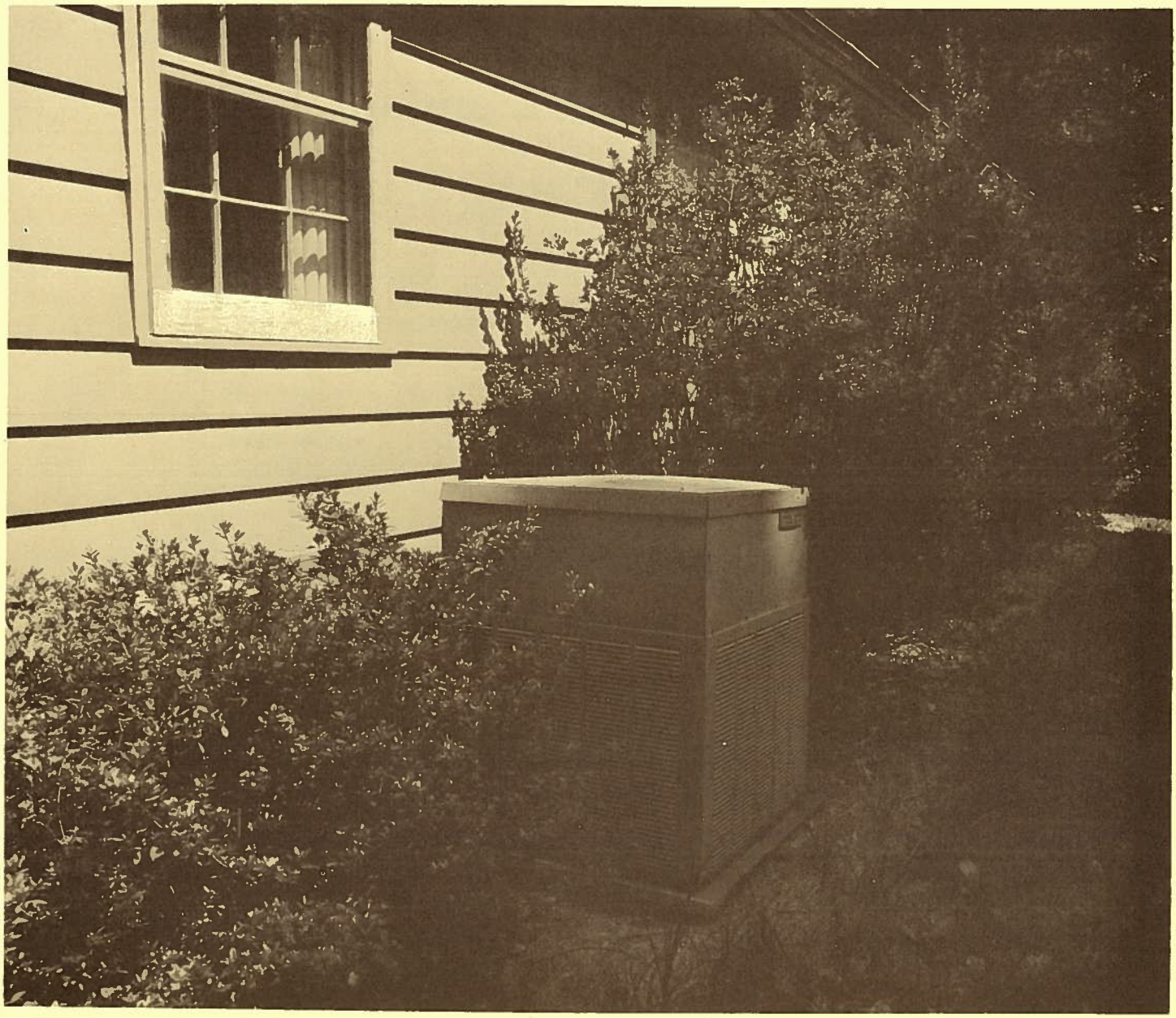

NBS BUILDING SCIENCE SERIES 155

Computer Modeling of the Vapor Compression Cycle With Constant Flow Area Expansion Device

U.S. DEPARTMENT OF COMMERCE • NATIONAL BUREAU OF STANDARDS

NATIONAL BUREAU OF STANDARDS

The National Bureau of Standards[1] was established by an act of Congress on March 3, 1901. The Bureau's overall goal is to strengthen and advance the Nation's science and technology and facilitate their effective application for public benefit. To this end, the Bureau conducts research and provides: (1) a basis for the Nation's physical measurement system, (2) scientific and technological services for industry and government, (3) a technical basis for equity in trade, and (4) technical services to promote public safety. The Bureau's technical work is performed by the National Measurement Laboratory, the National Engineering Laboratory, and the Institute for Computer Sciences and Technology.

THE NATIONAL MEASUREMENT LABORATORY provides the national system of physical and chemical and materials measurement; coordinates the system with measurement systems of other nations and furnishes essential services leading to accurate and uniform physical and chemical measurement throughout the Nation's scientific community, industry, and commerce; conducts materials research leading to improved methods of measurement, standards, and data on the properties of materials needed by industry, commerce, educational institutions, and Government; provides advisory and research services to other Government agencies; develops, produces, and distributes Standard Reference Materials; and provides calibration services. The Laboratory consists of the following centers:

Absolute Physical Quantities[2] — Radiation Research — Chemical Physics — Analytical Chemistry — Materials Science

THE NATIONAL ENGINEERING LABORATORY provides technology and technical services to the public and private sectors to address national needs and to solve national problems; conducts research in engineering and applied science in support of these efforts; builds and maintains competence in the necessary disciplines required to carry out this research and technical service; develops engineering data and measurement capabilities; provides engineering measurement traceability services; develops test methods and proposes engineering standards and code changes; develops and proposes new engineering practices; and develops and improves mechanisms to transfer results of its research to the ultimate user. The Laboratory consists of the following centers:

Applied Mathematics — Electronics and Electrical Engineering[2] — Manufacturing Engineering — Building Technology — Fire Research — Chemical Engineering[2]

THE INSTITUTE FOR COMPUTER SCIENCES AND TECHNOLOGY conducts research and provides scientific and technical services to aid Federal agencies in the selection, acquisition, application, and use of computer technology to improve effectiveness and economy in Government operations in accordance with Public Law 89-306 (40 U.S.C. 759), relevant Executive Orders, and other directives; carries out this mission by managing the Federal Information Processing Standards Program, developing Federal ADP standards guidelines, and managing Federal participation in ADP voluntary standardization activities; provides scientific and technological advisory services and assistance to Federal agencies; and provides the technical foundation for computer-related policies of the Federal Government. The Institute consists of the following centers:

Programming Science and Technology — Computer Systems Engineering.

[1]Headquarters and Laboratories at Gaithersburg, MD, unless otherwise noted; mailing address Washington, DC 20234.
[2]Some divisions within the center are located at Boulder, CO 80303.

NBS BUILDING SCIENCE SERIES 155

Computer Modeling of the Vapor Compression Cycle With Constant Flow Area Expansion Device

Piotr Domanski
David Didion

Building Equipment Division
Center for Building Technology
National Bureau of Standards
Washington, DC 20234

Partially Sponsored by:

Department of Energy
1000 Independence Avenue, S.W.
Washington, DC 20585

U.S. DEPARTMENT OF COMMERCE, Malcolm Baldrige, Secretary
NATIONAL BUREAU OF STANDARDS, Ernest Ambler, Director

Issued May 1983

ERRATA SHEET

NBS Building Science Series 155

Computer Modeling of the Vapor Compression Cycle

with Constant Flow Area Expansion Device

Piotr Domanski, David Didion

Page vii	Line 16;	is: 123,	should be: 121
	Line 17;	is: 124,	should be: 122
	Line 19;	is: 138,	should be: 136
	Line 23;	is: BSS 153,	should be: NBS BSS 155
Page xi	Line 5;	is: 68,	should be: 69
	Line 22;	is: 60,	should be: 61
Page xiv	Line 7;	is: 60,	should be: 61
Page 39	Line 23;	is: adequate	should be: inadequate
Page 43	Line 2;	is: $\frac{m_r}{A}$	should be: $\left(\frac{m_r}{A}\right)^2$
Page 48	Line 29;	is: $\frac{A}{m_r}^2$	should be: $\left(\frac{A}{m_r}\right)^2$
Page 67	Line 1;	is: h_w	should be: k_w
	Line 18;	is: wet (frost)	should be: water (frost)
Page 70	Line 15;	is: $(1 - x^2)$	should be: $(1 - x)^2$

Page 111 Coefficients in equation (E5) should read:

$$b = \frac{2[(v_V - v_L) \cdot v_L \cdot G^2 + i_V - i_L]}{G^2(v_V - v_L)^2}$$

$$c = \left[\frac{2(i_L - i_o)}{G^2} + v_L^2\right]\frac{1}{(v_V - v_L)^2}$$

Page 114 Symbols used in figure F1 are:

PEXIT = refrigerant pressure at tube exit
PFLASH = refrigerant flash pressure
P0 = refrigerant pressure before expansion device inlet
P1 = refrigerant pressure in expansion device inlet
X = refrigerant quality before expansion device inlet

Page 116 Symbols used in figure G1 are:

H = refrigerant enthalpy at tube end obtained from present calculation loop
H^* = refrigerant enthalpy at tube end obtained from previous calculation loop
H_E = refrigerant enthalpy at coil exit obtained from present calculation loop
H_E^* = refrigerant enthalpy at coil exit obtained from previous calculation loop

ABSTRACT

An analysis of the vapor compression cycle and the main components of an air source heat pump during steady-state operation has been performed with emphasis on fundamental phenomena taking place between key locations in the refrigerant system. The basis of the general heat pump model formulation is the logic which links the analytical models of heat pump components together in a format requiring an iterative solution of refrigerant pressure, enthalpy and mass balances.

The modeling effort emphasis was on the local thermodynamic phenomena which were described by fundamental heat transfer equations and equation of state relationships among material properties. In the compressor model several refrigerant locations were identified and the processes taking place between these locations accounted for all significant heat and pressure losses. Evaporator and condenser models were developed on a tube-by-tube basis where performance of each coil tube is computed separately by considering the cross-flow heat transfer with the external air stream and the appropriate heat and mass transfer relationships. A capillary tube model was formulated with the aid of Fanno flow theory.

The developed heat pump model has been validated by checking computer results against laboratory test data for full and part load operation for the cooling/dehumidifying mode as well as the heating mode under frosting conditions.

Key Words: air conditioner; capillary tube; coil; compressor; condenser; evaporator; expansion device; heat pump; modeling; vapor compression cycle.

PREAMBLE

This report is essentially the dissertation of Piotr Domanski which was submitted to the Catholic University of America in partial fulfillment of his Ph.D. requirements. David Didion was his major professor and dissertation director.

DISCLAIMER

In view of the presently accepted practice of the building industry in the United States and the structure of the computer software used in this project, common U.S. units of measurement have been used in this report. In recognition of the United States as a signatory to the General Conference of Weights and measures, which gave official status to the SI system of units in 1960, appropriate conversion factors have been provided in the table below. The reader interested in making further use of the coherent system of SI units is referred to: NBS SP330, 1972 Edition, "The International System of Units," or E380-72, ASTM Metric Practice Guide (American National Standard 2210.1).

METRIC CONVERSION FACTORS

Length	1 inch (in) = 25.4 millimeters (mm) 1 foot (ft) = 0.3048 meter (m)
Area	1 ft^2 = 0.092903 m^2
Volume	1 ft^3 = 0.028317 m^3
Temperature	F = 9/5 C + 32
Temperature Interval	1°F = 5/9°C or K
Mass	1 pound (lb) = 0.453592 kilogram (kg)
Mass Per Unit Volume	1 lb/ft^3 = 16.0185 kg/m^3
Energy	1 Btu = 1.05506 kilojoules (kJ)
Specific Heat	1 Btu/[(lb)(°F)] = 4.1868 kJ/[(kg)(K)]
Gallon	1 gallon = 0.0037854 m^3

TABLE OF CONTENTS

TABLE OF CONTENTS (Cont.)

LIST OF TABLES

LIST OF FIGURES

LIST OF FIGURES (Cont.)

LIST OF SYMBOLS

A = flow cross section area

A_f = fin surface area

A_h = heat transfer surface area

$A_{n,i}$ = coefficients in equation (68)

$A_{p,i}$ = pipe inside surface area

$A_{p,m}$ = pipe mean surface area

A_o = pipe total outside surface area

a1,a2,a3 = coefficients in equation (20)

CP = pressure drop parameter

CQ = heat transfer parameter

C_c = correction factor in equation (10)

C_e = clearance volume, in fraction of compressor stroke volume

Cp = specific heat at constant pressure

Cv = specific heat at constant volume

D = tube inside diameter

D_o = tube outside diameter

D_f = fin tip diameter

d1,d2 = dimensions representing arrangement of tubes in a coil, as per figure 21

E = electrical power input

F1,F2 = dimensionless parameters used in equation (60)

f = Fanning friction factor

$f_{tp,L}$ = friction factor for the liquid portion of two-phase flow, flowing alone in the tube

G = $\frac{m}{A}$, mass flux

G_{max} = air mass flux between two adjacent fins

h = heat transfer coefficient, $h_{c,o}$ refers to air-side mean convective heat transfer coefficient, $h_{d,i}$ refers to heat transfer coefficient for inside tube deposit, h_i refers to inside tube convection heat transfer coefficient

$h_{D,o}$ = air-side mass transfer coefficient

hp = horse power

i = enthalpy

i_{fg} = latent heat of evaporation or condensation

J = the mechanical equivalent of heat

K = flow contraction coefficient

k = thermal conductivity

L = tube length

Le = $\frac{h_{c,o}}{h_{D,o} Cp_a}$, Levis number

M = mass of refrigerant

m = mass flow rate

Nu = $\frac{h \cdot D}{k}$, Nusselt number

n = polytropic index

P = pressure

Pr = $\frac{\mu \cdot Cp}{k}$, Prandtl number

Q = heat transfer rate

R = rate of moisture removal per unit area

R' = rate of moisture removal per unit width of a fin

Re = $\frac{G \cdot D}{\mu}$, Reynolds number

$Re_{tp,L}$ = Reynolds number for the liquid portion of two-phase, flowing alone in the tube

RPM = compressor number of revolutions per minute

S = tube perimeter

s = entropy

T = temperature

$T_{f,b}$ = fin base temperature

$T_{f,m}$ = mean fin temperature

$T_{r,g}$ = refrigerant saturation temperature

t = fin thickness

U = overall heat transfer coefficient

V = velocity

Vs = compressor swept volume

$\forall$ = volume

v = specific volume

W_c = mechanical power available for compression process

W_e = mechanical power output

w_a = humidity ratio of air, $w_{a,i}$ refers to tube row inlet, $w_{a,e}$ refers to tube row outlet

w_w = humidity ratio of saturated air at temperature of wetted water film

$X_{tt} = \left[\frac{1 - x}{x}\right]^{0.9} \left[\frac{v_L}{v_V}\right]^{0.5} \left[\frac{\mu_L}{\mu_L}\right]^{0.1}$, Lockhard-Martinelli parameter

$x = \frac{m_V}{m_V + m_L}$, quality

x_p = pipe wall thickness

y = fin height

Z_{tp} = fraction of the tube in the two-phase region for the tube with liquid and two-phase flow

Z_V = fraction of the tube in the superheated vapor region for the tube with two-phase and superheated vapor flow

z = distance between adjacent fins

α = void fraction

β = exponent in equation (60)

γ = isentropic index

σ = liquid layer (frost) thickness

η_e = electric motor efficiency

η_m = mechanical efficiency of compressor

η_p = polytropic efficiency of compressor

η_v = volumetric efficiency of compressor

μ = absolute viscosity

ρ = density

τ = skin friction factor

Φ = correction factor for two-phase pressure drop

ϕ = fin efficiency

Subscripts:

a = air, a,d refers to dry air

e = exit

f = frost or fin

i = inlet

L = liquid

m = mean value

P = constant pressure process

r = refrigerant

s = constant entropy process

t = total value

V = vapor

v = constant volume process

w = water

1 to 13 = refrigerant key locations in a heat pump, as per figure 4, unless otherwise epxlained in the text

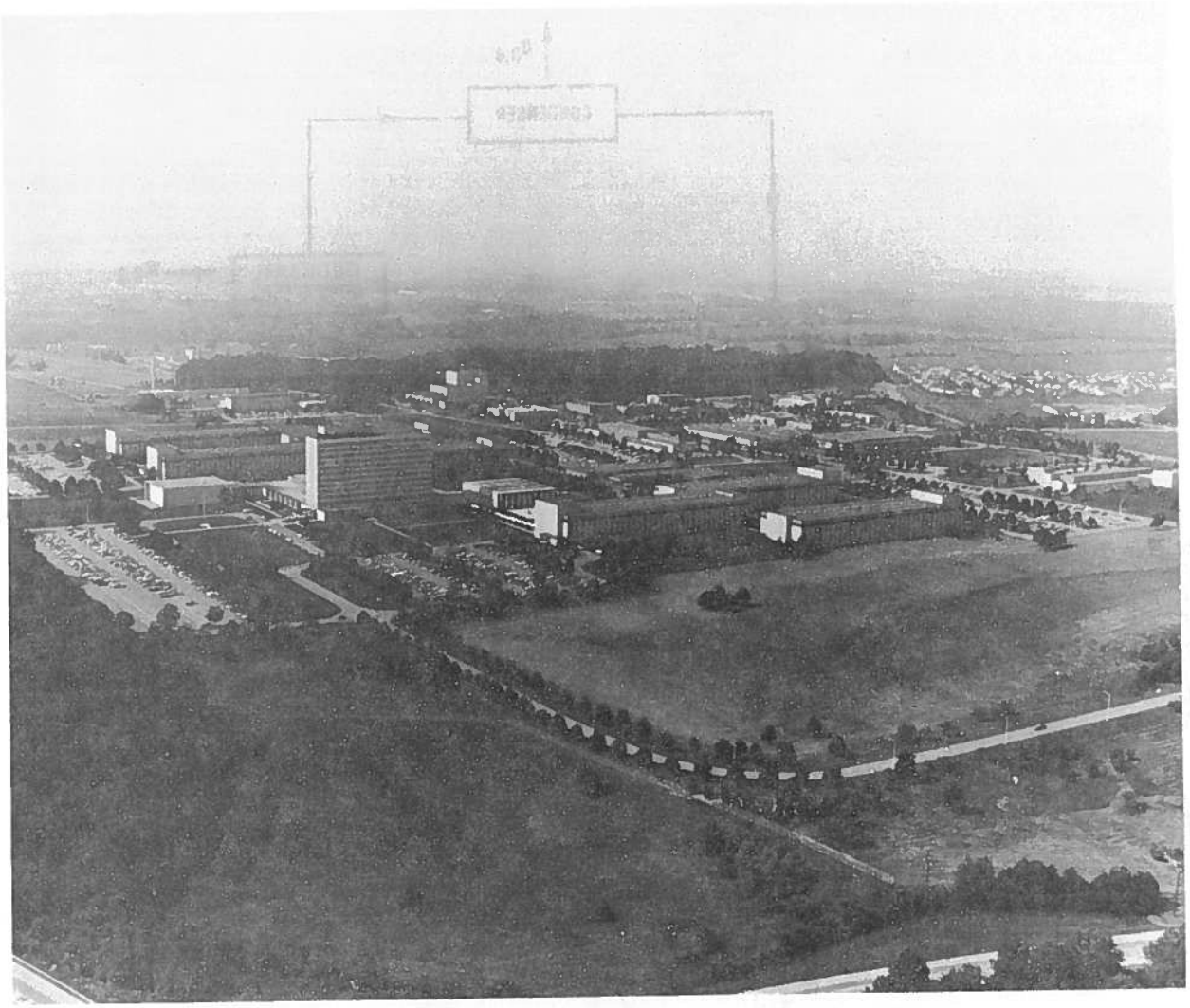

1. INTRODUCTION

Any power producing cycle, whose processes can be performed in the reverse direction and in the reverse order, will serve as a refrigerating cycle. The Carnot cycle is the model of perfection for a power producing cycle as well as for a refrigeration cycle. However, it is not practical to realize this perfect thermodynamic cycle with hardware (see figure 1). First, two compression machines, one realizing isentropic compression, the other realizing isothermal compression would be required. Second, the small amount of expansion work available does not support the idea of incorporating a work producing expander into the system.

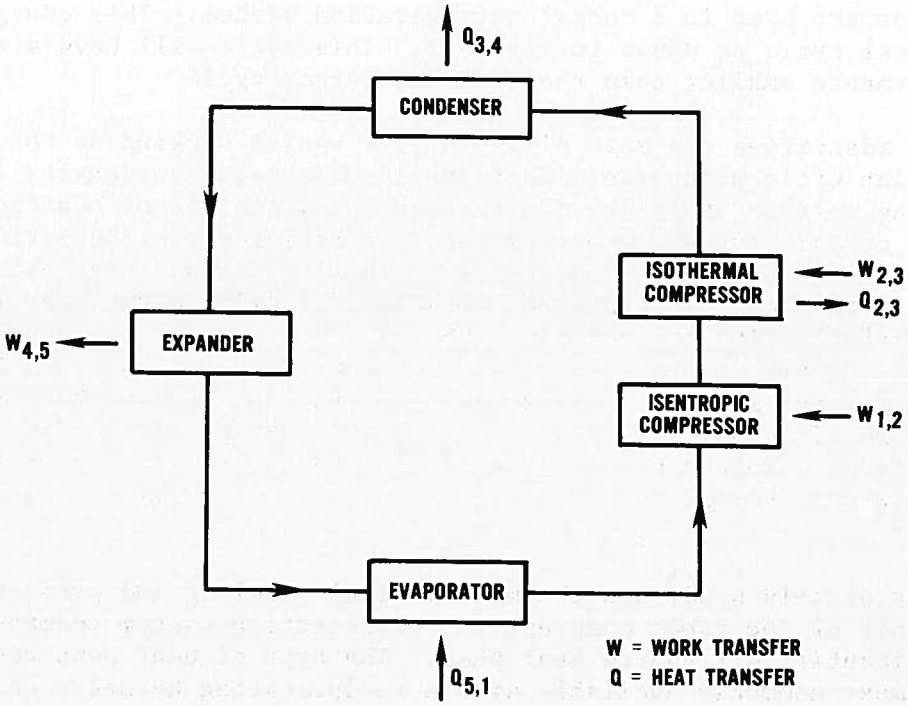

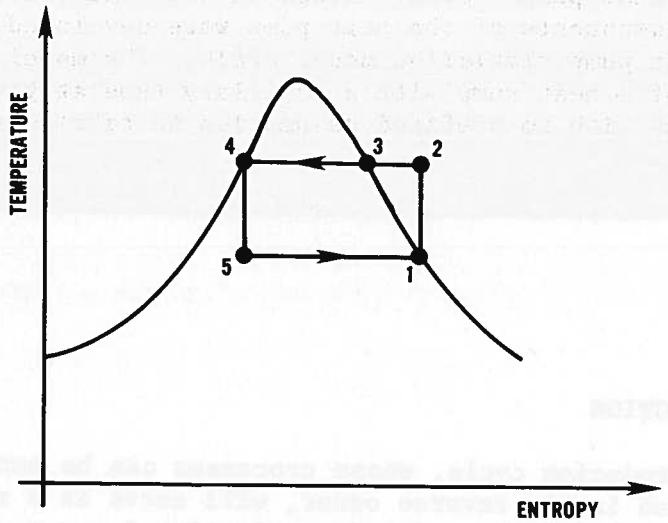

Figure 1. Carnot vapor compression cycle

Thus a simple isenthalic throttling expansion device and only one type of compressor are used in a normal refrigeration system. This changes the theoretical cycle as shown in figure 2. This cycle will have a coefficient of performance smaller than that for the Carnot cycle.

Figure 2 identifies the main elements of a system working on the vapor compression cycle principle. They are: compressor, condenser, evaporator and throttling valve. There are many concepts and designs of heat pump components, however, certain types are predominant. A reciprocating hermetic compressor is mostly used for vapor compression in small systems. Heat exchangers are usually in the form of staggered tubes with closely packed wavy fins (spine-fins or bristle-fins are sometimes used). There are basically two types of expansion devices in application today. Constant flow area restrictors are distinctly prevailing in small capacity units such as household refrigerators, window-type air conditioners and central residential air conditioners and heat pumps. Larger, more expensive residential units and commercial units are mostly equipped with a variable flow area device called a thermostatic expansion valve (TXV).

The focus of this study was the mathematical modeling and prediction of performance of the vapor compression refrigeration system commercially known as a residential air source heat pump. The type of heat pump considered is the one most commonly available with a reciprocating hermetic compressor, fin tube heat exchangers, and a constant flow area expansion device.

The present report discusses and analytically describes the phenomena taking place in the heat pump system. Based on this analysis, mathematical models of the main components of the heat pump were developed and linked together in a general heat pump simulation model HPSIM. The model HPSIM simulates the performance of a heat pump with a capillary tube at given outdoor and indoor air conditions with no prefixed assumption on refrigerant state at any point of the system.

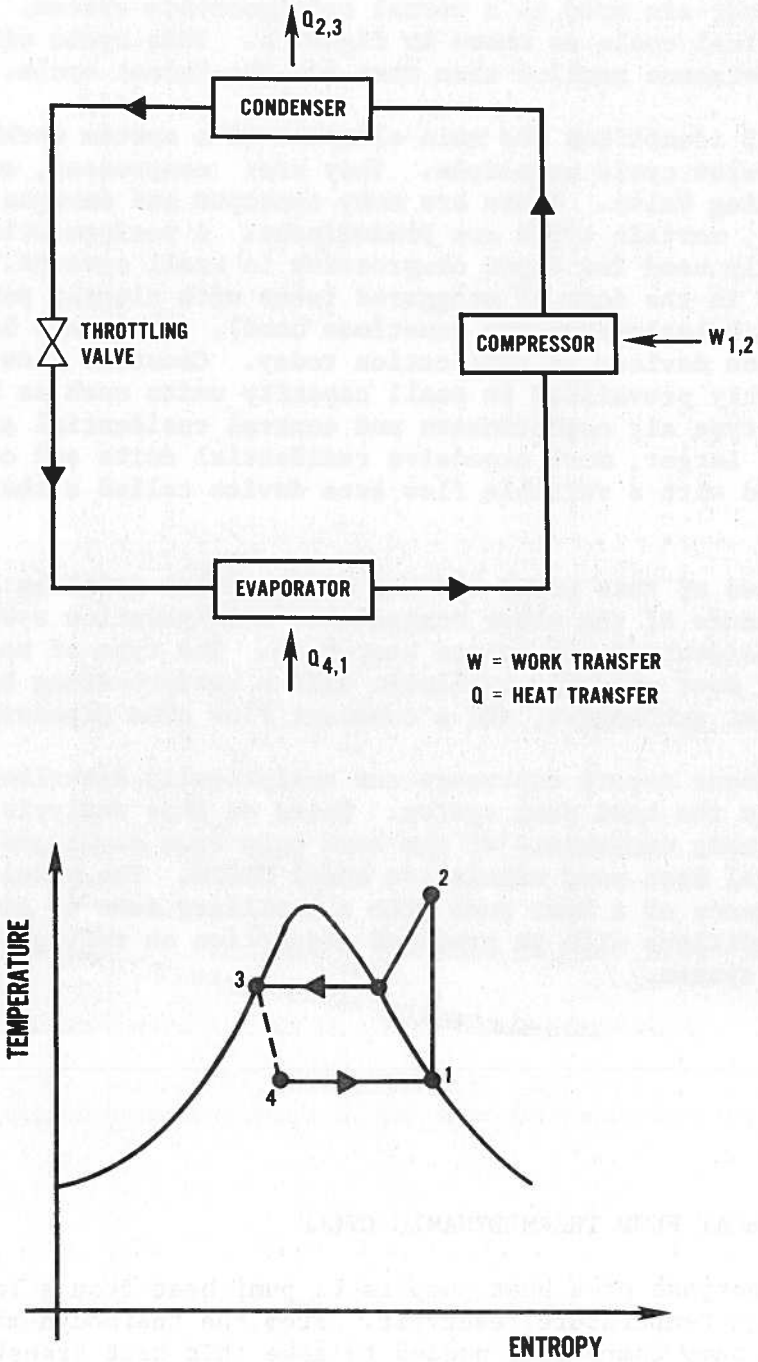

Figure 2. Theoretical vapor compression cycle

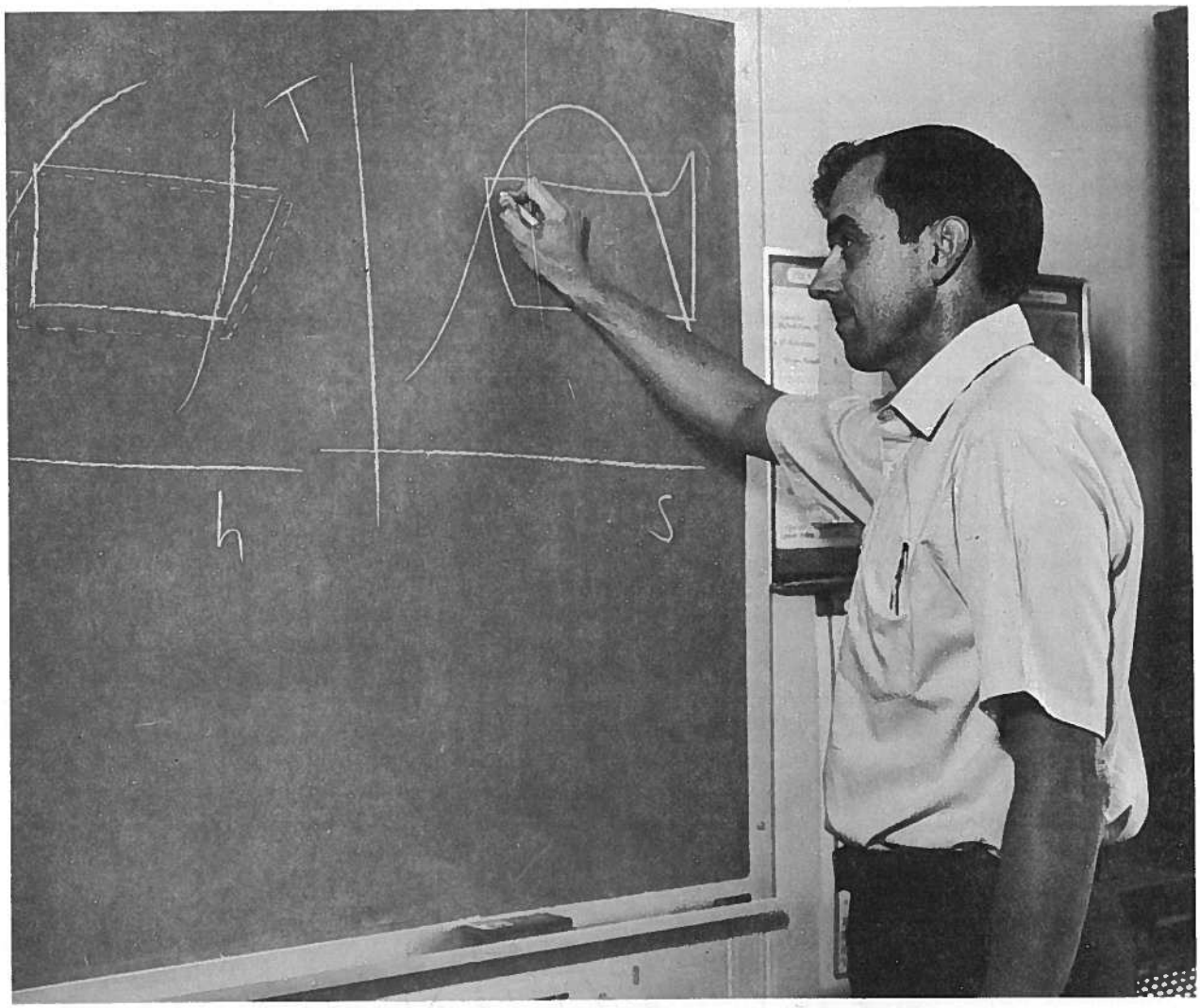

2. HEAT PUMP THERMODYNAMIC CYCLE

The purpose of a heat pump is to pump heat from a low temperature reservoir to a high temperature reservoir. From the thermodynamic point of view, the basic heat pump components needed to make this heat transfer feasible are: two heat exchangers, a compressor, and an expansion device. A heat pump thermodynamic cycle can be explained considering the processes that the refrigerant undergoes in these four components. The most convenient diagram for such explanation and performance analysis is that of a pressure vs. enthalpy coordinate system, as shown in figure 3. The compressor receives low pressure and temperature refrigerant at state 1 and compresses it to a high pressure. This compression process is associated with an increase of refrigerant temperature. At state 2,

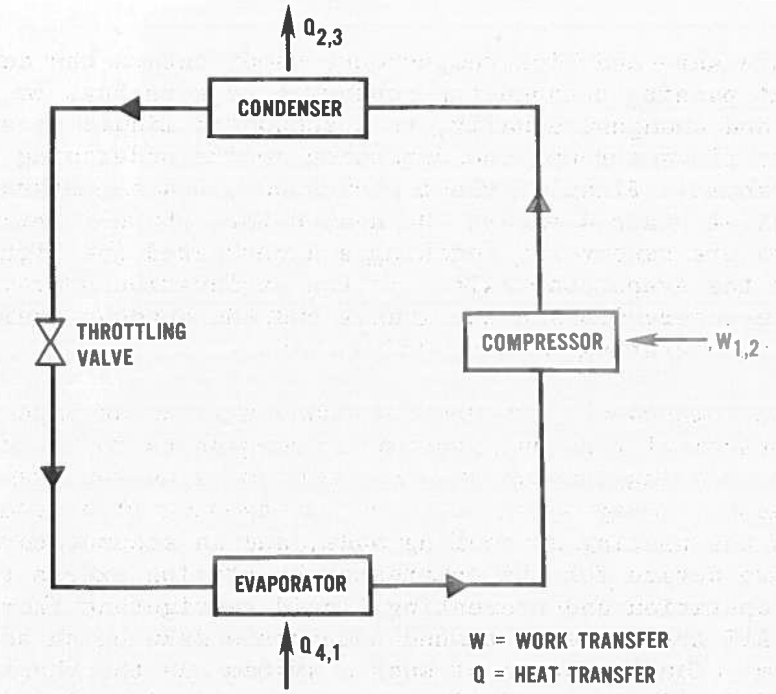

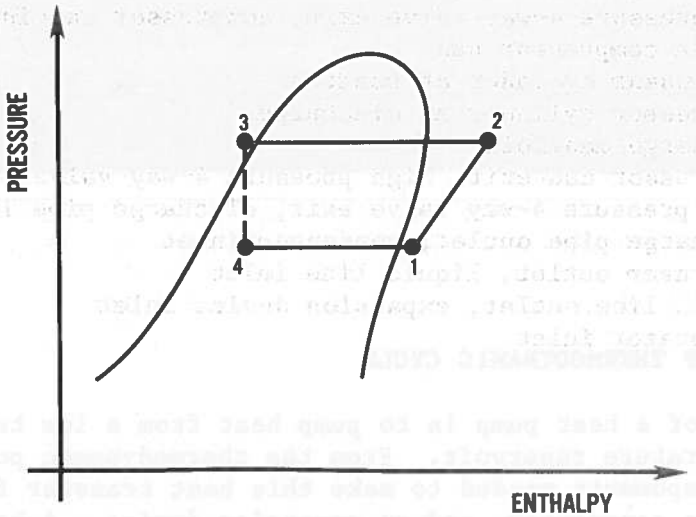

Figure 3. Oversimplified thermodynamic cycle of a heat pump

the high pressure and high temperature vapor enters the condenser. The refrigerant passing through the condenser rejects heat to the high temperature reservoir and changes, usually, to a subcooled liquid at state 3. Then, the refrigerant flows through the expansion device undergoing a drop in pressure and temperature. Finally, the low pressure, low temperature, and low quality refrigerant at state 4 enters the evaporator, where it picks up heat from the low temperature reservoir, reaching a superheated (or high quality) vapor state 1 at the evaporator exit. In the explanation above, the low and high temperature reservoirs are the indoor and the outdoor environment, when the heat pump is operating in the cooling mode.

Besides the compressor, two heat exchangers, and the expansion device, there are, for practical reasons, many other components in an actual heat pump system. Four modeling consideration, the most important are: tubes connecting basic elements, 4-way valve enabling refrigerant flow reversal for the unit to operate in the heating or cooling mode, and an accumulator, which acts as a protective device for the compressor by storing excess refrigerant during part load operation and preventing liquid refrigerant from entering the compressor. All the above mentioned components make up an actual vapor compression system. Configuration of such a system and the thermodynamic cycle are illustrated in figure 4 and figure 5, respectively. Refrigerant states in figure 5 correspond to particular locations in the system marked in figure 4, which are:

1 - evaporator exit, suction pipe inlet
2 - suction pipe outlet, low pressure 4-way valve inlet
3 - low pressure 4-way valve exit, compressor can inlet
4 - inside compressor can
5 - compressor cylinder at suction
6 - compressor cylinder at discharge
7 - discharge manifold
8 - compressor can exit, high pressure 4-way valve inlet
9 - high pressure 4-way valve exit, discharge pipe inlet
10 - discharge pipe outlet, condenser inlet
11 - condenser outlet, liquid line inlet
12 - liquid line outlet, expansion device inlet
13 - evaporator inlet

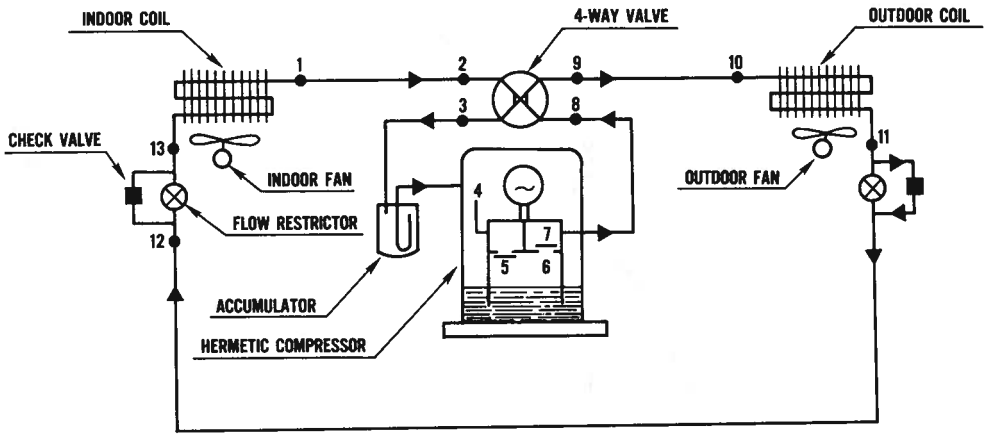

Note: 1. Refrigerant flow direction is marked as for cooling operation

2. Numbers 5 and 6 situated in the compressor correspond to refrigerant state before and after compression process

Figure 4. Schematic of a heat pump

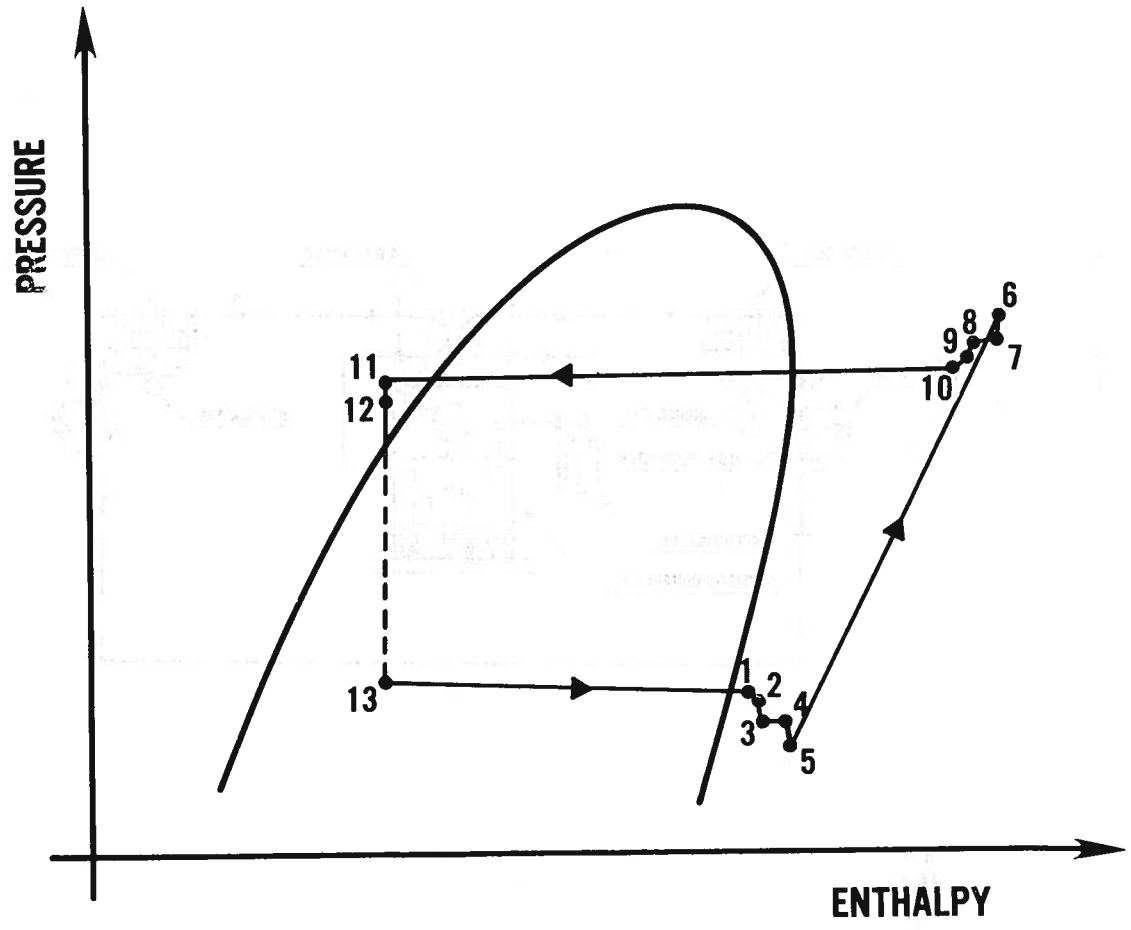

Figure 5. Thermodynamic cycle realized by a heat pump
(For number location refer to figure 4)

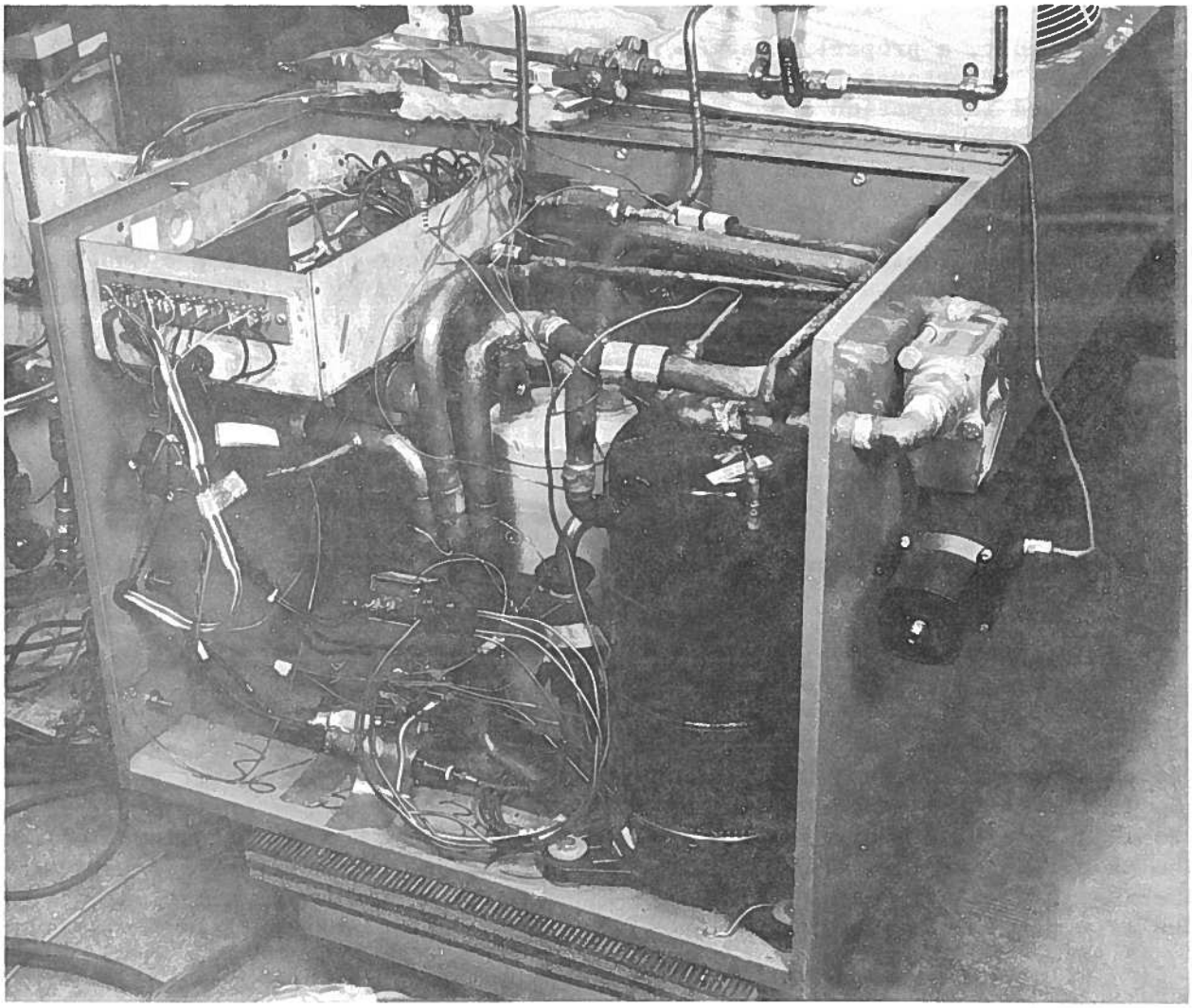

3. OPERATION OF AN AIR SOURCE HEAT PUMP WITH A CAPILLARY TUBE

Refrigerant state in key locations of a heat pump and heat pump performance are functions of many factors. From a macroscopic point of view they can be listed as follows:

- individual performance of heat pump components
- compatibility of components in the system
- properties of refrigerant
- refrigerant charge
- outdoor and indoor air conditions

Each of the above factors have an independent impact on heat pump capacity and efficiency.

In this report, a properly charged, commercially available heat pump is discussed. A customer receives a heat pump correctly precharged by a manufacturer and information about proper charge by weight of refrigerant is supplied on the heat pump name plates. Simple charts are also available to facilitate checking the state of charge of unit by reading compressor suction and head pressures at given operating conditions.

Manufacturers establish proper charge for a given heat pump during a laboratory test. It is usually a cooling test at standard operating conditions, which are:

outdoor air dry bulb temperature - 95°F
indoor air dry bulb temperature - 80°F
indoor air wet bulb temperature - 67°F

The measure of the refrigerant charge of the system is refrigerant superheat at the compressor can inlet. Superheat of about 15°F at this location is commonly accepted as an indication of a proper amount of refrigerant in the heat pump.

In a heat pump with a capillary tube, vapor superheat at the compressor inlet will vary with changing operating conditions. As a matter of fact, no single refrigerant parameter stays constant when indoor or outdoor air conditions are altered and the system seeks equilibrium under new conditions. To understand the phenomena that cause refrigerant state changes, consider a heat pump working in the cooling mode at constant indoor air conditions and the system response to a step increase of the outdoor temperature. For the purpose of the analysis it is assumed that the overall heat transfer coefficient for both heat exchangers does not vary. It is also assumed, as a first approximation, that the latent heat of evaporation, i_{fg}, is constant under the conditions discussed.

A step change in the outdoor air temperature first affects the performance of the condenser. Since the condenser environment temperature increase, the mean temperature difference between the air and the refrigerant decreases. Less heat is rejected by the refrigerant to the air and a smaller enthalpy change is realized in the coil. Consecutively, higher enthalpy, less subcooled liquid refrigerant enters the capillary tube. The capillary tube is sensitive to the amount of subcooling and with less subcooling the mass flow rate through the capillary tube decreases. Since the compressor capacity stays unchanged, pressure builds up in the condenser. Thus point 11 on the p - h diagram (refer to figure 5) moves in the direction of higher enthalpy and higher pressure.

The environment of the evaporator was not altered. However, refrigerant parameters in the evaporator change in response to the change of refrigerant state at location 11 as well as to the change in refrigerant mass flow rate. For pressure drop considerations, as a first approximation, the liquid line, the capillary tube, and the evaporator are viewed as one tube, in which a given flow experiences a certain pressure drop. As pressure of the refrigerant at

location 11 increases, it pulls up the refrigerant pressure in the evaporator. Conflicting phenomena affect the change of refrigerant enthalpy at point 1. Increased enthalphy at point 11 and reduced refrigerant mass flow rate work against the impact of the smaller temperature difference between the air and the refrigerant causing refrigerant enthalpy to slightly decrease. The significance of the change of the refrigerant state at location 1 depends on the move towards smaller vapor specific volume. Since the compressor, as a first approximation, is a constant intake volume pump, increase in gas density results in a higher mass flow rate.

The indicated phenomena will balance themselves further until the refrigerant in the key locations of the system acquires thermodynamic states that satisfy simultaneously all heat pump components. Since under steady-state operation, refrigerant mass flow rate through the compressor and the capillary tube have to match, the pressure in the condenser will rise to an appropriate level. Again, higher pressure in the condenser implies some increase of pressure (and saturation temperature) in the evaporator. Smaller temperature difference between the indoor air and the refrigerant, and higher refrigerant mass flow rate result in a smaller refrigerant enthalpy increase in the evaporator. Refrigerant state at point 1 with respect to point 11 is determined by this enthalpy change and appropriate pressure drop. Finally, when steady-state conditions are obtained, the following changes in refrigerant thermodynamic states can be noticed: higher refrigerant pressure in the condenser, higher refrigerant pressure in the evaporator, less superheat in the evaporator exit, and less refrigerant liquid subcooling at the condenser exit. A change of saturation temperature in the condenser corresponds approximately to a change in the outdoor air temperature. The change of pressure in the evaporator equals to a fraction (approximately 15 percent) of the pressure change in the condenser. Though the refrigerant is circulated in the system at a higher mass flow rate, capacity of the heat pump is decreased due to smaller refrigerant enthalpy change in the evaporator. Efficiency also drops since, in addition to a smaller cooling effect, energy input for the compression process increases due to higher refrigerant mass flow rate and higher compression rate. A decrease of the outdoor air temperature would induce the opposite trends.

A change of refrigerant parameters is illustrated in figure 6, where results of three heat pump tests are plotted on the pressure-enthalpy diagram. (Test results are those of system 2 discussed later in section 6.1). In these tests, the indoor air conditions were held constant while the outdoor air dry bulb temperature was changed inducing modification of the realized thermodynamic cycle.

For the heating mode operation, refrigerant flow is reversed by reset of the 4-way valve. Flow direction of the refrigerant in the system is the opposite to that in the cooling mode, with the exception of the compressor. The indoor coil becomes a condenser while the outdoor coil serves as an evaporator. It is worthwhile to note the effect this change has on the system. Since pressures in heat pump heat exchangers are functions of environment temperatures, the pressure in the evaporator is now much lower than during cooling operations. Consequently, the density of the refrigerant at the evaporator exit is smaller and less refrigerant is being pumped by the compressor. In order to maintain a

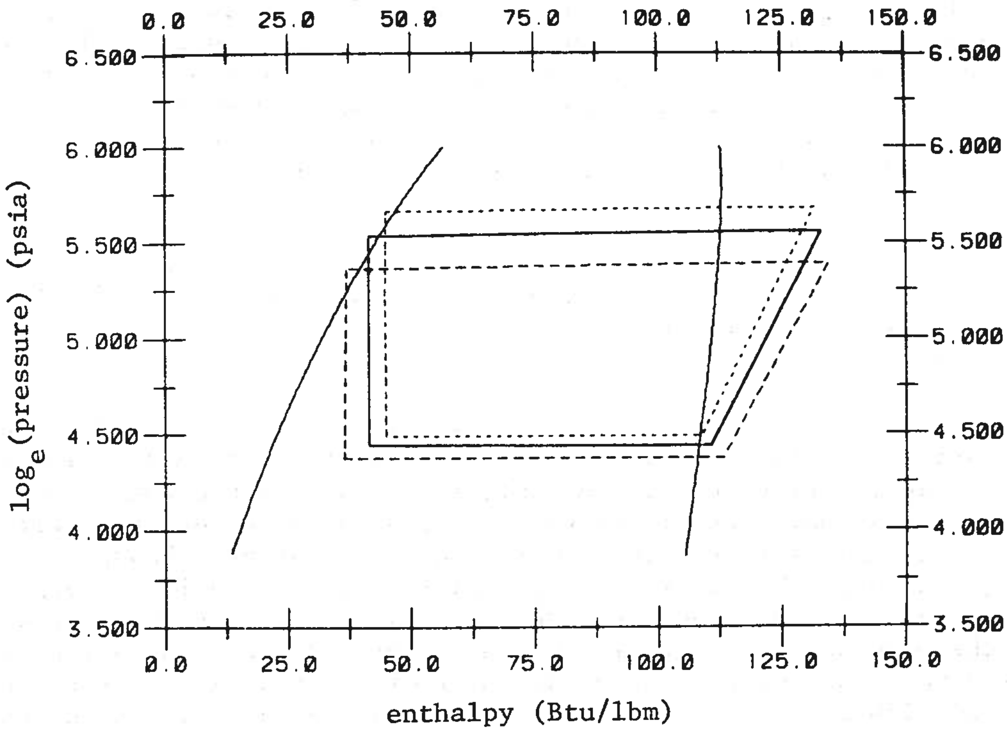

Indoor conditions (all three tests): air dry bulb temperature - 80°F
air wet bulb temperature - 67°F

Outdoor dry bulb temperature: ------------------------------------ - 105°F

———————————————— - 95°F

— — — — — — — — — — — — — — — - 82°F

Note: 1. Saturation lines have been generated by means of equations presented in appendix A.

2. Refrigerant states in a heat pump were obtained from laboratory tests 2.1, 2.2., and 2.3 discussed in section 6.1.

Figure 6. Simplified thermodynamic cycle realized by a heat pump in the cooling mode at different outdoor conditions

proper pressure in the condenser, another, properly sized capillary tube is now used in the system, while the one used in the cooling mode is bypassed.

An indoor coil is usually much smaller than an outdoor coil. Need for good dehumidification performance is the primary reason. The indoor coil working as the condenser cannot hold as much refrigerant as the outdoor coil during cooling operation. Since the condenser holds the bulk of working refrigerant in the system, excess refrigerant has to be stored somewhere during heating operation. For storage purposes in heat pumps equipped with a capillary tube, an accumulator is provided.

A schematic of an accumulator is given in figure 7. The accumulator is a closed container with two pipes. The longer, bent pipe has a small diameter hole on the bottom side, and is connected to the compressor. The other pipe connects the tank with the evaporator exit.

If superheated vapor leaves the evaporator, vapor only is contained in the accumulator and no special function is fulfilled by the accumulator in this case. If wet vapor enters the accumulator, liquid droplets accumulate on the bottom of the tank, while saturated vapor enters the pipe leading towards the compressor. Some liquid refrigerant enters the vapor stream through the hole in the pipe, driven by the static pressure difference in the liquid-vapor stream interface. It should be noted that during steady-state operation with liquid in the accumulator, qualities of the vapor entering and leaving the accumulator have to be equal. Since the small diameter hole allows for a small rate of liquid flow into the saturated vapor stream, vapor taken in by the compressor is close to its saturation state. Such a situation at the compressor inlet prevails in the heating mode since, with a possible exception to operation at high outdoor temperature, there is always liquid refrigerant stored in the accumulator.

This discussion has been for the heat pump employing a constant flow area expansion device. Thermostatic expansion valves, TXV's, are variable opening orifice devices. The amount of opening is varied according to some control function, usually constant vapor superheat at the evaporator exit. In heat pumps employing TXV's, vapor superheat at the compressor inlet does not depend on operating conditions but rather has a constant preset value.

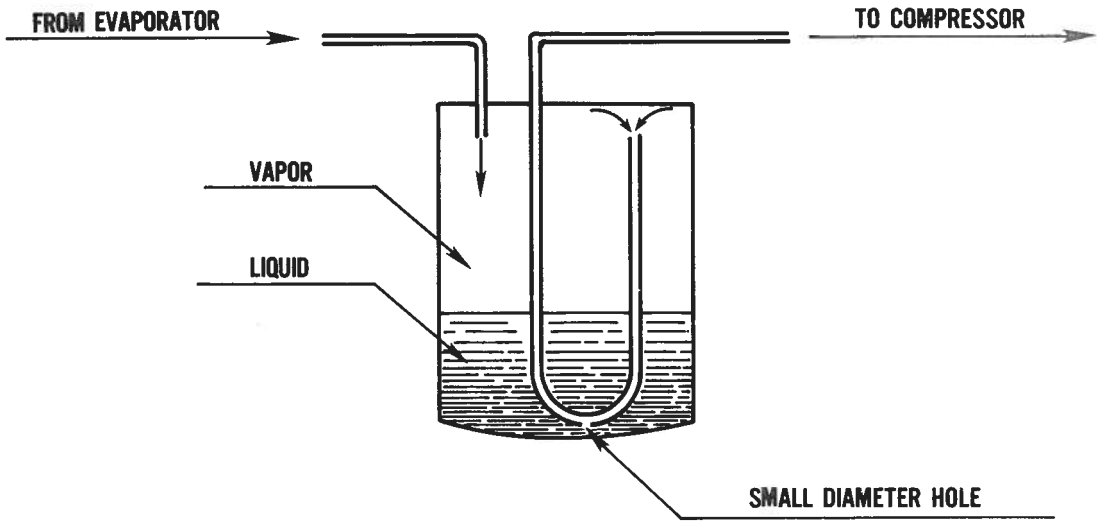

Figure 7. Schematic of an accumulator

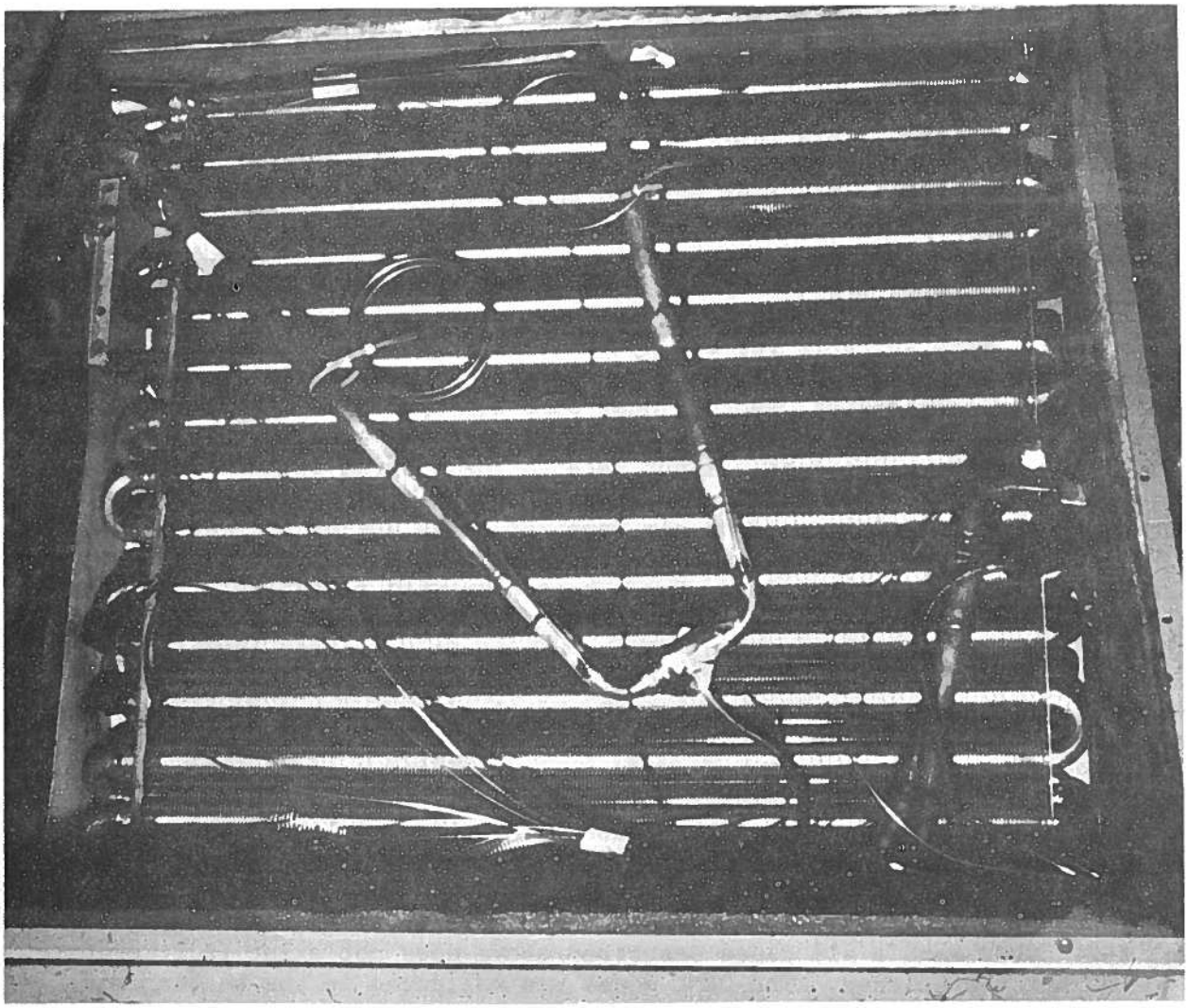

4. PREVIOUS WORK IN STEADY-STATE VAPOR COMPRESSION CYCLE MODELING

Modeling of the vapor compression cycle has to be performed by modeling essential processes taking place in the system. A review of state-of-the-art steady-state vapor compression cycle modeling will be conducted at two levels. On one level, presently available heat pump models will be discussed. On another level, the discussion will deal with the available models of particular components of a heat pump. The latter discussion will take place in later sections.

Although some equipment manufacturers have highly developed proprietary models, one of the first sophisticated steady-state models of the vapor compression

cycle was published at Massachusetts Institute of Technology [1]. The MIT model simulates a heat pump in the heating mode equipped with a thermostatic expansion valve, TXV, maintaining a constant refrigerant vapor superheat at the evaporator exit. Input data required to the program, besides heat pump data, are indoor air conditions, saturation refrigerant temperature at the evaporator exit, and refrigerant vapor superheat at the same location. Heat pump capacity, power input, and outdoor air temperature are obtained as results of a simulation run. If heat pump performance data at given operating conditions are required, several simulation runs have to be performed in order to be able to interpolate to get desired results.

The Oak Ridge National Laboratory developed a heat pump simulation model [2] based on the study performed at MIT. The ORNL program includes a new compressor model, more suitable for use by an averaging user. In addition to a thermostatic expansion device available in the MIT version, a capillary tube model has been incorporated, hence a heat pump equipped with either type of an expansion device can be simulated by the ORNL program. the general structure of MIT model has been retained. Input data to the program include refrigerant saturation temperature and refrigerant vapor superheat at the evaporator outlet while as in the MIT model, outdoor air temperature is one of the outputs of the program[1/]. A limitation appears in the simulation of a system employing a constant flow area expansion device. For a heat pump with a capillary tube, superheat is usually known only at one set of standard operating conditions (function of refrigerant charge only). Then, when a change in operating conditions occurs, the superheat will also change. The ORNL model does not provide a means for calculating the change in superheat; it is required as input data, which can be approximated at best. An additional limitation also results from the capillary tube model. The model depends on curve fitting of capillary tube capacity charts presented in ASHRAE Guide and Data Book [4]. These charts cover performance of a long capillary tube with subcooled liquid entering. Thus, the model cannot handle either a capillary tube when there is incomplete condensation in the condenser (that does happen, particularly during heating operation), or very short constant bore flow restrictors. A capillary tube model that could handle all cases described above does not exist in literature to the author's knowledge. The ORNL model was validated in the heating mode only.

A mathematical model of a heat pump was also developed at the National Bureau of Standards [3]. The model simulates the performance of a heat pump employing a TXV as an expansion device. The general logic of the model is similar to those of the MIT and ORNL models. Heat pump data, indoor air conditions, refrigerant saturation temperature, and refrigerant vapor superheat at the evaporator exit are required as input. Output consists of performance information (capacity,

---

1/ At the stage of completion at this report documentation on a new heat pump model was published by Oak Ridge National Laboratory (December 1981) [55]. This latest model, representing an upgraded version of the model described in [2], allows the user to specify heat pump operating conditions.

power input, efficiency) and the outdoor temperature. The NBS model was validated in the heating mode only.

The above review outlines the available, general models of a heat pump, their applicability and limitations. Considering the formulation of a model of a heat pump with a capillary tube, the following conclusions can be made:

1. The only program available in the literature for simulating a heat pump with a capillary tube is provided by ORNL. The program has limitations which result from the logic of the program and from the capillary tube model itself. As input data, refrigerant vapor superheat at the evaporator exit is required, and the program is unable to simulate the heat pump when a two-phase flow condition exists at the capillary tube inlet. Also, the model cannot handle a short capillary tube.

2. The logic in the existing models is adequate for simulation of a heat pump with TXV, however, it is insufficient for modeling a system employing a capillary tube. A new logic allowing for calculation of the vapor superheat should be formulated.

3. There is no capillary tube model available in the literature which can simulate its performance regardless of refrigerant state (two-phase or subcooled liquid) at the tube inlet, and which can simulate tubes of a short length. Such a model should be formulated.

4. Models of a compressor, an evaporator, and a condenser are available in the literature. They may be used in original or modified form in any new simulation heat pump model.

5. None of the available models accepts operating conditions as input data. A model providing heat pump performance data at given operating conditions is most desirable and appropriate logic should be developed.

6. All discussed models have been verified in the heating mode only. Verification of a model in heating and cooling operation would be desirable.

These conclusions led to the development of the new model described in this report. It was felt that the model should simulate an air-to-air heat pump equipped with a constant flow area expansion device with no prefixed refrigerant state in any system location required in a set of input data.

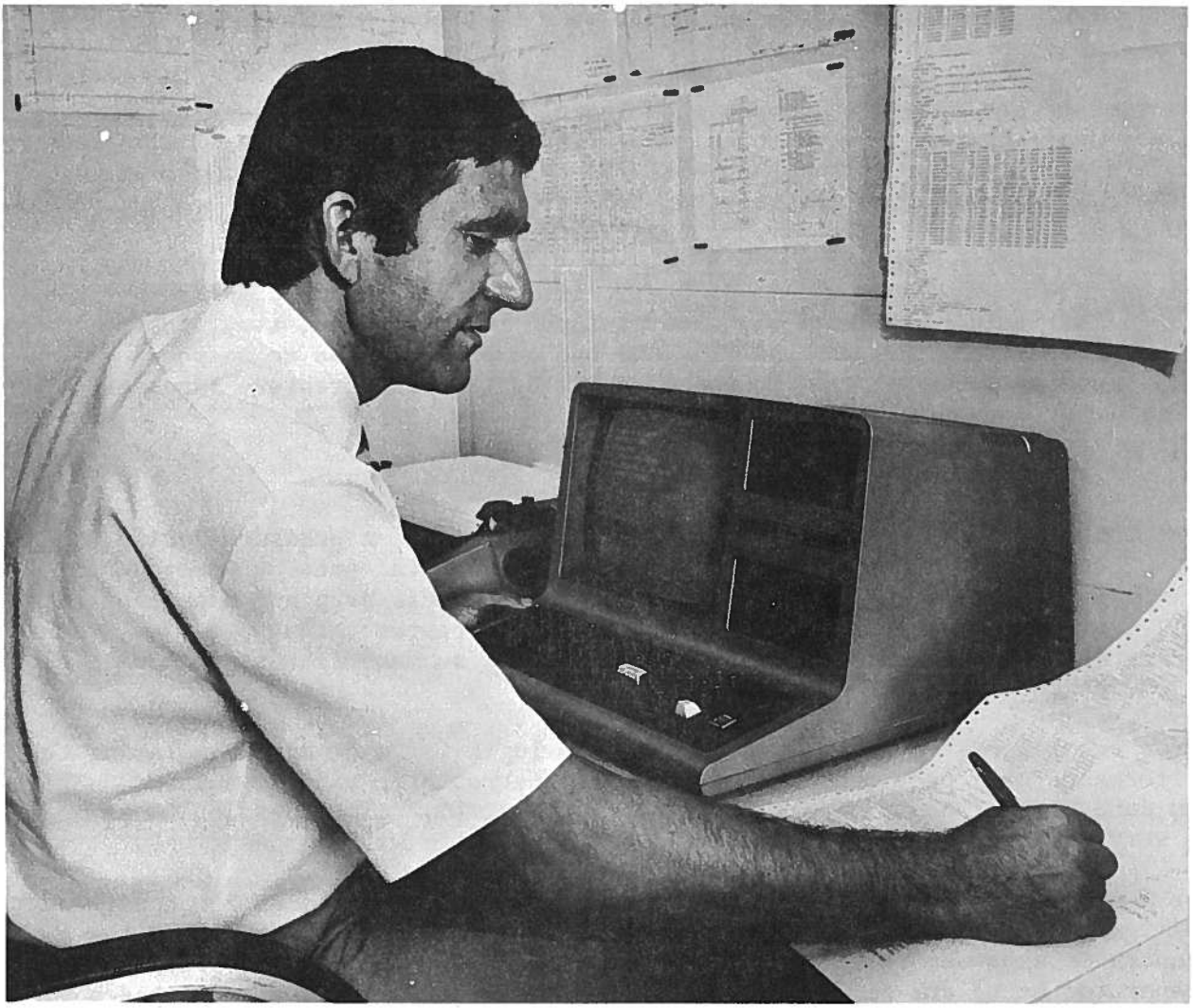

5. MODELING A HEAT PUMP WITH A CONSTANT FLOW AREA EXPANSION DEVICE

5.1 MODELING OF THE SYSTEM

5.1.1 Structure of Available Heat Pump Models

During heat pump operation, refrigerant parameters at any location are established at a level which satisfies the respective components of the system. There is a one-to-one relationship between working medium parameters and operating conditions, i.e., for given outdoor and indoor air conditions, there is no alternative but just one set of refrigerant parameters at any location within

the system which constitute steady state operation. This unique set of refrigerant parameters has to be sought by a heat pump simulation program in an iterative process.

In order to set up a heat pump system logic, balances taking place during steady state operation have to be recognized. From the fact that a thermodynamic cycle is a closed loop, an analysis of a heat pump cycle on a pressure-enthalpy diagram allows statement of two balances:

- Enthalpy Balance

  This balance implies that energy input to the system, i.e., to the evaporator, the suction line and the compressor, has to be equal to energy rejected by the system, i.e., by the high pressure line and the condenser.

- Pressure Balance

  This balance implies that increase of refrigerant pressure during the compression process has to be equal to the total pressure drop during other processes forming the cycle. As pressure drop and mass flow rate are strictly related, this balance may be restated that pressure drop through each component has to be adequate so mass flow rate in each component is the same.

These two balances are sufficient to set up logic for a program simulating the performance of a heat pump equipped with a thermostatic expansion valve. This was done for all three models reviewed [1], [2], [3]. The logic of these models is very similar, so only one, the N.B.S. model logic will be described.

For the heating mode simulation, besides heat pump data, indoor air conditions, refrigerant saturation temperature, and refrigerant vapor superheat at the evaporator exit are required. These data (including refrigerant state at the evaporator exit) are fixed for the run. A set of input data also includes compressor head pressure and outdoor air temperature, which are input as initial estimates.

The compressor is simulated first to estimate refrigerant mass flow rate. Then an enthalpy balance is sought simulating the condenser and the evaporator. If refrigerant enthalpy at the condenser outlet and the evaporator inlet do not match, outdoor air temperature is altered and the evaporator is simulated until the balance is reached. It is assumed reasonably well, that a change in outdoor temperature has negligible effect on compressor performance. Next, the thermostatic expansion valve is simulated. If refrigerant mass flow rate through the TXV is not equal to that through the compressor, the compressor discharge pressure is changed and the whole procedure is repeated again.

The above logic is relatively simple, since all iterative processes take place with a fixed refrigerant state at the evaporator exit. The evaporator environment temperature is calculated and is part of the simulation run output. If

performance of the unit at particular outdoor conditions is needed, a few simulation runs have to be performed in order to allow for interpolation. Of course, this results in increased computing time and imposes a need to reduce output data. A similar logic can be used to simulate the cooling mode, however, with similar inefficiencies.

5.1.2 New System Logic

Two balances, an enthalpy balance and a pressure balance, are sufficient to set up the logic for a program simulating steady state performance of a heat pump with a thermostatic expansion valve because this expansion device maintains a constant refrigerant vapor superheat at evaporator outlet. A constant flow area expansion device does not provide any fixed control of refrigerant superheat or any other flow parameter. It can be generally stated, that for heat pumps with capillary tubes during cooling mode operation, the vapor superheat at the compressor can inlet increases with rising indoor temperature and humidity, and with decrease of outdoor temperature. Logically then, the superheat decreases with respective opposite trends. During cooling operation, superheat may vary from 0 to 40°F. During heating mode operation, very low or no superheat is observed at the compressor inlet.

In as much as refrigerant superheat is a new unknown, an additional balance has to be used to establish superheat values for each operating condition. It is proposed, that superheat be evaluated by means of conservation of mass, as expressed by the equation:

$$\frac{D}{Dt} \int_{\Psi} \rho d\Psi = 0 \qquad (1)$$

where ρ = density
Ψ = system volume

Equation (1) implies, that the amount of working medium in the system is the same at all times, for any operating conditions.

The logic is based on three balances, enthalpy, pressure, and refrigerant mass as explained below. It provides means for calculation of vapor superheat and allows for heat pump simulation at implied operating conditions. Explanation of the logic, for sake of clarity, is done considering only four main components of a heat pump, i.e., a compressor, a condenser, a capillary tube, and an evaporator.

Required input consists of outdoor and indoor conditions, and heat pump data. The simulation process starts with guessed refrigerant pressure and vapor superheat at the compressor inlet, and the compressor discharge pressure. Using these data, compressor performance is simulated yielding refrigerant mass

flow rate. Next, the condenser and the capillary tube are simulated[2/] and a mass flow balance is sought by comparing refrigerant mass flow rate through the compressor and capillary tube. If compared mass flows are not equal, simulation of the compressor, the condenser, and the capillary tube is redone with an unchanged refrigerant state at the compressor can inlet and a modified guess of compressor discharge pressure. Increasing this pressure reduces refrigerant mass flow rate through the compressor. Then the condenser works with this smaller mass flow rate and at a higher saturation temperature. Consequently, refrigerant reaching the expansion device inlet is at higher pressure and has more subcooling. Both factors promote greater mass flow rate through the capillary tube. Thus, increase in discharge pressure has a clear and opposite impact on mass flow rates through the compressor and thr~ugh the capillary tube and the appropriate discharge pressure can be found ,r which mass flow balance exists.

Once mass flow balance is reached, simulation of the evaporator is performed with the known refrigerant state at the evaporator exit and the refrigerant mass flow rate. Since the thermodynamic process in a capillary tube may be viewed as adiabatic, refrigerant enthalpy at the evaporator inlet should be equal to the enthalpy at the condenser outlet. If these enthalpies are not equal (enthalpy balance is not reached), a new calculation starts from the beginning with a modified guess on the refrigerant pressure at the compressor can inlet. From the condenser operation point of view, a change in compressor suction presure induces a change in refrigerant mass flow rate and modification of the condenser saturation temperature caused by the system flow balance search. These two changes have opposite effects on refrigerant enthalpy at the condenser exit, leaving it only slightly altered. On the other hand, the same change of compressor suction pressure has a strong effect on refrigerant enthalpy at the evaporator inlet by a change in the evaporator saturation temperature and refrigerant mass flow rate, both working to change the enthalpy in the same direction. Thus an appropriate suction pressure at the compressor inlet can always be found for which an enthalpy balance exists.

Once enthalpy and pressure balances are established, two out of three refrigerant parameters guessed at the beginning are determined. However, these two parameters, compressor suction and discharge pressure, are only as good as the third guessed parameter, the refrigerant superheat at the compressor inlet, which has not yet been verified. For this parameter verification, the refrigerant mass balance in the system is used. Specifically, a refrigerant mass inventory is made. It is based on refrigerant states in the system which are found to satisfy enthalpy and pressure balances with asumed vapor superheat at the compressor can inlet. Then the amount of refrigerant obtained from mass inventory calculations is compared to the actual refrigerant mass input (known

---

2/ Simulation of a capillary tube can be performed at this time even without precise knowledge of the evaporator inlet pressure. For a heat pump pressure operation range, capillary tube capacity is a weak function, if not independent of evaporator pressure. For the first calculation pressure at the evaporator inlet may be assumed to be the same as at the evaporator outlet. Refer to section 5.3.

as design parameter). If the amount of refrigerant calculated is smaller than refrigerant input into the heat pump, the superheat guess has to be decreased and all calculations have to be repeated from the beginning.

The logic described above is presented graphically in figure 8. Details about the above program flow chart can be found in appendix H. Refrigerant mass inventory is discussed in section 5.6.

5.2 MODELING OF A RECIPROCATING, HERMETIC COMPRESSOR

5.2.1 Compressor Operation

The compressor is mechanically the most complex component of a heat pump. A reciprocating, hermetic compressor is most commonly used in heat pump systems. A schematic of this type of compressor is shown in figure 9. The compressor consists of a shell containing an electric motor, a cylinder/piston assembly with valves and manifolds and pipes. The electric motor is coupled to the compressor eccentric. Lubricating oil is collected on the bottom of the can and is in free contact with the refrigerant.

Flow of the refrigerant is from location 3 to location 8, as marked in figure 9. Low pressure refrigerant enters the compressor can and is directed towards the electric motor to cool motor windings. Enthalpy of the refrigerant changes due to this and other heat transfer with other surrounding surfaces; namely, the compressor can, manifolds, the discharge pipe and the cylinder body. Then the refrigerant at state 4 undergoes the cylinder process, which in case of positive displacement compressors consists of: expansion through the suction valve and mixing the residual gas, compression, expansion through the discharge valve, and re-expansion of residual gas. Compressed, high temperature and high pressure refrigerant vapor leaves the compressor through the discharge manifold and discharge line after giving up some heat to the low pressure refrigerant at state 4.

Numbers marked in figure 9 identify key compressor locations and corresponding refrigerant states. Even during steady state operation it is difficult to talk about steady parameters in the compressor can, where, pressure changes in a manner of pulses. This pulsation is initiated by the periodic compression and suction processes and valve behavior. Because a certain pressure difference is needed for valve opening, pressure in the cylinder at the end of compression is considerably above discharge manifold pressure. Similarly, pressure during intake falls below suction manifold pressure. Particularly strong pressure peaks are observed in case of spring equipped valves. These pressure differences vary from compressor to compressor because of valve and manifold design, but also vary for the same compressor with compressor speed, compression pressure ratio, refrigerant, and mass flow rate.

Since processes taking place in a compressor are dynamic in nature, the most correct way of modeling a compressor would require dynamic simulation of valve motion, cylinder-manifold pressure interaction, and cylinder heat transfer. Such models exist and are described in [5], [6], and [7]. However, these models

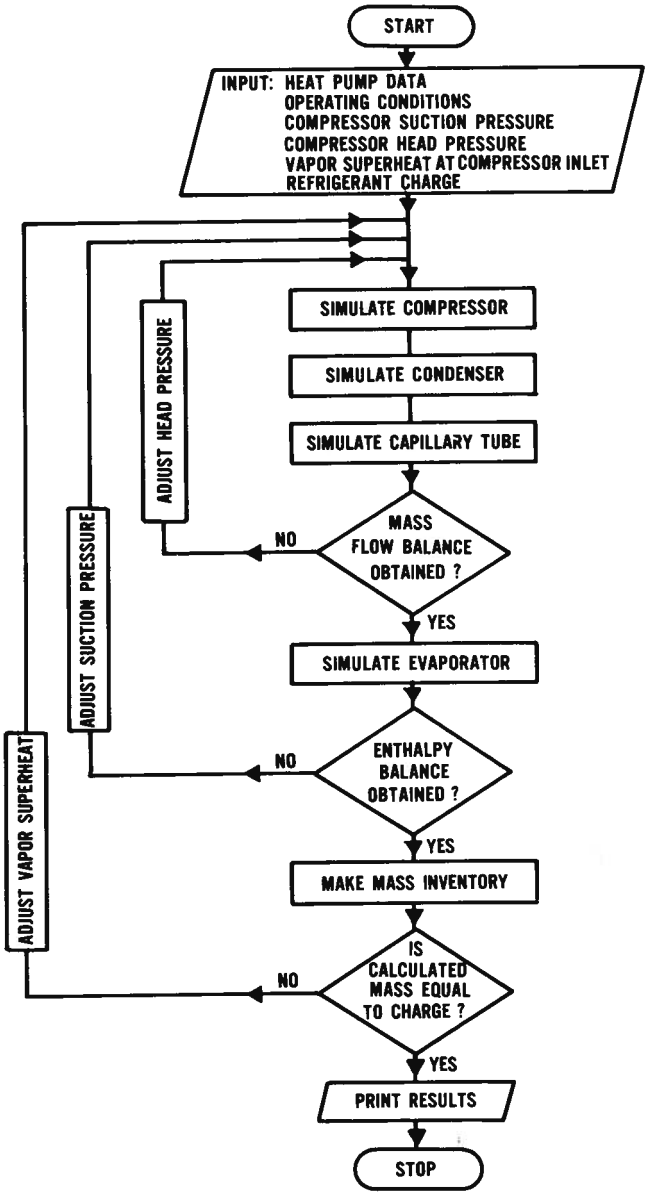

Figure 8. Overall logic of a program simulating a heat pump with constant flow area expansion device

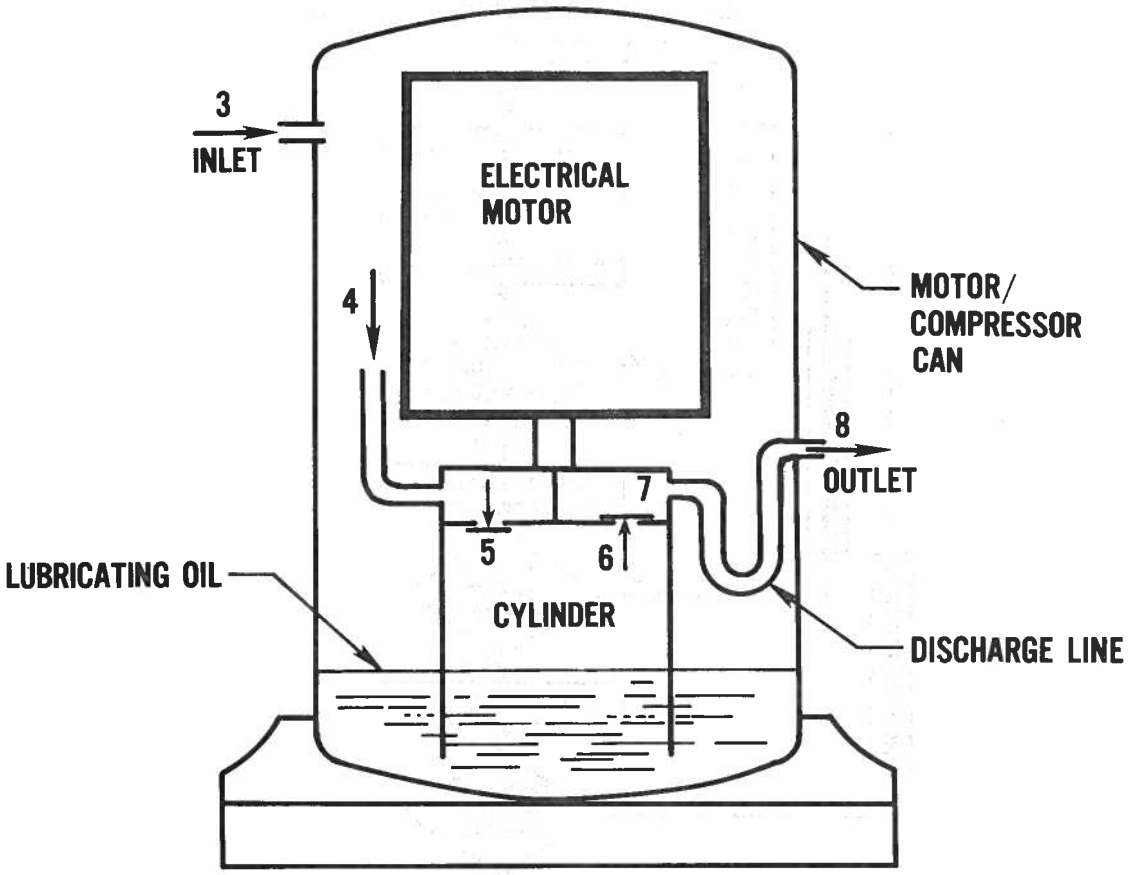

Figure 9. Schematic of a hermetic compressor

usually require some very detailed experimental data or design information, not necessarily readily available for the prospective user of a heat pump simulation program. That is why a relatively simpler, but certainly still adequate compressor model from [3] was adopted for this study.

5.2.2 Theory and Governing Relations

Several assumptions are made for model formulation. The basic assumption is that the highly dynamic process in the compressor results in steady gas parameters through the can. Pressure and temperature in the cylinder and in suction and discharge manifolds are assumed to have constant values. Refrigerant is considered to have uniform thermodynamic properties throughout the space assigned to the particular location. Refrigerant flow through the compressor is assumed to be one-dimensional, so one-dimensional steady flow equations can be used. Though the model does not simulate valve dynamic behavior, it allows for valve representation by a steady difference between manifold and cylinder pressures.

In order to derive equations governing compressor balances, the thermodynamic irreversibilities taking place in the hermetically sealed compressor have to be identified. These losses can be put into four categories:

1. Those associated with incomplete conversion of electric energy into a mechanical energy available for vapor compression.

2. Those associated with non-isentropic conversion process inside the cylinder.

3. Those due to heat transfer at different locations.

4. Those due to pressure drop at difference locations.

All of these losses contribute to the overall compressor efficiency on the order of 60 percent (first law basis) and have to be considered in the modeling effort.

Conversion of Electrical to Mechanical Energy

Electric energy is supplied to an electric motor to be converted into mechanical work. This conversion has losses due to windage, friction, winding resistance, and hysteresis, which are accounted for by a motor efficiency η_e. By definition

$$\eta_e = \frac{W_e}{E} \tag{2}$$

where E = electric power input
W_e = mechanical power output

Electric motor efficiency, η_e, depends on load and is customarily given as a function of the fraction of actual mechanical power output to the maximum power output. In heat pumps with usual power requirements below 5 hp, single phase electric motors are mostly used. They are permanent split-capacitor or capacitor-start capacitor-run types. A typical efficiency versus load curves for a permanent split-capacitor 2 pole electric motor is shown in figure 10 [14].

The electric motor is coupled to the compressor eccentric. Moving compressor parts experience friction and a power loss accounted for by the compressor mechanical efficiency η_m. By definition

$$\eta_m = \frac{W_c}{W_e} \tag{3}$$

where W_c = mechanical power available for compression

A common value of compressor mechanical efficiency falls in range of 0.95 to 0.98.

Compression Process

A simplified indicator diagram is shown in figure 11. It shows assumed constant suction and discharge pressures in a cylinder. In modeling the cylinder process, both compression and re-expansion processes are assumed to be polytropic with the same polytropic index, n, following the equation:

$$P \cdot v^n = \text{const} \tag{4}$$

where n = polytropic index
P = pressure
v = refrigerant vapor specific volume

Since constant pressure and temperature are assumed during the discharge process, this implies no change in specific volume between points "c" and "d" (figure 11); consequently, the compression and re-expansion polytropic curves will coincide. This further means, that the net work required for compression of the residual gas is zero.

The refrigerant enthalpy increase during polytropic compression, $i_6 - i_5$ (refer to figure 5), can be evaluated by the equation derived from the expressions for isentropic and polytropic work of compression at the same compression ratio. Equating these expressions results in the equation:

$$i_6 - i_5 = (i_{6s} - i_5)\frac{\frac{n}{n-1}}{\frac{\gamma}{\gamma-1}} \frac{\left(\frac{P_6}{P_5}\right)^{\frac{n-1}{n}} - 1}{\left(\frac{P_6}{P_5}\right)^{\frac{\gamma-1}{\gamma}} - 1} \tag{5}$$

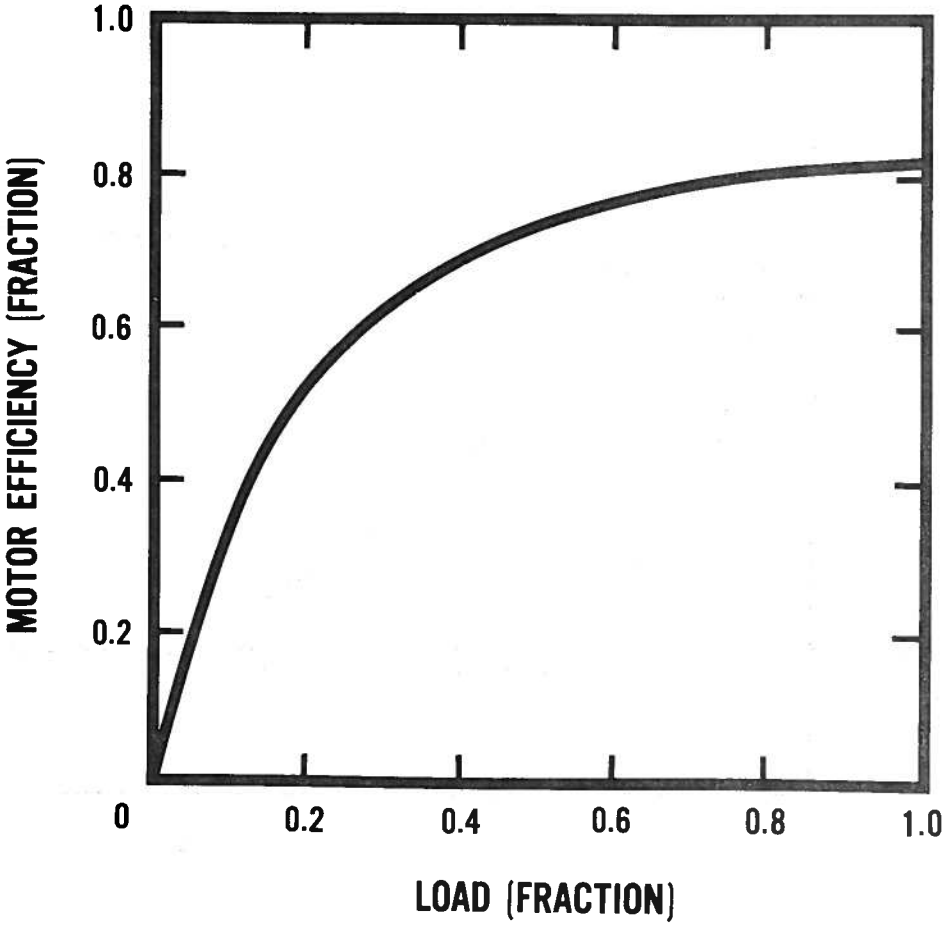

Figure 10. Typical efficiency versus load curve for a permanent split-capacitor 2 pole electric motor [4]

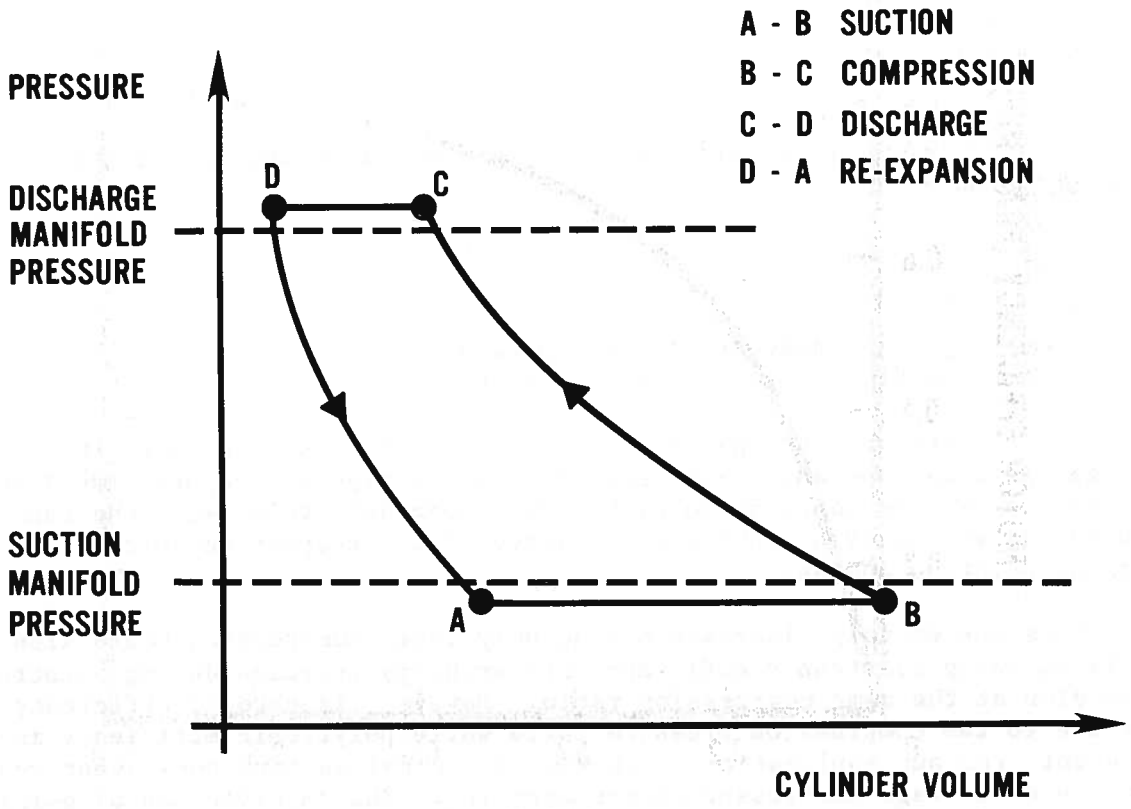

Figure 11. Simplified indicator diagram for a reciprocating compressor

where i_5 = refrigerant enthalpy before compression
i_6 = refrigerant enthalpy after compression
i_{6s} = refrigerant enthalpy after isentropic compression, defined by pressure P_6 and entropy s_5
n = polytropic index
P_5 = suction pressure
P_6 = discharge pressure
γ = isentropic index

The isentropic index, γ, and the polytropic index n, are related by the polytropic efficiency of the compressor:

$$\eta_p = \frac{\frac{\gamma - 1}{\gamma}}{\frac{n - 1}{n}} \tag{6}$$

The isentropic index, γ, equals the ratio of specific heats, as in the following formula:

$$\gamma = \frac{Cp}{Cv} \tag{7}$$

where Cp = specific heat at constant pressure
Cv = specific heat at constant volume

The specific heats of ideal gases are constant, thus the isentropic index of an ideal gas is also constant. For real gases as refrigerant vapors, specific heats vary along the compression path. To accommodate this fact, the isentropic index can be evaluated by taking the average of the respective specific heat ratios at points 5 and 6s.

The refrigerant enthalpy increase during polytropic compression could also be calculated using isentropic efficiency and enthalpy increase during isentropic compression at the same compression ratio. However, isentropic efficiency is sensitive to the compression pressure ratio while polytropic efficiency is more consistent from one application to another and provides more consistent representation of average compressor performance [8]. The imperfection of using isentropic efficiency may be traced to the general thermodynamic relation:

$$\left(\frac{\partial i}{\partial s}\right)_P = T \tag{8}$$

where i = enthalpy
P = pressure
s = entropy
T = temperature

requiring that pressure lines diverge on a Mollier chart.

The refrigerant mass flow rate pumped by a compressor can be calculated by the following formula:

$$m_r = \frac{60 \cdot RPM \cdot Vs}{v_5} \eta_v \tag{9}$$

where m_r = refrigerant mass flow rate
RPM = compressor speed (number of revolutions per minute)
Vs = compressor swept volume per revolution
v_5 = refrigerant specific volume at piston before compression
η_v = volumetric efficiency

The RPM of a compressor is equal to that of an electric motor and is a function of load on the motor. A typical speed (RPM) versus load curve for a permanent split-capacitor 2-pole elctric motor is shown in figure 12.

With assumptions stated so far for the compression and re-expansion processes, the following formula for volumetric efficiency of a compressor can be derived:

$$\eta_v = C_c \left[1 - C_e \left(\frac{P_6}{P_5}\right)^{\frac{1}{n}} - 1\right] \tag{10}$$

where C_c = correction factor for leakage from piston, valves and for throttling effect, assumed to be 0.96, [9]
C_e = clearance volume, in fraction of stroke volume

Heat Transfer Relations

Electrical energy supplied to an electric motor is in part transferred to the refrigerant and in part is dissipated to the compressor environment. This compressor heat balance can be expressed by the following equation:

$$E + m_r (i_3 - i_8) - Q_{C,A} = 0 \tag{11}$$

where E = electric power input
i_3, i_8 = refrigerant enthalpy at respective locations (refer to figure 9)
$Q_{C,A}$ = rate of heat rejected to ambient air

Reference is made to figure 9, where key locations of refrigerant in the hermetic compressor are marked. In order to solve the compressor heat balance represented by equation (11), the following heat transfer losses are considered in the compressor model:

1. Heat transfer between the compressor can and ambient air, $Q_{C,A}$

2. Heat transfer between the refrigerant in the compressor can and the compressor can, $Q_{4,C}$

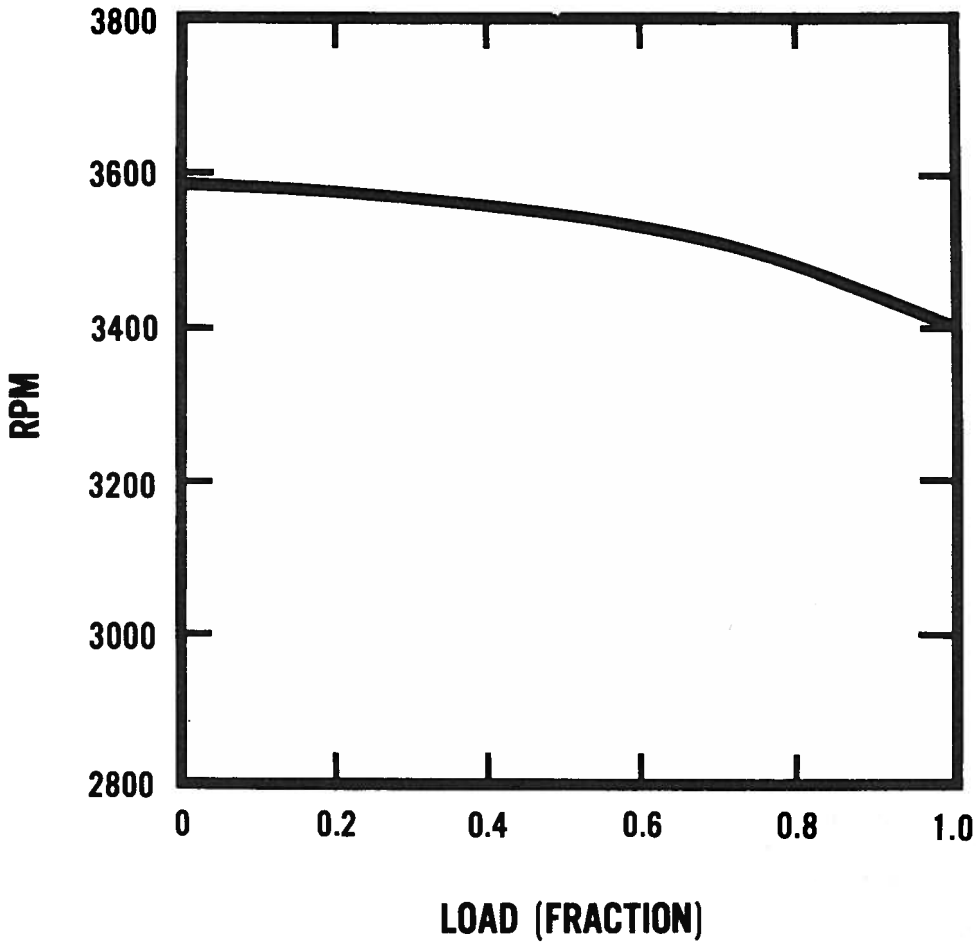

Figure 12. Typical speed (RPM) versus load curve for a permanent split-capacitor 2 pole electrical motor [4].

3. Heat transfer between the inlet refrigerant and the suction manifold and valve, $Q_{4,5}$

4. Heat transfer between the discharge refrigerant and the discharge valve and manifold, $Q_{6,7}$

5. Heat transfer between the refrigerant in the compressor can and the refrigerant in the discharge line, $Q_{7,8}$

According to general heat transfer equation of Péclet:

$$Q = U \cdot A_h \cdot \Delta T \tag{12}$$

The heat transfer rate, Q, for a given temperature difference, ΔT, can be calculated if the overall coefficient of heat transfer, U, and heat transfer area, A_h, are known. The heat transfer between the compressor can and ambient air (item 1) is governed by free convection (radiation is negligible). A simple correlation is available to estimate the free convection heat transfer coefficient in air [10], i.e.,

$$h \propto \Delta T^{0.333} \tag{13}$$

where h = convection heat transfer coefficient
ΔT = temperature difference between air and heat transfer surface

Hence, the heat transfer rate between ambient air and the compressor shell, $Q_{C,A}$, can be calculated by the equation:

$$Q_{C,A} = CQ_{C,A}(T_c - T_a)^{1.333} \tag{14}$$

where $CQ_{C,A}$ = heat transfer parameter
T_a = ambient air temperature
T_c = compressor shell temperature

Heat transfer inside the compressor shell between the shell and refrigerant vapor (item 2) is governed by forced convection, for which the non-dimensional heat transfer parametric expression in terms of Nusselt, Reynolds and Prandtl numbers is in the form:

$$Nu \propto Re^{0.8} \cdot Pr^{0.333} \tag{15}$$

where $Nu = \frac{h \cdot L}{k}$ Nusselt number

$Pr = \frac{\mu \cdot Cp}{k}$ Prandlt number

$Re = \frac{G \cdot L}{\mu}$ Reynolds number

$G = \frac{m_r}{A}$, refrigerant mass flux

L = characteristic dimension

k = refrigerant thermal conductivity

μ = refrigerant dynamic viscosity

Using equation (15) the forced convection heat transfer coefficient, h, can be expressed as:

$$h = C \cdot m_r^{0.8} \cdot k^{0.667} \cdot Cp^{0.333} \cdot \mu - 0.467 \quad (16)$$

where C = constant of proportionality, a fuction of wetted surface geometry

Combining equations (12) and (16) yields the following expression for heat transfer rate between the compressor can and refrigerant:

$$Q_{4,C} = C \cdot A_h \cdot m_r^{0.8} \cdot k_4^{0.667} \cdot Cp_4^{0.333} \cdot \mu_4 - 0.467 \ (T_4 - T_c)$$

or

$$Q_{4,C} = CQ_{4,C} \cdot m_r^{0.8} \cdot k_4^{0.667} \cdot Cp_4^{0.333} \cdot \mu_4 - 0.467 \ (T_4 - T_c) \quad (17)$$

where $CQ_{4,C}$ = heat transfer parameter

Obviously, heat transfer rates $Q_{C,A}$ and $Q_{4,C}$ are equal. Derivations of equations for the heat transfer rates between the inlet refrigerant and the suction manifold and valve, $Q_{4,5}$, and between the discharge refrigerant and the discharge manifold valve, $Q_{6,7}$, is similar to the derivation just performed for $Q_{4,C}$, since in these two cass heat transfer is also by forced convection. Resulting expressions for the heat transfer rates are:

$$Q_{4,5} = CQ_{4,5} \cdot m_r^{0.8} \cdot k_{4,5}^{0.666} \cdot Cp_{4,5}^{0.333} \cdot \mu_{4,5} - 0,467 \ (T_6 - T_4) \quad (18)$$

$$Q_{6,7} = CQ_{6,7} \cdot m_r^{0.8} \cdot k_{6,7}^{0.667} \cdot Cp_{6,7}^{0.333} \cdot \mu_{6,7} - 0.467 \ (T_7 - T_4) \quad (19)$$

Heat transfer between refrigerant in the compressor can and refrigerant in the discharge line (item 5) is modeled as forced convection heat transfer between the fluids separated by a barrier non-resistant to heat flow. Assuming that the temperature of refrigerant in the shell does not change (as a result of other heat transfers in the can and mixing) and applying the logarithmic mean temperature difference, the following expression for heat transfer rate $Q_{7,8}$ can be derived:

$$Q_{7,8} = CQ_{7,8} \cdot m_r^{0.8} \frac{a1}{a2 + a3} (T_7 - T_8) / \ln \frac{T_7 - T_4}{T_8 - T_4} \quad (20)$$

where $a1 = (Cp_4 \cdot Cp_{7,8})^{0.333}(k_4 \cdot k_{7,8})^{0.667}$

$a2 = \mu_4^{0.467} \cdot Cp_{7,8}^{0.333} \cdot k_{7,8}^{0.667}$

$a3 = \mu_{7,8}^{0.467} \cdot Cp_4^{0.333} \cdot k_4^{0.667}$

Subscripts 3 through 8 refer to refrigerant key locations in the compressor as per figure 9. If separated by a comma, the average value is implied.

The heat transfer to/from the following refrigerant changes the refrigerant enthalpy as per equation:

$$Q = m_r \cdot \Delta i \tag{21}$$

where Δi = refrigerant enthalpy change

Combining equations (18), (19), (20), and (21) yields the following expressions for the refrigerant enthalpy change during flow between respective locations of the compressor:

$$i_5 - i_4 = CQ_{4,5} \cdot k_{4,5}^{0.667} \cdot Cp_{4,5}^{0.333} (T_6 - T_4)/(m_r^{0.2} \cdot \mu_{4,5}^{0.467}) \tag{22}$$

$$i_6 - i_7 = CQ_{6,7} \cdot k_{6,7}^{0.667} \cdot Cp_{6,7}^{0.333} (T_7 - T_4)/(m_r^{0.2} \cdot \mu_{6,7}^{0.466}) \tag{23}$$

$$i_7 - i_8 = CQ_{6,7} \frac{a1}{a2 + a3} (T_7 - T_8)/(m_r^{0.2} \cdot \ln \frac{T_7 - T_4}{T_8 - T_4}) \tag{24}$$

where a1, a2, a3 are as in equation (20)

Derived heat transfer relations contain heat transfer parameters $CQ_{C,A}$, $CQ_{4,5}$, $CQ_{6,7}$, and $CQ_{7,8}$. These parameters are functions of heat transfer surface geometry mainly and have to be found empirically. If required laboratory test data of a given compressor are not available, typical compressor test data can be used. A large number of experimental compressor measurements have been published. The summary of these data and a list of references can be found in [1].

Pressure Drop Relations

Total pressure drop ΔP_{tot} experienced by a flowing fluid results from pressure drops due to friction, momentum change, and gravity, i.e.,

$$\Delta P_{tot} = \Delta P_{friction} + \Delta P_{accel} + \Delta P_{gravity} \tag{25}$$

Pressure drop due to gravity in the hermetic compressor may be disregarded based on an order of magnitude analysis. On the same grounds, pressure drop of flowing refrigerant between certain compressor locations may be attributed to either viscous effect or dynamic effect.

Pressure drop due to the dynamic effect, ΔP_{accel}, is proportional to velocity head, i.e.,

$$\Delta P_{accel} \propto \rho \cdot V^2 \tag{26}$$

which can be written, using the continuity equation:

$$\Delta P_{accel} = CP \cdot m_r^2/\rho \tag{27}$$

where CP = pressure drop parameter
m_r = refrigerant mass flow rate
V = refrigerant velocity
ρ = refrigerant density

The relation for the pressure drop due to viscous effect, $P_{friction}$, can be derived from the classical Fanning equation for pressure drop in a tube:

$$\Delta P_{friction} = 2f \cdot \rho \cdot V^2 \cdot L/D \tag{28}$$

where f = friction factor
D = tube diameter
L = tube length

The friction factor, f, in the equation above is approximately proportional to the Reynolds number to the -0.2 power. Considering this fact and applying the equation of continuity, equation (28) becomes:

$$\Delta P_{friction} = CP \cdot \mu^{0.2} \cdot m_r^{0.8}/\rho \tag{29}$$

Pressure drop of the refrigerant in the compressor can is modeled by evaluating individual pressure drops between refrigerant key locations as per figure 9. Based on equations (27) and (29), and attributing pressure drop between particular compressor locations either to the viscous or friction effect, the following pressure drop relations are proposed:

$$P_3 - P_4 = CP_{3,4} \cdot m_r^2/\rho_{3,4} \quad \text{for compressor can inlet} \tag{30}$$

$$P_4 - P_5 = CP_{4,5} \cdot m_r^2/\rho_{4,5} \quad \text{for suction manifold and valve} \tag{31}$$

$$P_6 - P_7 = CP_{6,7} \cdot m_r^2/\rho_{6,7} \quad \text{for discharge valve and manifold} \tag{32}$$

$$P_7 - P_8 = CP_{7,8} \cdot m_r^{1.8} \cdot \mu_{7,8}^{0.2}/\rho_{7,8} \quad \text{for discharge line} \tag{33}$$

Pressure drop parameters $CP_{3,4}$, $CP_{4,5}$, $CP_{6,7}$, and $CP_{7,8}$ have to be found experimentally for a given compressor or can be calculated using test data for a similar compressor. For sources of such data, the reader may refer to [1].

Equations derived in this section make it possible to carry out an energy balance of a hermetic compressor solving it in an iterative process for electrical energy input, for heat lost to the ambient air, and for refrigerant parameters in compressor key locations. The variety of designs of refrigerant flow passages in the compressor caused the modeling of pressure drop and heat transfer

to be done in an approximate manner in this general compessor model. In spite of several assumptions that were made to simplify the modeling process and reduce computing time, the model still retains sufficient details of the underlying physical principles to allow designers to determine which specific changes in the compressor design lead to increased efficiency of the compressor and the heat pump system.

5.3 MODELING OF A CONSTANT FLOW AREA EXPANSION DEVICE

A constant flow area expansion device, as used in heating/air conditioning systems, is commonly called a capillary tube or a refrigerant flow restrictor. Usually it is a small bore tube of length as short as one-half inch up to a few feet, connecting the outlet of the condenser (or a liquid line) to the inlet of the evaporator. The main task of the constant flow area expansion device is to maintain the minimum pressure at the condenser at which all the flowing refrigerant can condense. Many researchers have investigated flow through a capillary tube and a bibliography on the subject can be found in [4]. The objective of this research was to explain capillary tube phenomena and develop a mass flow rate prediction method. None of the metods found in the literature were computer oriented or could analyze both single-phase and two-phase flow in the restrictor. Thus there was a need to develop a more comprehensive capillary tube routine that could be incorporated into a heat pump simulation program.

5.3.1 Available Capillary Tube Performance Data

Capillary tube is a traditionally accepted name for a constant flow area expansion device used in heat pump systems. This name is adequate and misleading since for tube diameters in the neighborhood of 1/16 of an inch, capillary forces are negligible for the task the capillary tube performs. The pressure drop consists practically of:

- loss due to sudden contraction at the entrance
- loss due to flow in the tube
- loss due to sudden enlargement at the exit to the evaporator

The flow of refrigerant through a constant bore tube is more complex than the geometric simplicity of the device would first indicate. The pressure and temperature distribution along a typical capillary tube is shown in figure 13. Bolstad's description of the flow is as follows:

> At the entrance to the tube, section 0-1, there is a slight pressure drop which was usually unreadable on the gages. From point 1 to point 2 the pressure drop is linear. In the portion of the tube 0-1-2 the refrigerant is entirely in the liquid state and at point 2 the first buble of vapor forms. From point 2 to the end of the tube the pressure drop is not linear, the pressure drop per unit length increasing as the end of the tube is approached. For this portion of the tube, both the saturated liquid and saturated vapor phases are present, the percent and volume of vapor increasing in the direction of flow . . . .

> With a saturation temperature scale corresponding to the pressure scale superimposed along the vertical axis, it is possible to plot the observed temperatures in a more meaningful way than if a uniform temperature scale were used. The temperature is constant for the first portion of the tube 0-1-2. At point 2, the presence has dropped to the saturation pressure corresponding to this temperature. Further pressure drop beyond point 2 is accompained by a corresponding drop in temperature, the temperature being saturation temperature corresponding to the pressure. As a consequence, the pressure and temperature lines coincide from point 2 to the end of the tube [11].

The point of the tube where the first bubble forms is called a bubble point or a flash point. The pressure at the point is called the flash pressure. Bolstad also presented an analytical method of solution for adiabatic flow through the capillary based on the Fanno flow theory.

Mikol [12] performed a capillary tube investigation from which his conclusions can be summarized as follows:

- Fluid flow through small bore tubes conforms to continuum flow as established for large bore tubes and pipes.

- the friction factor correlation of Moody and any others consistent with Moody's correlation [13] is applicable to single-phase flow in small bore tubes.

- the phenomena of metastability, persistence of the liquid state to pressure less than the saturation pressure corresponding to its local temperature, has been found to occur.

- the phenomenon of choked flow in two-phase flow occurs in the same way and for the same reasons as in the case of gaseous flow. Sonic velocity occurs at the tube exit.

One of Mikol's findings, existence of superheated liquid in a small portion of a tube was not observed by Bolstad [11]. However, it was reported by Cooper [14] and Rezk [15]. Investigators have found that delayed evaporation is affected by initial disturbances and flow agitation, but there is not enough data in the current literature to assess all the factors promoting/eliminating this phenomena and making it possible to consider metastability in a capillary tube model at this time.

Refrigerant mass flow rate through the capillary tube always increases with an increase of inlet pressure. It also increases with a decrease in external outlet pressure down to a critical pressure below which the flow does not change. Sensitivity of the flow to external outlet pressure decreases significantly at low outlet pressure before the flow is choked.

Pressure and temperature distributions along a capillary tube as shown in figure 13 occur at design operating conditions of a long (a few feet) capillary. Part of the capillary is filled with flowing liquid, while two-phase flow exists in

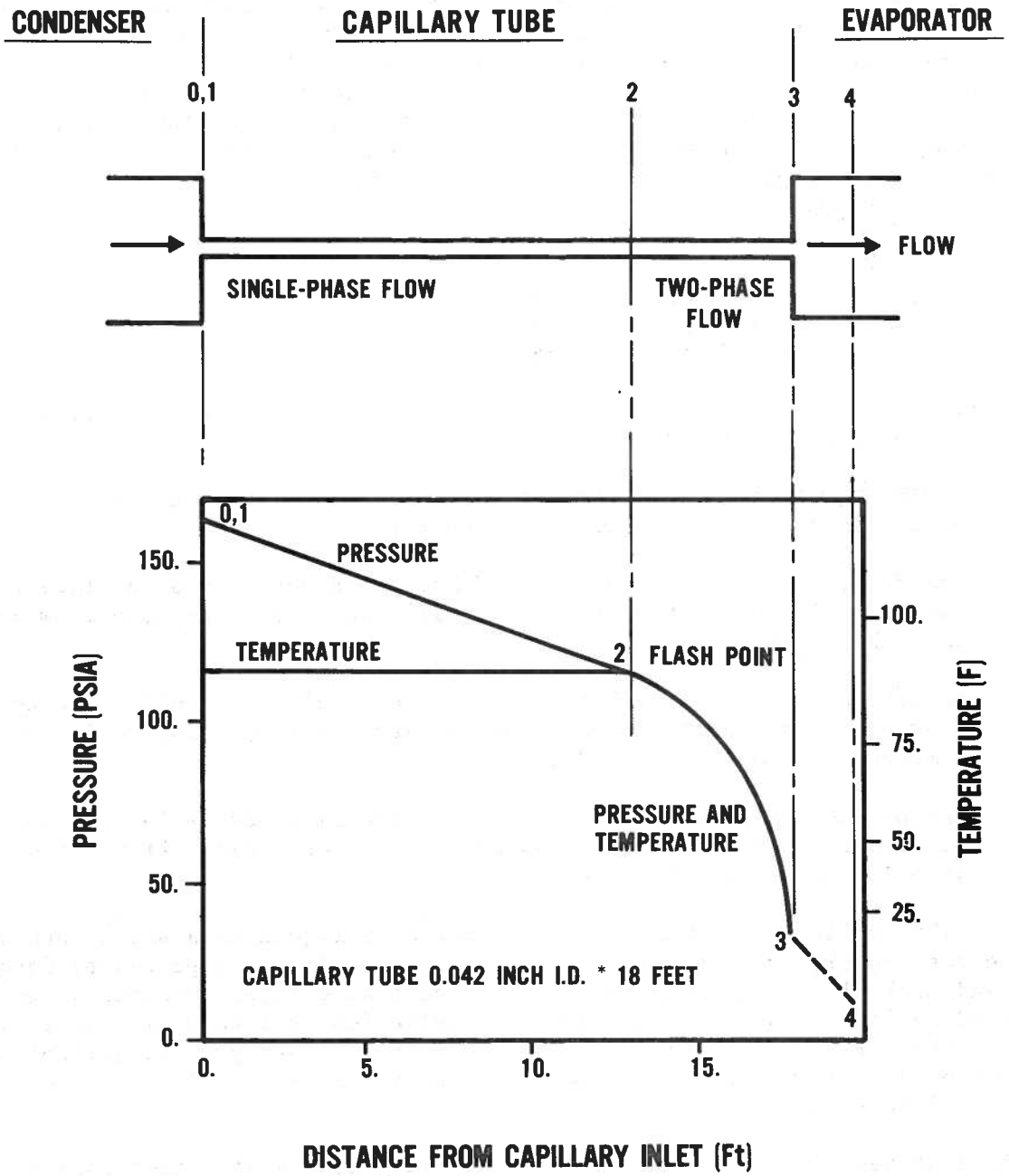

Figure 13. Pressure and temperature distribution along typical capillary tube [11]

the other part. However, there are also other possible modes of operation, i.e., with only two-phase flow in the capillary (the case of incomplete condensation in the condenser) or with only liquid flow (the case of a short restrictor). All these cases are observed in practice and have to be simulated by a general model of the constant flow area expansion device.

Based on the experimental evidence and the theory of large tube fluid mechanics, the following assumption were set up for model formulation:

1. The capillary tube is a straight, horizontal, constant inner diameter tube

2. Flow in the capillary is one-dimensional and homogeneous

3. Flow in the capillary is adiabatic

4. Flow resistance in the capillary tube can be subdivided into

   a. resistance due to the entrance effect

   b. resistance due to flow in a tube which consists, in the general case, of single-phase liquid flow resistance from the entrance to the flash point, and two-phase mixture flow resistance in the rest of the tube. Existence of delayed evaporation phenomena is neglected. Resistance due to the exit effect is neglected as meaningless for a choked flow and insignificant for a non-choked flow [11].

5. Choked flow phenomenon for two-phase is governed by the same laws as for single-phase flow, and can be modeled accordingly.

5.3.2 Critical Flow in a Capillary Tube

Refrigerant mass flow rate through a given capillary tube will depend on the inlet refrigerant state and on pressure that will be established at the tube outlet. This pressure may equal the evaporator pressure or may have a higher value if the flow is choked. Since pressure at the capillary tube exit is one of the parameters affecting the flow, it has to be known for proper refrigerant mass flow rate prediction.

The assumption that the flow in the capillary is one-dimensional and homogeneous enables the two-phase flow in the capillary to be treated as single-phase flow with uniform properties at any cross-section of the flow and allows use of the single-phase, one-dimensional form of the governing equations as presented in figure 14, 15, and 16.

Adiabatic flow through a capillary tube is a classical example of so called Fanno flow; adiabatic flow with friction in a constant area duct. The energy equation for such flow has the form:

$$di + V \cdot dV = 0 \quad \text{or} \quad i_o = i + V^2/2 = \text{const} \tag{34}$$

which, when combined with the equation of continuity yields:

$$i_o = i + \frac{m_r}{A} \cdot v^2/2 = i + G^2 \cdot v^2/2 \qquad (35)$$

where A = tube cross-sectional area

$G = \frac{m_r}{A}$, refrigerant mass flux

i = refrigerant enthalpy
i_o = refrigerant stagnation enthalpy
m_r = refrigerant mass flow rate
V = flow velocity
v = refrigerant specific volume

Graphical representation of equation (35) on the enthalpy-entropy diagram, as shown in figure 17, is called a Fanno line. Fanno flow as an irreversible adiabatic process, can sequentially exist only in the direction of increasing entropy. The upper branch of the Fanno line corresponds to subsonic, accelerating flow while the lower branch is the supersonic, decelerating flow. Both flows tend towards point C where the sonic velocity is reached.

The Fanno line implies that fluid cannot reach the velocity of sound inside a constant area duct, because, if this happened, further flow in the duct would have to be associated with a decrease of entropy, as per figure 17, and that would be in violation of the Second Law of Thermodynamics. Thus, the only location of a tube at which sonic velocity can be reached is the tube exit, and choking will never occur inside the capillary regardless of external outlet pressure. Evaluation of the critical pressure for two-phase Fanno flow is discussed in appendix E.

It is intuitively felt, based on compressible gas theory, that if the critical pressure is greater than the pressure in an evaporator, the critical pressure will be established at the capillary tube outlet. However, it is not clear what pressure would actually exist at the end of a capillary which is fed with a subcooled liquid, if the calculation choking pressure is higher than the saturated liquid pressure resulting from the liquid temperature[3/]. Before this is explained, some information on sonic velocity phenomena is reviewed.

The velocity of sound is calculated by the formula:

$$a = \left(\frac{\partial P}{\partial \rho}\right)_s^{0.5} \qquad (36)$$

3/ It is assumed here, for discussion purposes only, that choking pressure can be found independently from refrigerant mass flow rate and then mass flow rate can be calculated. In fact, mass flow rate and choking pressure (and other factors of operation) are interrelated and have to be found simultaneously in an iterative process.

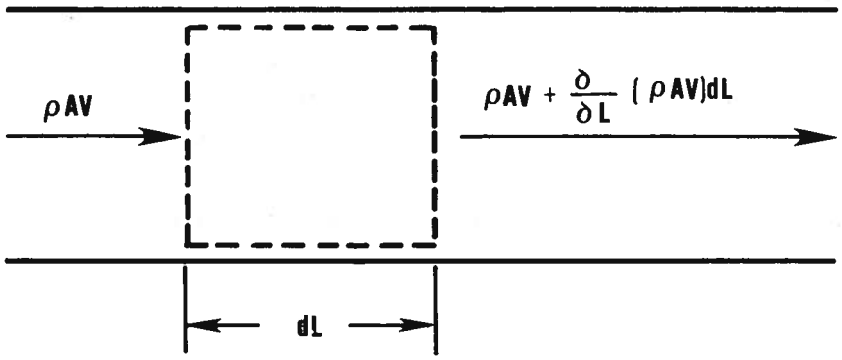

CONTINUITY EQUATION: $d(\rho V) = 0$

Figure 14. Mass balance for an element of fluid in one-dimensional steady flow in a constant area duct

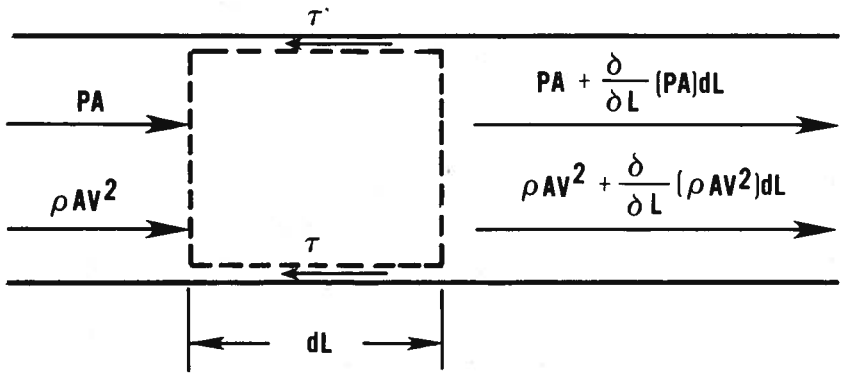

MOMENTUM EQUATION: $AdP + \rho AVdV + \tau SdL = 0$

Figure 15. Momentum balance for an element of fluid in one-dimensional steady flow in a horizontal, constant area duct

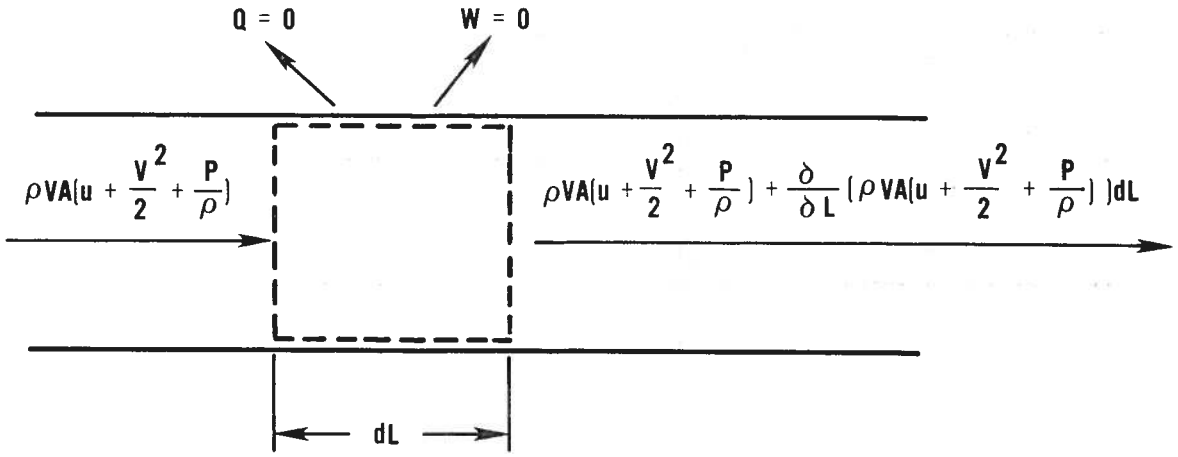

Figure 16. Energy balance for an element of fluid in one-dimensional adiabatic, steady flow in a horizontal, constant area duct

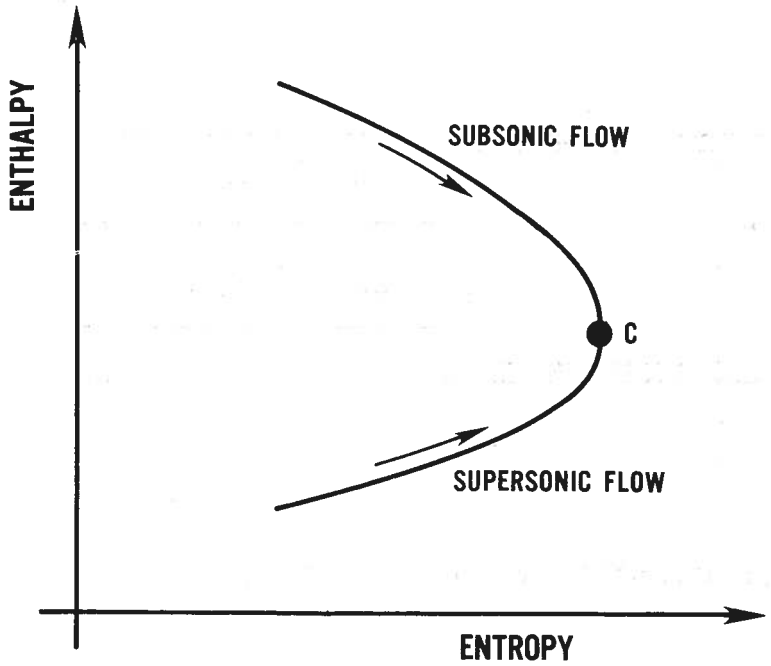

Figure 17. Fanno line

where a = velocity of sound
P = pressure
ρ = density
s = entropy

For a liquid, in which the density is hardly affected by pressure, the velocity of sound assumes a very high value, typically in the range of 5000 ft/s. Liquid flow in capillary tubes is never accelerated to such high velocities. However, the velocity of sound for a two-phase state containing a small amount of vapor is drastically smaller, e.g., sonic velocity of two-phase flow of quality less than 0.0001 and temperature of 100°F is on the order of 1 ft/s. Sonic velocity increases with temperature and quality and assumes a value of about 500 ft/s close to the critical state. Thus, the velocity of sound in a liquid is much different than in the two-phase state and a sharp discontinuity in sonic velocity takes place at the boundary of single and two-phase flow [16].

In the case of a capillary tube working at design conditions, there is a single-phase liquid flow in the beginning part of the tube and single component two-phase mixture flow in the latter tube portion. Though there is basically one substance flowing, the relation between pressure and density along the path of flow will be different for each part of the flow in the tube. Theoretically, a separate Fanno line could be drawn for each flow, with an intersection point corresponding to a flash point. Also, two sonic velocities could be considered, but a limitation of sonic velocity in the liquid is disregarded as it is too high to be reached in a capillary tube under any operational conditions.

Consider several capillary tubes of the same bore but different lengths. All the capillaries receive subcooled liquid at the same condition and are working at the same pressure in the evaporator. The various possible flows are shown in figure 18. If a capillary tube is sufficiently long (a), it will be able to realize a pressure drop down to the evaporator pressure and choking will not occur. With a shorter capillary tube such as (b) and (c), the mass flow rate is greater, and the critical pressure which is established at the tube exit, exceeds the pressure in the evaporator. Tube (d) has the length at which the critical pressure equals the flash pressure. The critical pressure in the case of tube (e) is greater than the flash pressure and the latter is established at the tube exit due to the flash that will occur from the sudden expansion. Thus, any tube shorter than tube (d) will have flash pressure at the exit. To prove this last case, which is least evident, other flow situations than that proposed must be considered. First, eliminated the possibility of pressure at the tube exit being greater than the flash pressure because otherwise it would imply the liquid is choked at other than its critical pressure, which is physically impossible. Another alternative is to assume that the liquid reaches saturation pressure within the tube and changes into a two-phase mixture. With the two-phase mixture critical pressure being higher than saturation pressure, it would mean a change from single-phase subsonic flow into two-phase supersonic flow. Such flow is also impossible since it would require the flow to experience a decrease in quality in its progress and would be converted back to liquid flow immediately. The liquid flow also could not proceed any further because vapor bubbles would form. Thus the only possible situation for flow

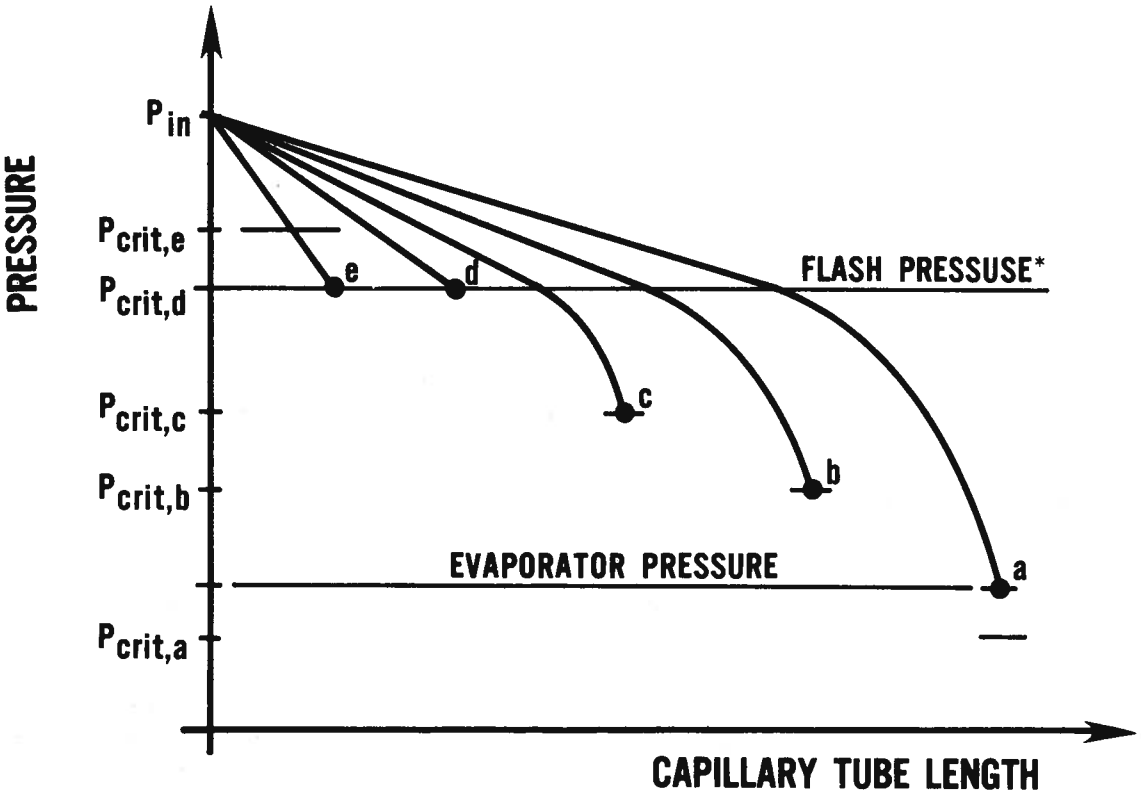

* Actual flash pressure is not constant. It increases slightly with capillary tube length.

Figure 18. Pressure distribution along different length capillary tubes at the same operating conditions

with the critical pressure greater than the liquid saturation pressure is to be choked at the tube exit where the flow is at the liquid saturation pressure.

5.3.3 Model Formulation

Refrigerant flow from the liquid line into the capillary tube experiences a pressure drop due to sudden contraction. This pressure drop consists of an acceleration loss and entrance friction loss and is usually expressed by a decrease in the Bernoulli head and a contraction coefficient referred to the kinetic energy of the flow in the section of smaller flow area:

$$\frac{P_0 - P_1}{\rho_{0,1}} + \frac{V_0^2 - V_1^2}{2} = K \frac{V_1^2}{2} \tag{37}$$

Subscripts in eq. (37) refer to sections shown in figure 13. Combining with the equation of continuity, the above can be rearranged to:

$$P_0 - P_1 = \Delta P = (1 + K)\rho_{0,1} \cdot \frac{V_1^2}{2} \tag{38}$$

The contraction coefficient, K, given in the literature is stricly empirical and is represented as a function of the contraction area ratio. Several sources are in disagreement about its value. The value of K = 0.15, used here is from a derivation based on Kay's general formula [17]. It was calculated for a normal range of contraction area ratios for capillary tubes with slightly beveled entrances.

The equation of motion for steady flow in a constant cross-section area pipe has the following form:

$$\rho \cdot A \cdot dV + A \cdot dP + \tau \cdot S \cdot dL = 0 \tag{39}$$

The skin friction coefficient, τ, can be expressed in terms of the friction coefficient, f, and the velocity head:

$$\tau = \frac{1}{2} f \cdot \rho \cdot V^2 \tag{40}$$

The flow velocity term, V, can be eliminated by means of the equation of continuity:

$$d(V \cdot \rho) = 0 \tag{41}$$

Substituting and rearranging; the equation of motion assumes the following form:

$$\left(\frac{A}{m_r}\right)^2 \cdot \int_{P_i}^{P_{i+1}} \rho \cdot dP + \frac{2}{D} \cdot \int_{L_i}^{L_{i+1}} f \cdot dL + \ln \frac{\rho_i}{\rho_{i+1}} = 0 \tag{42}$$

As discussed before, flow in a capillary tube, in the general case, can be subdivided into two parts separated by a flash point: the liquid flow part and the two-phase mixture part. The same equation will be applicable for both flows through in the case of liquid flow, it can be simplified on grounds of incompressibility. In fact, it reduces to the Fanning pressure drop formula in the following form:

$$\Delta P = \frac{2f \cdot G^2 \cdot L}{\rho \cdot D} \tag{43}$$

where the friction factor, f, can be evaluated by the empirical formula:

$$f = 0.046 \cdot Re^{-0.2} \tag{44}$$

For the two-phase mixture flow, equation (42) has to be solved in its full form. This was done by Whitesel, [18] and [19], but with significant over-simplified approximations for refrigerant properties. In solving equation (42), difficulty arises with evaluating the first term because it depends directly on the pressure-density relation along the path of flow. However, the relation can be obtained by considering the adiabatic flow case. The specific volume at a given pressure can be expressed in terms of the property values for saturated liquid and vapor and in terms of quality:

$$v = v_L + x(v_v - v_L) \tag{45}$$

where v = specific volume
x = quality
Subscripts L and V are for liquid and vapor, respectively

The quality of the flow in the Fanno path can be found as explained in appendix E. Thus integration of refrigerant density over a given pressure interval can be done numerically. Still another problem is faced in evaluating the second term of equation (42), which includes a two-phase friction factor as a function of tube length. Erth [20] made an effort to correlate two-phase average friction factor in a capillary tube. His regression analysis, based on four sets of data from four different experiments, yielded the following correlation for a two-phase flow mean friction factor, f_m, as a function of the inlet conditions only:

$$f_m = \frac{0.775}{Re^{0.5}} \exp[(1 - x_i^{0.25})/2.4] \tag{46}$$

where x_i = quality of refrigerant entering capillary tube

$$Re = \frac{G \cdot D}{\mu_L + x_i (\mu_V - \mu_L)} \text{, two-phase Reynolds number} \tag{47}$$

Using this mean friction factor, f_m, equation (42) may be written for the two-phase portion of the flow in the following form:

$$m_r = A \left[\frac{-\int_{P_2}^{P_3} \rho \, dP}{\frac{2}{D} f_m \cdot (L_3 - L_2) + \ln (\rho_2/\rho_3)} \right]^{0.5} \qquad (48)$$

where numbers used as subscripts denote location consistent with figure 13.

The above equations have to be solved in a highly iterative process since choking pressure, friction factor, fraction of capillary tube length with liquid and two-phase flow, and the velocity head used to correct enthlapy are functions of refrigerant mass flow rate which has yet to be found.

5.4 MODELING OF AN EVAPORATOR AND A CONDENSER

5.4.1 Modeling Methodology

There are two heat exchangers in a heat pump: an indoor coil and an outdoor coil. Both coils are made in a similar way and both serve as an evaporator or condenser depending on the heat pump opertional mode. Schematic of a typical heat pump heat exchanger is shown in figure 19. It consists of a set of finned tubes connected in a specifically designed circuit configuration. An example of the coil circuitry is illustrated in figure 20. The refrigerant is pumped through the tubing while air is forced to flow over the outside of the coil.

Heat exchanger models in the MIT and ORNL heat pump simulation programs, [1] and [2], are very similar. Coil performance calculations in these models are based on the effectiveness-NTU method for a cross-flow heat exchanger with both fluids umixed. These models can rigorously simulate only certain regular tube arrangements and are insenitive to different coil circuitry patterns. The heat exchanger models in [3] are based on the so called tube-by-tube simulation method which depends on imaginary isolation of one tube with appropriate fin surfaces from the coil assembly and calculating the performance of this tube independently[4/]. The heat transfer to/from a tube is calculated with the aid of heat exchanger cross-flow theory. This is done for each tube in a proper sequence and the summation results in total coil capacity. An even more detailed method of heat exchanger simulation would be to apply the finite-difference technique. Such a model would subdivide an analyzed tube of the coil into arbitrary small elements and would solve heat transfer equations for each element marching in space from the tube inlet to the tube outlet. Since for this study the cost of computing time required for such simulation would be prohibitive, the tube-by-tube approach was adopted.

In the tube-by-tube simulation method, the performance of one tube is calculated at one time and the general finned coil problem is reduced to a single tube problem. In order to conduct heat transfer calculations, fin surfaces associated

---

[4/] At the stage of completion of this report a new tube-by-tube computer model of a condenser coil was published by ORNL [56].

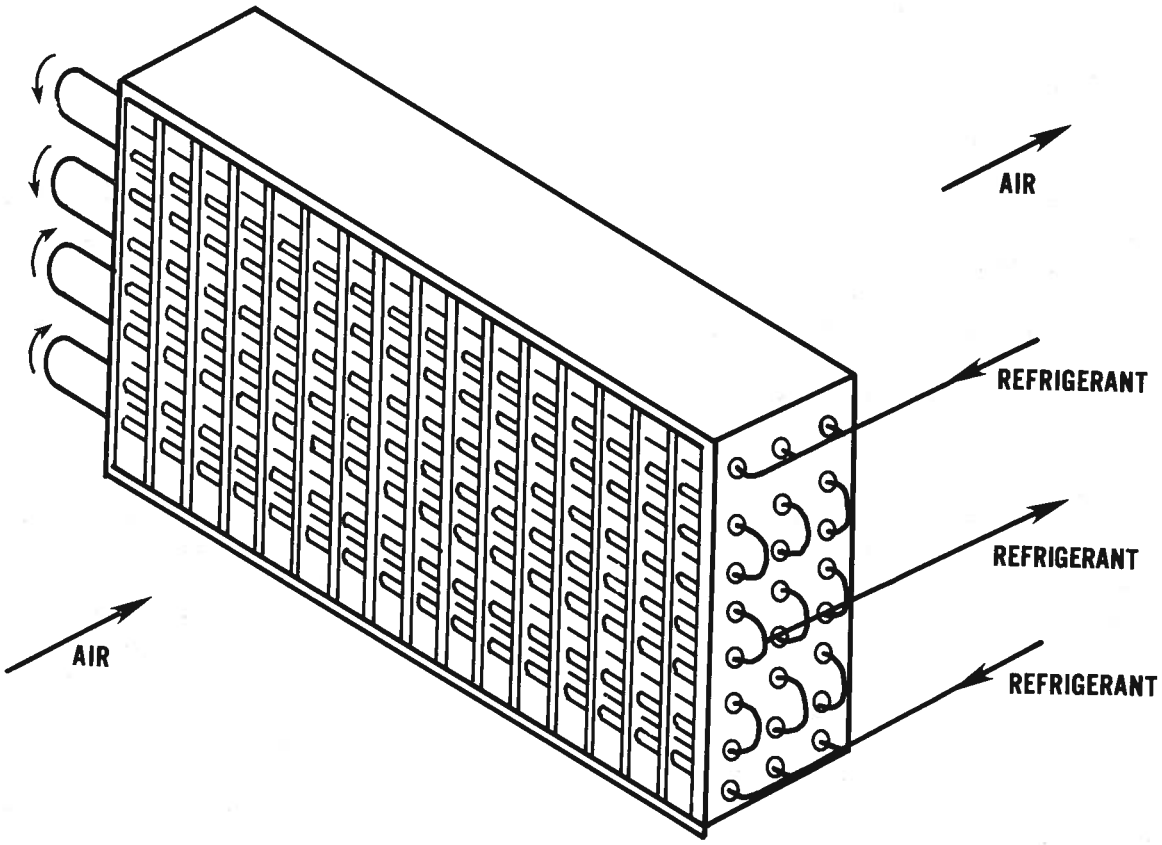

Figure 19. Schematic of a heat pump heat exchanger

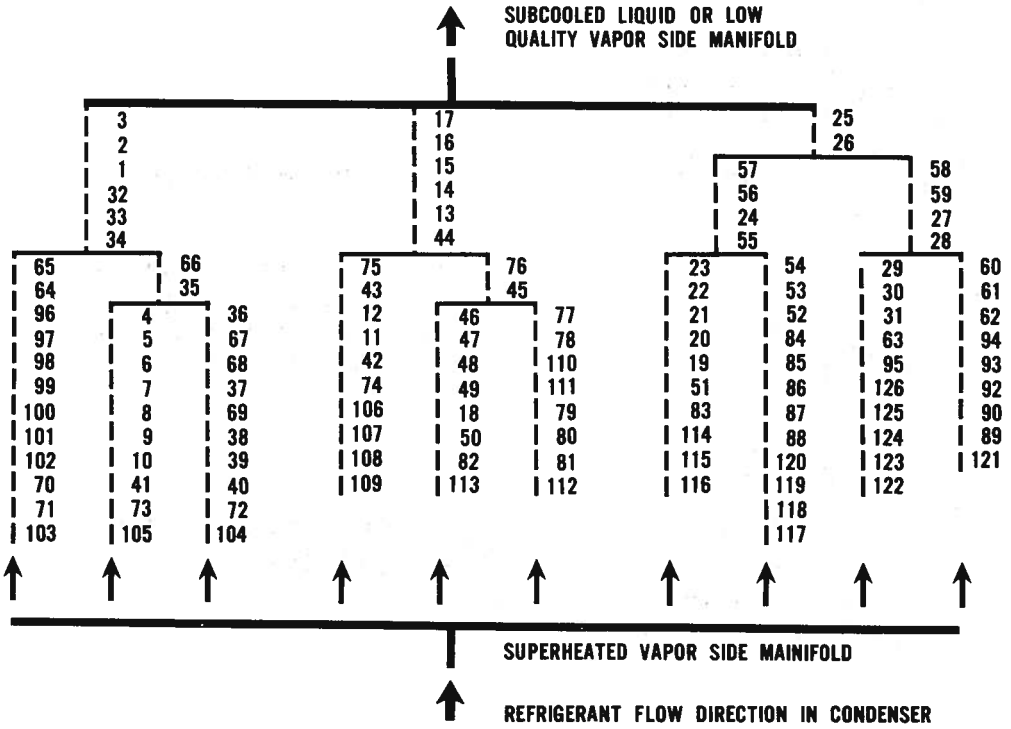

Figure 20. Example of coil circuitry

with the tubes must be defined. Following Carrier and Anderson [22], it was assumed that fin area served by each tube is equivalent in performance to a circular-plate fin of equal area. Thus a single tube is considered with a circular fin of diameter, D_t, as shown in figure 21.

5.4.2 Heat Transfer Rate for a Tube in a Cross-Flow Arrangement

Usually a heat pump coil employs some form of cross-flow arrangement. If a separate tube is considered, the problem is one of pure cross-flow. Fortunately, this kind of arrangement has received much attention in theoretical investigations. According to the Péclet heat transfer equation:

$$Q = U \cdot A_h \cdot \Delta T \tag{49}$$

where A_h = heat transfer surface area
U = overall coefficient of heat transfer
ΔT = temperature difference

In case of a pure cross-flow arrangement, one of two mean temperature differences applies for ΔT, [23]:

$$\Delta T_m = \frac{t_2 - t_1}{\ln \frac{T_2 - t_1}{T_1 - t_2}}$$

when temperature of one of the fluids does not change (temperature of that fluid is denoted by T) (50)

$$\Delta T_m = \frac{t_2 - t_1}{\ln \frac{\frac{T_1 - T_2}{t_2 - t_1}}{\frac{T_1 - T_2}{t_2 - t_1} + \ln \frac{T_2 - t_1}{T_1 - t_1}}}$$

when temperature of both fluids changes (51)

where T = temperature of one fluid
t = temperature of another fluid
ΔT_m = mean temperature difference

subscripts 1 and 2 refer to tube inlet (upstream) and outlet (downstream) conditions

The enthalpy change of the fluid will be according to the equation:

$$Q = m \cdot (i_2 - i_1)$$

or

$$Q = m \cdot Cp \cdot (T_2 - T_1) \tag{52}$$

$$D_t = 2\left(\frac{d1 \cdot d2}{\pi}\right)^{0.5}$$

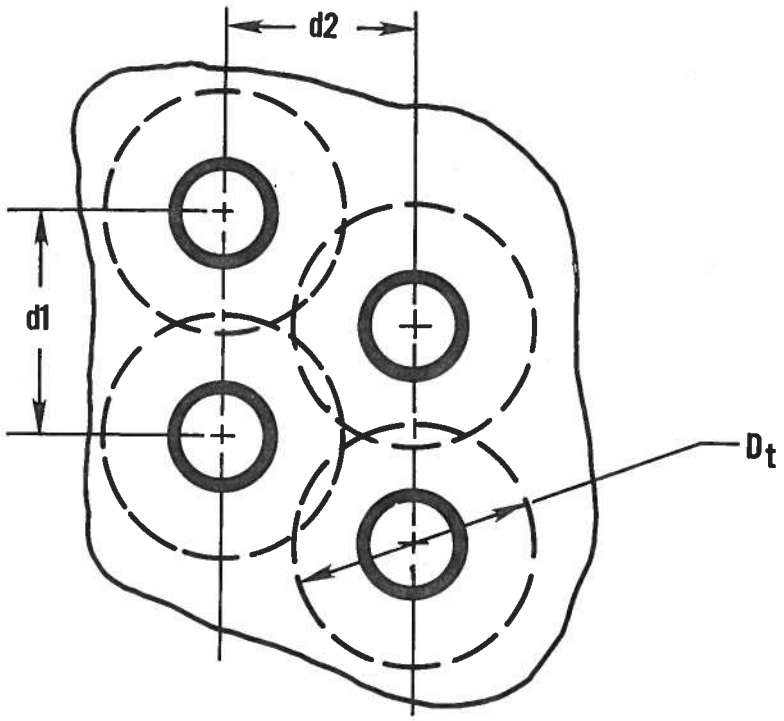

Figure 21. Approximation method for treating a rectangular-plate fin of uniform thickness in terms of a flat circular-plate fin of equal area

where Cp = specific heat of fluid
i = enthalpy
m = mass flow rate

Looking at any vapor compression cycle P-h or T-s diagram, it can be realized that the single-phase and two-phase refrigerant flow usually exists in a given heat exchanger. Also, both flow patterns can actually exist in one tube. That means the refrigerant flowing in the tube may maintain approximately constant temperature (two-phase) or its temperature may vary (single-phase). Not only the mean temperature difference between fluids but also the refrigerant pressure drop is affected by the flow pattern. Equations presented below, derived from equations (49), (50), (51), and (52), allow for detailed consideration of these problems. The heat transfer rate for each mentioned flow condition can be calculated as follows:

- single-phase flow only, refrigerant is superheated or subcooled at both inlet and outlet

$$Q = Cp_r \cdot m_r(T_{r,i} - T_{a,i})\left(1 - \exp\left(-\frac{Cp_a \cdot m_a}{Cp_r \cdot m_r}\left(1 - \exp\left(-\frac{U \cdot A_o}{Cp_a \cdot m_a}\right)\right)\right)\right) \quad (53)$$

- two-phase flow only, refrigerant is in two-phase at both inlet and outlet

$$Q = Cp_a \cdot m_a \left(1 - \exp\left(-\frac{U \cdot A_a}{Cp_a \cdot m_a}\right)\right)(T_{r,g} - T_{a,i}) \quad (54)$$

- superheated vapor at tube inlet, two-phase at the tube outlet

$$Q = m_r(i_{r,i} - i_{r,V}) + Cp_a \cdot m_a(1 - Z_V)\left(1 - \exp\left(-\frac{U \cdot A_o}{Cp_a \cdot m_a}\right)\right)(T_{r,g} - T_{a,i}) \quad (55)$$

where Z_v = fraction of the tube length in the superehated region which can be calculated by the equation:

$$Z_v = \frac{-Cp_r \cdot m_r \cdot \ln\left(1 - \frac{i_{r,i} - i_{r,g}}{Cp_r(T_{r,i} - T_{a,i})}\right)}{Cp_a \cdot m_a\left(1 - \exp\left(1 - \frac{U \cdot A_o}{Cp_a \cdot m_a}\right)\right)} \quad (56)$$

- two-phase at tube inlet, subcooled liquid at the tube outlet

$$Q = Cp_r \cdot m_r(T_{r,g} - T_{a,i})\left(1 - \exp\left(-\frac{Cp_a \cdot m_a(1-Z_{tp})}{Cp_r \cdot m_r}\left(1 - \exp\left(-\frac{U \cdot A_o}{Cp_a \cdot m_a}\right)\right)\right)\right)$$

$$+ m_r(i_{r,i} - i_{r,L}) \quad (57)$$

where Z_{tp} = fraction of the tube length in the two-phase region which can be calculated by the equation:

$$Z_{tp} = \frac{m_r(i_{r,i} - i_{r,L})}{Cp_a \cdot m_a(1 - \exp(-\frac{U \cdot A_o}{Cp_a \cdot m_a}))(T_{r,i} - T_{a,i})} \quad (58)$$

In equations (53) through (58) the following nomenclature was used:

A_o = total exterior surface area associated with the tube wetted by air
Cp_a = air specific heat at constant pressure
Cp_r = refrigerant specific heat at constant pressure
$i_{r,i}$ = refrigerant enthalpy at the tube inlet
$i_{r,L}$ = enthalpy of refrigerant saturated liquid
$i_{r,V}$ = enthalpy of refrigerant saturated vapor
m_a = air mass flow rate associated with the tube
m_r = refrigerant mass flow rate in the tube
$T_{a,i}$ = air temperature upstream of the tube
$T_{r,g}$ = refrigerant saturation temperature
$T_{r,i}$ = refrigerant temperature at the tube inlet
U = overall tube heat transfer coefficient

A desirable feature in the above equations is that they do not involve any of the outlet temperatures or any of the outlet fluid parameters. Hence, the heat transfer rate can be calculated based on total heat transfer area, overall tube heat transfer coefficient, inlet fluid parameters, and their mass flow rates.

5.4.3 Refrigerant and Air Mass Flow Rates Associated with a Tube

Refrigerant Mass Flow Rate

During flow through a heat pump heat exchanger, the refrigerant undergoes a change of phase in the course of evaporation or condensation. The change of phase is associated with a dramatic change of density which affects the velocity and pressure drop of the working fluid. In order to prevent a high pressure drop, tubes in some heat pump coils are connected to form branched circuits. An example of such coil circuitry has been shown in figure 20.

Refrigerant flow direction marked in figure 20 is for the coil working as a condenser. Superheated vapor enters the vapor side manifold and is distributed into 10 tubes. On its flow path, refrigerant merges several times and finally merges in the liquid manifold to enter the liquid line. For the coil operating as an evaporator, the direction of flow is opposite to that marked in the figure. Low quality refrigerant enters the coil and the flow is subdivided into three circuits. On its way through the coil the refrigerant evaporates and splits several times on its way towards the exist where it is finally collected into one bigger diameter vapor line. The mass flow rates through the particular circuits of the coil are self-adjusting so the pressure at merging (splitting) tubes is the same.

To perform a simulation of a coil by the tube-by-tube method, refrigerant mass flow rate for each tube has to be known. Since total refrigerant mass flow rate supplied to the coil is known, the problem reduces to the determination of refrigerant distribution. In [3], refrigerant distribution is found by considering the coil working as an evaporator and assuming that refrigerant splits equally among tubes at any splitting point of tubing circuitry. Thus the fraction of the total flow is assigned to each tube based on circuit geometry and is used in both the heating and cooling mode simulation.

The method for determination of refrigerant flow distribution used in [3] was checked by examining calculated refrigerant pressures at the ends of all circuit branches. These pressures should be equal if the assumed distribution is right; however, the pressures were found to be different by as much as 3 psi. Of course, refrigerant flow distribution could be corrected in an iteration process. This would require repeating all coil simulation calculations several times, hence making coil simulation prohibitively expensive.

Another approach was tried to determine refrigerant flow distribution. Since most of the coil total pressure drop may be expected to result from superheat vapor and two-phase flow, it was assumed that the refrigerant flow is uniformly distributed among tubes connected to the vapor side manifold and that mass flow rates in other tubes may be found by following the refrigerant path with direction of flow as marked in figure 20. The resulting distribution was checked as before. The maximum pressure discrepancy found was equal to 0.3 psi which represented less than a 0.2°F variation in the saturation temperature between merging tubes. This was considered satisfactory and the method was adopted in this study for determining refrigerant mass flow rate distribution in a coil.

Air Mass Flow Rate

Air mass flow rate was assumed to be distributed uniformly over the whole coil face regardless of the coil and fan respective locations, so each coil was associated with the same air mass flow. It was also assumed that there were enough turbulence in the air stream passing through the coil to provide effective mixing so that air of uniform properties enters each tube bank.

5.4.4 Overall Heat Transfer Coefficient for a Dry Finned Tube

Dry fined tube analysis is applicable to a condenser and also to an evaporator if no dehumidifcation takes place. The overall heat transfer coefficient, U, for a dry finned tube can be derived by summing the individual resistances between the refrigerant and the air, [23]:

$$U = \left[\frac{A_o}{A_{p,i} h_i} + \frac{A_o}{A_{p,i} h_{d,i}} + \frac{A_o x_p}{A_{p,m} k_p} + \frac{1}{h_{c,o}\left(1 - \frac{A_f}{A_o}(1 - \phi)\right)} \right]^{-1} \qquad (59)$$

where A_f = fin surface area
A_o = total exterior surface area wetted by air

$A_{p,i}$ = pipe inside surface area
$A_{p,m}$ = pipe mean surface area
$h_{c,o}$ = convection heat transfer coefficient at exterior surface
$h_{d,i}$ = heat transfer coefficient for inside tube deposit
h_i = inside tube convection heat transfer coefficient
k_p = thermal conductivity of pipe material
x_p = thickness of pipe wall

$$\phi = \frac{T_{f,m} - T_a}{T_{f,b} - T_a}, \text{ fin efficiency}$$

T_a = air temperature
$T_{f,b}$ = fin base temperature
$T_{f,m}$ = mean fin temperature

The third term of equation (59) can be evaluated if the heat exchanger material and geometry are known. The heat transfer coefficient for inside tube deposit, $h_{d,i}$, was assumed to be 5000 Btu/(h • ft^2 • F) [23] which allows for evaluation of the second term. Terms 1 and 4, which refer to the inside and outside convection resistance respectively, required considerably more analysis to establish the proper algorithm for determining the heat transfer coefficient.

5.4.5 Forced Convection Heat Transfer Inside a Tube

Analyzing the problem for both an evaporator and a condenser, the following modes of forced convection are encountered:

- single-phase forced convection
- two-phase forced convection with condensation
- two-phase forced convection with evaporation

The physics of these phenomena are very much different and they have to be considered separately.

Single-Phase Forced Convection

Single-phase forced convection takes place in a condenser, at the entrance section where the superheated vapor is being cooled, and a the exit section where a subcooled liquid is being cooled. It is also applicable in the evaporator, as the superheated vapor passes through the exit tubes. The non-dimensional heat transfer parameter describing this phenomena, Nusselt number, is related to the non-dimensional Reynolds and Prandtl numbers in the following form:

$$Nu = 0.023 \cdot Re^{0.8} \cdot Pr^{0.333} \qquad (60)$$

where $Nu = \frac{h \cdot D}{k}$, Nusselt number

$Pr = \frac{\mu \cdot Cp}{k}$, Prandtl number

$$Re = \frac{G \cdot D}{\mu}, \text{ Reynolds number}$$

Cp = specific heat at constant pressure
D = inside diameter of a tube
G = refrigerant mass flux
h = convection heat transfer coefficient
k = refrigerant thermal conductivity
μ = refrigerant absolute viscosity

Two-Phase Forced Convection with Condensation

The predominant flow pattern during condensation in a heat pump condenser is annular flow with liquid refrigerant flowing on the pipe wall and vapor refrigerant flowing in the core. Traviss, Baron, and Rohsennow [24] performed experimental and analytical studies of vapor condensation in annular flow with refrigerants R-12 and R-22. They assumed von Karman universal velocity distribution in the condensate flow (like on a flat plate), calculated pressure drops using the Lockhart-Martinelli method [25], and applied momentum and heat transfer analogy for calculation of the condensation heat transfer coefficient. The correlation proposed by them has the following form:

$$Nu = \frac{Re_L^{0.9} \cdot Pr_L \cdot F1^{\beta}}{F2} \tag{61}$$

where $Nu = \frac{h \cdot D}{k_L}$

h = condensation heat transfer coefficient
D = tube inside diameter
k_L = thermal conductivity of liquid refrigerant

$$Re_L = \frac{G(1 - x)D}{\mu_L}$$

G = refrigerant mass flux
x = quality
μ_L = liquid refrigerant absolute viscosity

$$Pr_L = \frac{\mu_L \cdot Cp_L}{k_L}$$

$\beta = 1$ for $F1 \leq 1$, $\beta = 1.15$ for $F1 > 1$

F1 and F2 in equation (61) are dimensionless parameters expressed as follows:

$$F1 = 0.15 \left(X_{tt}^{-1} + 2.85\, X_{tt}^{0.524}\right) \tag{62}$$

$$F2 = 0.707 \cdot Pr_L \cdot Re_L^{0.5} \qquad \text{for } Re_L < 50$$

$$F2 = 5 \cdot Pr_L + 5 \cdot \ln(1 + Pr_L(0.09636 \cdot Re_L^{0.585} - 1)) \quad \text{for } 50 < Re_L < 1125$$

$$P2 = 5 \cdot Pr_L + 5 \cdot \ln(1 + Pr_L) + 2.5 \cdot \ln(0.00313 \cdot Re_L^{0.812}) \quad \text{for } Re_L < 1125 \tag{63}$$

Parameter X_{tt}, formulated by Lockhart-Martinelli [25] with the assumption of no radial pressure gradient and a smooth pipe, has the following form:

$$X_{tt} = \left(\frac{1 - x}{x}\right)^{0.9} \left(\frac{v_L}{v_V}\right)^{0.5} \left(\frac{\mu_L}{\mu_V}\right)^{0.1} \tag{64}$$

Parameter X_{tt} is inversely proportional to flow quality and refers to turbulent vapor and turbulent liquid flow. Physically it is equal to the square roof of the ratio of pressure drop of the liquid phase to the frictional pressure drop of the vapor phase if these phases were flowing independently and alone in the tube, i.e.:

$$X_{tt} = \left[\frac{\left(\frac{dP}{dL}\right)_L}{\left(\frac{dP}{dL}\right)_V}\right]^{0.5} \tag{65}$$

Equation (61) is applicable where conditions for annular condensation in a tube exist. Such conditons may be assumed to exist for flow qualities ranging from 0.1 to 0.9. At qualities larger than 0.9, the whole tube inner surface is not covered by a liquid film and part of the heat transfer is just that of single-phase convection. At qualities less than 0.1, flow was observed to be in the slug regime [24]. It is assumed, that in the quality range 0.0 to 0.1 and 0.9 to 1.0, the heat transfer coefficient changes linearly from a two-phase flow value to a single-phase flow value and is calculated using linear interpolation between values obtained from equations (60) and (61).

Two-Phase Forced Convection with Evaporation

Refrigerant enters an evaporator from an expansion device at quality about 20 percent and forms an annular flow instantly. The quality increases with the proceeding flow and the annular flow pattern is maintained until the quality reaches about 0.90, at which refrigerant vapor has enough kinetic energy to gradually destory the liquid layer and patches of dry wall appear.

There are many correlations for calculating the forced convection evaporation heat transfer coefficient (nucleation effect for mass fluxes taking place in heat pump evaporators at qualities greater than 20 percent is insignificant, even if it happens). Anderson, Rich, and Geary [26] performed laboratory measurements to obtain the forced convection evaporation heat transfer coefficient under conditions closely approximating those existing in refrigerant evaporators.

They also examined six generally known correlations checking heat transfer coefficient predictions with their laboratory results. They found best agreement with Pierre's [27] correlation, which correlate reasonably well with experimental data at high mass velocities (above 10^5 lb/(h • ft^2)) and provided an excellent agremeent at lower mass velocities.

Pierre's correlation, based on experimental work with refrigerants R-12 and R-22, has the following form:

$$Nu = \frac{h \cdot D}{k_L} = 0.0009 \cdot \frac{G \cdot D}{\mu_L} \cdot \left[\frac{J \cdot \Delta x \cdot i_{fg}}{L}\right]^{0.5} \qquad (66)$$

where
- D = inner diameter of the tube
- G = refrigerant mass flux
- h = heat transfer coefficient
- i_{fg} = latent heat of evaporation
- J = the mechanical equivalent of heat
- k_L = thermal conductivity of liquid refrigerant
- L = length of the tube
- Δx = refrigerant vapor quality change in the tube
- μ_L = absolute viscosity of liquid refrigerant

Pierre's correlation is applicable for a Nusselt number value within the limit:

$$28.5 < Nu < 753 \qquad (67)$$

which falls in the range of heat pump evaporator operation, and for a quality range from 0.15 to 0.90. For refrigerant quality greater than 0.09, similar to the condensation case, the evaporative heat transfer coefficient may be obtained by averaging between the values yielded by equation (66) and the single-phase forced convection correlation, equation (60).

5.4.6 Forced Convection Heat Transfer at the Air-Side of a Flat-Finned Tube

In order to evaluate the forced convection heat transfer outside a flat-finned tube (term 4 of equation (59)), the total exterior surface area, A_o, the fin area, A_f, the air-side heat transfer coefficient, $h_{c,o}$, and fin efficiency, ϕ, have to be known.

From the number of air-side heat transfer correlation available in the literature, the one proposed by Briggs and Young [28] is most applicable here. This correlation was developed after extensive tests on 18 tube banks of different fin geometry. A regression analysis of the test data yielded the following equation:

$$Nu = \frac{h_{c,o} \cdot D_o}{k_a} = 0.134 \cdot Re_a^{0.681} \cdot Pr_a^{0.333} \cdot \left(\frac{z}{y}\right)^{0.2} \cdot \left(\frac{z}{t}\right)^{0.1134} \qquad (68)$$

where
- D_o = outside tube diameter
- G_{max} = air mass flux at minimum cross section
- $h_{c,o}$ = air-side mean convective heat transfer coefficient

k_a = air thermal conductivity

$$Pr_a = \frac{\mu_a \cdot Cp_a}{k_a}, \text{ Prandtl number}$$

$$Re_a = \frac{G_{max} \cdot D_o}{\mu_a}, \text{ Reynolds number}$$

t = fin thickness
y = fin height
z = distance between adjacent fins

The geometry parameters affecting the heat tranfer are illustrated in figure 22. The adequacy of equation (68) was further verified by Jones and Russell [29].

The addition of fins to the tubes greatly increases the outer heat transfer area but at the expense of decreasing the mean temperature difference between the surface and the air stream. The parameter, fin efficiency, ϕ, is used to rate the thermal effectiveness of a fin. As mentioned in section 5.4.1, it is assumed in this study for heat transfer analysis, that each tube is served by a circular-plate fin of equivalent surface area, as per figure 21. Gardner [30] solved the diferential equation for describing the temperature distribution in a circular fin and presented fin efficiency curves in terms of two parameters.

$$D_o/D_t \text{ and } y\left(\frac{2 \cdot h_{c,o}}{k_f \cdot t}\right)^{0.5}$$

Exact theory results are correlated well by the following equation proposed in [3] (see also figure 23):

$$\phi = \sum_{i=1}^{8} \left(A_{1,i} + A_{2,i} \frac{D_o}{D_t} + A_{3,i} \left(\frac{D_o}{D_t}\right)^2\right)\left(y\left(\frac{2 \cdot h_{c,o}}{k_f \cdot t}\right)^{0.5}\right)^{i-1} \qquad (69)$$

where $h_{c,o}$ = air-side convective heat transfer coefficient
k_f = fin material thermal conductivity

The geometry parameters are indicated in figure 22. The coefficients, $A_{n,i}$, are given in table 1.

5.4.7 Overall Heat Transfer Coefficient for a Wet Finned Tube

Wet finned tube analysis is applicable to an evaporator when its temperature is below the dew point temperature of ambient air. In such a case, moisture is being removed from an air stream and is transferred to an evaporator external surface. If the evaporator temperature is above 32°F, a water film flows down the fin under force of gravity. If the exterior evaporator temperature is below 32°F, frost is accumulated.

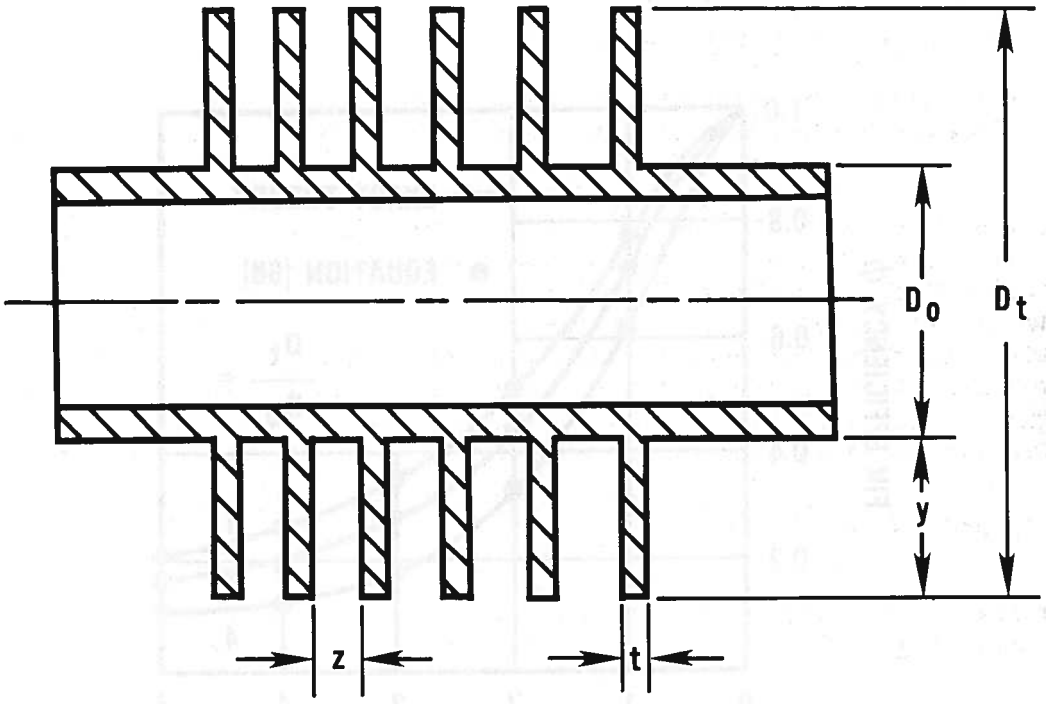

D_o = TUBE OUTSIDE DIAMETER
D_t = FIN TIP DIAMETER
y = FIN HIGHT
t = FIN THICKNESS
z = DISTANCE BETWEEN ADJACENT FINS

Figure 22. Cross section of a flat-finned tube indicating parameters which affect the air-side heat transfer coefficient

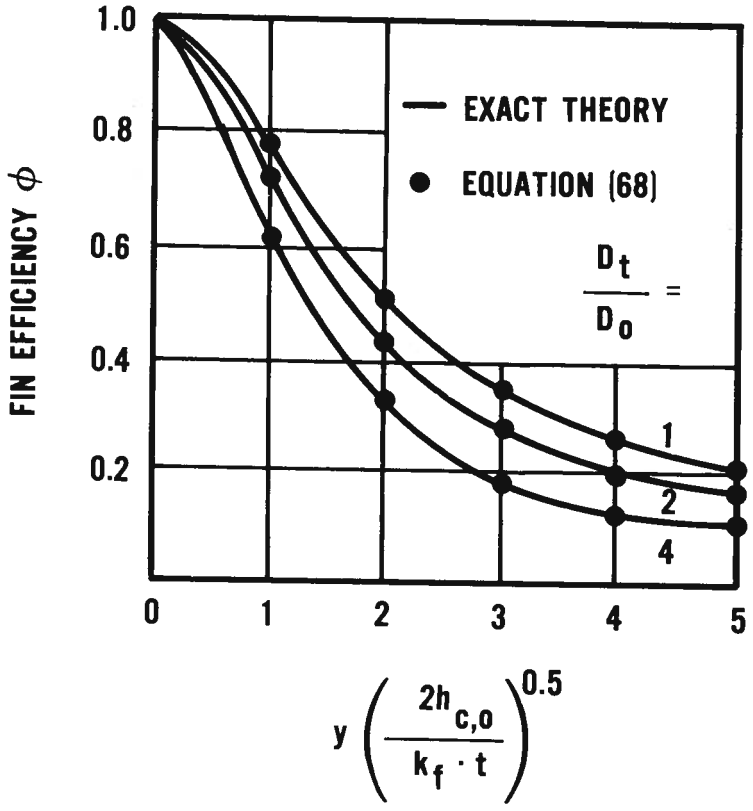

Figure 23. Efficiency for a circular-plate fin of uniform thickness. Comparison of exact theory results with those obtained by equation (69)

Table 1. Coefficients to be Used in Correlation for Fin Efficiency (Equation (69))

i	$A_{1,i}$	$A_{,2i}$	$A_{3,i}$
1	1.0	0.0	0.0
2	-0.22920E-01	-0.13755E+00	0.20130E-01
3	0.16106E+00	0 81890E-01	-0.11440E-01
4	-0.64975E+00	-0.55500E-01	-0.28753E-01
5	0.53491E+00	0.18040E-01	0.42477E-01
6	-0.19286E+00	0.36494E-03	-0.20335E-01
7	0.32564E-01	-0.10660E-02	0.40947E-02
8	-0.20972E-02	0.12410E-03	-0.29673E-03

Looking at the heat transfer phenomena from refrigerant to air, one can realize that the dehumidification process will alter the heat transfer situation on the external surface of the finned tube, while other processes in the tube and refrigerant stay unaffected and are governed by relations already proposed in previous sections. Thus only processes connected with dehumidification need to be discussed.

The heat transfer rate between the air stream and the water surface is described by the following equation:

$$dQ = (h_{c,o}(T_a - T_w) + h_{D,o}(w_a - w_w)i_{fg,w})dA_o \tag{70}$$

The first term in equation (70) accounts or sensible heat and the second term accounts for latent heat transfer. Noting that for air at atmospheric pressure the Lewis number,

$$Le = \frac{h_{c,o}}{h_{D,o}Cp_a}, \tag{71}$$

is close to 1, equation (70) assumes the following form for a flat finned tube:

$$dQ = h_{c,o}(1 + \frac{i_{fg,w}(w_a - w_w)}{Cp_a(T_a - T_w)})(1 - \frac{A_f}{A_o}(1 - \phi))(T_a - T_w)dA_o \tag{72}$$

Symbols used in equations (70), (71), and (72) denote:

A_f = fin area
A_o = total external area
Cp_a = specific heat of air
$h_{c,o}$ = air-side forced convection heat transfer coefficient
$h_{D,o}$ = air-side mass transfer coefficient
$i_{fg,w}$ = latent heat of condensation for water
T_a = temperature of air
T_w = temperature of liquid water (frost)
Q = heat transfer rate
w_a = humidity ratio of air
w_w = humidity ratio of saturated air at T_w temperature

$\phi = \frac{T_{w,m} - T_a}{T_{w,b} - T_a}$, fin efficiency

$T_{w,m}$ = mean temperature of water film (frost)
$T_{w,b}$ = temperture of water film (frost) at fin base

The one-dimensional heat conduction across the condensate (frost) film can be expressed by equation:

$$dQ = h_L \cdot \Delta T_L \cdot dA_o \tag{73}$$

where $h_L = \frac{h_w}{\delta}$, heat transfer coefficient for condensate (frost) film

k_w = thermal conductivity of water (frost)

δ = thickness of condensate (frost) film

ΔT_L = temperature difference across condensate (frost) film

Using equations (72) and (73) and referring to equation (59), the following relation for overall heat transfer coefficient for a wet finned tube can be derived:

$$U = \left[\frac{A_o}{h_i A_{p,i}} + \frac{A_o}{h_{d,i} A_{p,i}} + \frac{A_o x_p}{A_{p,m} k_p} + \frac{1}{h_L} + \frac{1}{h_{c,o}\left(1 + \frac{i_{fg,w}(w_a - w_w)}{Cp_a(T_a - T_w)}\right)\left(1 - \frac{A_f}{A_o}(1 - \phi)\right)} \right]^{-1} \quad (74)$$

where symbols used are defined as in equations (59) and (72).

In the above formulation of the overall heat transfer coefficient, it is assumed that the temperature difference across the liquid film (frost) is uniform. The calculated value for wet fin efficiency is affected by the change of the air-side heat transfer coefficient caused by air passage geometry alternation by liquid (frost) accumulation, and by released latent heat of condensation (sublimation). The effect of water (frost) conductance on fin efficiency is neglected. In summary the heat transfer phenomena that occurs during dehumidification on the air-side may be itemized as follows:

(1) layer of wet (frost) offers additional heat flow resistance
(2) air-side heat transfer resistance is decreased due to effect of condensation
(3) air-side heat transfer coefficient, $h_{c,o}$, since it is sensitive to external surface geometry, has an increased value (see equation (68))
(4) fin efficiency has decreased value as $h_{c,o}$ is increased (see figure 23)
(5) the cross sectional area of the air flow passage between the fins has decreased, decreasing the flow rate and the heat exchange.

In order to evaluate water (frost) layer thickness, consider the mass transfer equation:

$$m_{a,d} \cdot dw_a = - h_{D,o}(w_a - w_w)dA_o \quad (75)$$

For the Lewis number equal to 1 and for a finned tube differential surface area, equation (75) assumes the following form:

$$m_{a,d} \cdot dw_a = - \frac{h_{c,o}}{Cp_a}(w_a - w_w)\left(1 - \frac{A_f}{A_o}(1 - \phi)\right)dA_o \quad (76)$$

Variation of air humidity ratio can be calculated by integrating equation (76), which yields:

$$w_{a,e} = w_{a,i} - (w_{a,i} - w_w)\left(1 - \exp \frac{-h_{c,o} \cdot A_o\left(1 - \frac{A_f}{A_o}(1 - \phi)\right)}{Cp_a \cdot m_{a,d}}\right) \quad (77)$$

The rate of moisture removal per unit area, R, can be now calculated:

$$R = m_{a,d}(w_{a,i} - w_{a,e})/A_o \quad (78)$$

where $m_{a,d}$ = mass flow rate of dry air
$w_{a,e}$ = humidity ratio of air at tube row exit
$w_{a,i}$ = humidity ratio of air at tube row inlet

If the evaporator temperature is below the freezing point, moisture removed from the air stream accumulates on the evaporator external surface in the form of frost. Its thickness, δ_f, can be evaluated by integrating the rate of moisture removal with respect to time, i.e.:

$$\delta_f = \int_0^t \frac{R}{\rho_f}\, dt \quad (79)$$

where t = time
R = rate of moisture removal per unit area
δ_f = frost layer thickness
ρ_w = frost density

In case of evaporator temperature above 32°F, condensate flows down on the fin. Assuming no drag on the liquid layer, the condensate thickness, δ_w, can be found by solving the Navier-Stokes equation. The resulting expression for a finned tube situation is:

$$\delta_f = 1.083 \left(\frac{\mu_w \cdot R'}{g \cdot \rho_w^2}\right)^{1/3} \quad (80)$$

where g = gravitational acceleration
R' = condensation rate per unit width of a fin
μ_m = water dynamic viscosity
ρ_w = water density

5.4.8 Pressure Drop in a Tube

As expressed by equation (25), the total pressure drop experienced by a flowing fluid results from pressure drops due to friction, momentum change, and gravity. In an actual heat pump heat exchanger, pressure drop due to gravity effect is very small and may be neglected. Only pressure drop due to friction and due to

momentum change will be considered with distinction between different flow patterns in a tube.

Single-Phase Flow

Frictional pressure drop for a single-phase in a tube can be calculated by the Fanning equation with the Fanning friction factor as per equations (43) and (44):

$$\Delta P = \frac{2f \cdot G^2 \cdot L}{D \cdot \rho} \tag{81}$$

$$f = 0.046\ Re^{-0.2} \tag{82}$$

Pressure drop due to momentum change can be calculated by the following equation:

$$\frac{dP}{dL} = - G^2 \frac{dv}{dL} \tag{83}$$

where G = refrigerant mass flux
L = tube length
v = refrigerant specific volume

Two-Phase Flow with Condensation

Frictional pressure drop for two-phase flow with condensation can be calculated by the method proposed by Lockhard and Martinelli [25]. They performed a semi-empirical study of adiabatic two-phase flow with air and different liquids including benzene, kerosene, water, and various oils in pipes varying in diameter form 0.586 to 1.017 inch. They related pressure drop of two-phase flow to the pressure drop of the liquid portion of the flow flowing alone in the pipe, by the dimensionless parameter X_{tt}, i.e.:

$$\frac{\Delta P_{tp}}{\Delta P_L} = f(X_{tt}) = \Phi \qquad \Delta P_{tp} = \Delta P_L \cdot \Phi \tag{84}$$

where ΔP_L = frictional pressure drop of the liquid portion of two-phase flow flowing alone in the tube
ΔP_{tp} = frictional pressure drop of two-phase flow
Φ = correction factor for two-phase pressure drop
X_{tt} = as given by equation (64)

The pressure drop, ΔP_L, can be calculated by the single-phase pressure drop relation with calculated liquid Reynolds number and friction factor as follows:

$$Re_{tp,L} = \frac{(1 - x)G \cdot D}{\mu_L} \tag{85}$$

$$f_{tp,L} = 0.046 \cdot Re_{tp,L}^{-0.2} \tag{86}$$

where $f_{tp,L}$ = friction factor for the liquid portion of two-phase flow flowing alone in the pipe

$Re_{tp,L}$ = Reynolds number for the two-phase liquid portion flowing alone in the pipe
x = quality
μ_L = liquid dynamic viscosity

A correction factor for two phase pressure drop, Φ, can be correlated by the following equation:

$$\Phi = 10^{\sum_{i=1}^{5} A_i (\log X_{tt})^{i-1}} \tag{87}$$

where $A_1 = 1.4$
$A_2 = -0.87917$
$A_3 = 0.14062$
$A_4 = 0.0010417$
$A_5 = -0.00078125$

Combining equations (84), (85), (86), and (87), the two-phase pressure drop equation assumes the form:

$$\Delta P_{tp} = 2 f_{tp,L} \cdot G^2(1 - x^2)L \cdot \Phi/(D \cdot \rho_L) \tag{88}$$

The pressure drop due to momentum change for separated two-phase flow can be estimated by the following equation:

$$\frac{dP}{dL} = - G^2 \frac{d}{dL} \left(\frac{v_V \cdot x^2}{\alpha} + \frac{v_L(1 - x)^2}{(1 - \alpha)}\right) \tag{89}$$

where x = quality
v_L = specific volume of liquid
v_V = specific volume of vapor
α = void fraction

Void fraction, α, percent of tube filled with vapor, was shown by Lockhard and Martinelli to be a function of X_{tt} under any flow conditions for separated flow with both phases turbulent. Wallis [31] correlated their results in the following form:

$$\alpha = (1 + X_{tt}^{0.8})^{-0,378} \tag{90}$$

This expression was found to correlate well with data presented in [25] for values of $X_{tt} \leq 10$. For X_{tt} greater than 10, another curve fitted formula is used:

$$\alpha = 0.823 - 0.157 \cdot \ln X_{tt} \tag{91}$$

Two-Phase Flow with Evaporation

The pressure drop for two-phase flow with evaporation can be calculated by the correlation proposed by Pierre [32], based on his experiments with refrigerants R-12 and R-22. Pierre's correlation has the following form:

$$\Delta P = \left(f \frac{L}{D} + \frac{\Delta x}{x_m}\right) G^2 \cdot v_m \qquad (92)$$

where f = friction factor (calculated by equation (93))
x_m = mean quality
Δx = quality change
$v_m = v_L + x_m(v_v - v_L)$, mean specific volume

The friction factor to be used in equation (92) was correlated by Pierre from his experimental data by the following empirical equation:

$$f = 0.0185 \left(Re \frac{L}{J \cdot i_{fg} \cdot \Delta x}\right)^{0.25} \qquad (93)$$

where $Re = \frac{G \cdot D}{\mu_L}$, Reynolds number

The correlation proposed by Pierre is in the conventional format for the single pressure drop formula. The first term of equation (92) is for frictional pressure drop while the second is for pressure drop due to change of momentum. The formula for the friction factor contains conventionally the Reynolds number divided by the term $J \cdot i_{fg} \cdot \Delta x/L$, referrred to as a boiling number, making friction factor sensitive to vapor generation rate at the vapor-liquid interface. Pierre's correlation was verified in [26] providing overall better agreement with experimental data for pressure drop of refrigerants R-12 and R-22 than the other popular correlation of Martinelli and Nelson [33].

5.5 MODELING OF ADDITIONAL HEAT PUMP COMPONENTS

In the previous sections, modeling of the main heat pump components has been discussed. The analysis included a compressor, a constant flow area expansion device, a condenser, and an evaporator. Additional components that have to be considered for a more accurate heat pump performance prediction by the model are: vapor suction and discharge lines, liquid line, and a four-way valve. Their modeling is briefly explained below.

Vapor Lines

A suction line connects an evaporator with a compressor. A compressor and a condenser are connected by a discharge line. In both lines, single-phase flow exists in the form of either saturated or superheated vapor. In heat pump systems vapor lines are usually insulated. Heat transfer rates between refrigerant vapor flowing in these pipes and ambient air can be calculated by a general heat transfer equation for a circular duct with insulation [10]. Single-phase forced convection is assumed inside the tube (equation (60)) and

free convection is assumed outside the tube. The following equation is used for calculation of the free convection heat transfer coefficient for a horizontal pipe [38]:

$$h = 0.27 \left(\frac{\Delta T}{D_o}\right)^{0.25} \tag{94}$$

for Grashof numbers from 10^3 to 10^9

where ΔT = temperature between tube wall and air
D_o = tube outside diameter

Pressure drop in vapor lines can be calculated by the single-phase pressure drop equation (43).

Liquid Line

A liquid line connects an evaporator and a condenser. This line is filled with subcooled liquid or low quality two-phase flow. The pressure drop can be calculated by equations (43) or (88), depending on the flow pattern. Heat loss from the liquid line to the ambient air is neglected.

Four-Way Valve

The main function of a four-way valve is to direct refrigerant flow from the compressor to the indoor or outdoor coil depending on the mode of operation (heating or cooling). The side effects of flow through a four-way valve are changes in the refrigerant thermodynamic state due to pressure drop and heat exchange. Assuming an adiabatic exterior wall, all heat lost by the discharge refrigerant is gained by the suction refrigerant. Heat transfer rate and refrigerant pressure drop in the valve can be evaluated by formulas similar to equations (20) and (30), respectively. Heat transfer and pressure drop parameters in these formulas have to be found empirically.

5.6 REFRIGERANT MASS INVENTORY IN A HEAT PUMP

The mass, M, of a substance occupying a known volume, $\forall$, may be determined by:

$$M = \int_{\forall} \rho \cdot d\forall \tag{95}$$

where ρ = local density

In reality, the mass of refrigerant in the system can be fund by estimating masses of the refrigerant in each system component and adding them up. For this purpose, equation (95) can be written in the form:

$$M = \Sigma M_i \tag{96}$$

$$M_i = \forall_i \cdot \rho_{m,i}$$

where M_i = mass of refrigerant in particular component i
V_i = internal volume of component i
$\rho_{m,i}$ = mean fluid density in component i

The heat pump components taken into account in the mass inventory calculations are shown in figure 24. The refrigerant phase in each of the components as indicated in the figure is based on the following consideration:

Discharge line - receives and is filled with superheated vapor from the compressor.

Condenser - receives superheated vapor from a discharge line. In the course of passage through the condenser tubes, vapor temperature is brought to saturation temperature. Starting at this point, a thin condensed liquid layer forms on the tube walls. Depending on the mass flux, this liquid film may be swept and entrained within the vapor as a mist forming a dispersed flow. With more condensed vapor, the velocity decreases, a permanent liquid film is formed on the wall, and flow proceeds further as annular flow or semiannular flow. The quality decreases and flow slows down in the direction of flow. Gravity forces result in a stratifying effect and liquid flowing in the bottom of the tube periodically wets the upper tube wall (slug flow). If full condensation is reached, there will be subcooled liquid at the condenser exit.

Thus there are four two-phase flow patterns in the refrigerant condensers, i.e.:

dispersed flow, annular flow, semi-annular flow, slug flow

as identified by Traviss and Rohsenow [34]. Soliman and Azer [35] identified nine flow regimes; however, five of them may be considered as transition regimes and can be put into the above basic four categories. The effect of return bends connecting condenser tubes was investigated in [36]. It was found that this effect is insignificant and that the annular flow pattern "recovers" almost immediately in a tube after passing a return bend.

Liquid line - receives refrigerant from a condenser and delivers it to an expansion device. Entering the small bore restrictor at the end of the liquid line, the flow experiences a sudden contraction. The entrance presure drop depends upon the mass flow rate and fluid density. This along with capillary sensitivity to the amount of subcooling, provides a flow controlling mechanism for the system. It is common practice to design a capillary tube so the refrigerant mass flow rate through it would balance with the mass flow rate through the compressor when a liquid seal exists before the capillary tube. Temporary existence of vapor before the capillary tube would decrease the mass flow rate and build up the pressure. This would provide better conditions for condensation in the condenser and thus cause a return to a subcooled liquid or very low quality two-phase flow in the liquid line.

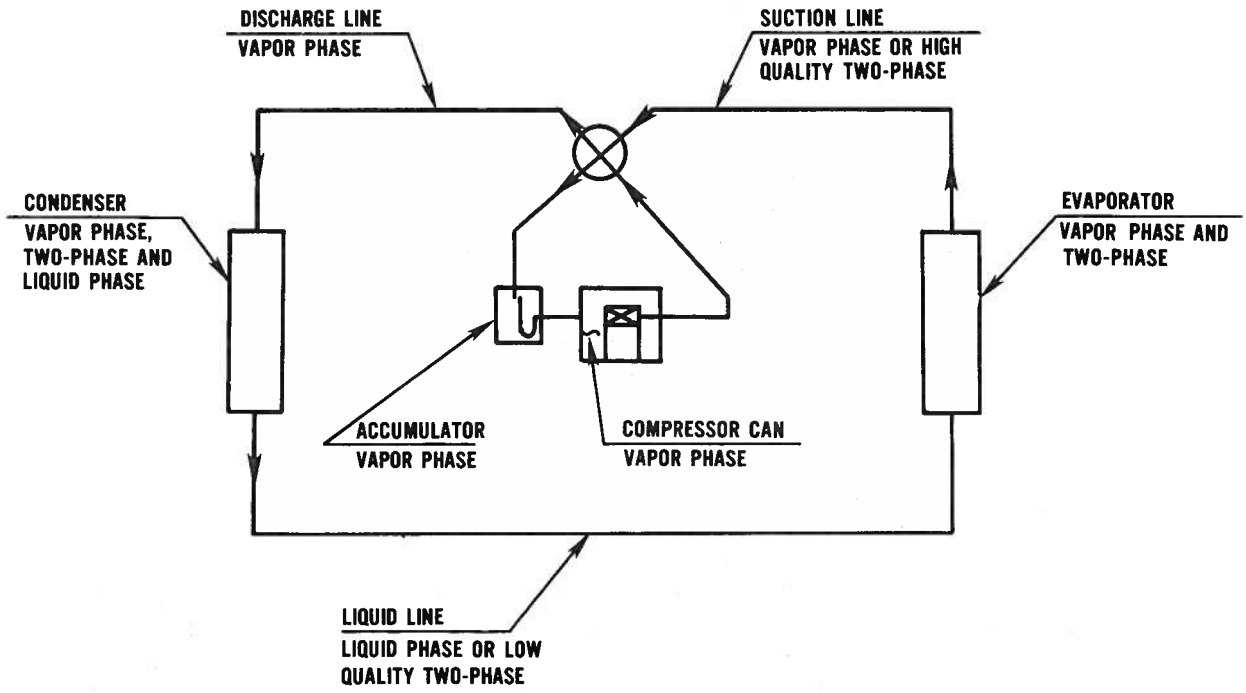

Figure 24. Refrigerant phase in heat pump components

Capillary tube - due to small internal volume may be disregarded for mass inventory purposes.

Evaporator - receives refrigerant from a capillary tube in the form of homogeneous flow of about 20 percent quality, at sonic or close to sonic velocity. This flow experiences a sudden deceleration and is assumed to form an annular or semi-annular flow pattern very quickly having a void fraction about 0.8 [37]. The liquid phase flows along the tube in the form of an annulus and the vapor phase flows in the core. This type of flow prevails in most of the evaporator. With increasing quality, the velocity of the vapor increases and becomes eventually high enough to entrain small liquid drops and tear the liquid film apart. This results in a dry mist flow at qualities close to 1. Finally, the flow may reach the evaporator exit in a superheated vapor state.

Suction line - receives refrigerant from the evaporator as a mist flow or superheated vapor flow and the same flow pattern exists at the exit.

Accumulator - receives the refrigerant from a suction line after some heat was added in the four-way valve. Saturated vapor or superheated vapor may be expected. (This does not account for refrigerant liquid that may be accumulated on the accumulator bottom.)

Compressor can - receives refrigerant from the accumulator as a saturated or superheated vapor which is further superheated due to heat transfer from an electric motor, discharge line, and compressor cylinder body.

According to the above analysis, refrigerant in the accumulator, compressor can, suction line, and discharge line is in (or close to) a homogeneous vapor state. In the liquid line, homogeneous liquid flow or two-phase flow exists but in a state so close to saturation that both liquid and vapor would travel at about the same velocity. For mass inventory purposes, the flow may be assumed to be homogenous. The mass of refrigerant in these components can be then calculated in a similar manner since refrigerant densities in the components described above will be known as a result of the simulation program iteration process.

In the case of both coils, the refrigerant flow in part is homogeneous; however, in most of the coil some type of annular flow prevails. For a separated flow regime like an annular flow, density of the flowing fluid results from vapor and liquid densities and the fractions of tube volume occupied by the liquid and vapor phase:

$$\rho_m = \frac{M_t}{\forall_t} = \frac{\rho_L \cdot \forall_L + \rho_V \cdot \forall_V}{\forall_t} = \rho_L(1 - \alpha) + \rho_V \cdot \alpha \qquad (97)$$

where M = mass
$\forall$ = occupied volume
ρ = density
$\alpha = \forall_V/\forall_t$, void fraction

subscripts refer to:

L = liquid phase
m = mean value
t = total value
V = vapor phase

It should be pointed out that for a two-phase flow of given quality, mean density depends not only on the thermodynamic parameters affecting densities of the liquid and vapor, but also on the ratio of mean velocities of the vapor and liquid referred often as the slip ratio. This can easily be noticed by looking at the equation for void fraction, which can be derived considering mass flow rates of each phase:

$$\alpha = \frac{1}{1 + \frac{1 - x}{x} \frac{V_V}{V_L} \frac{\rho_V}{\rho_L}} \tag{98}$$

where V = velocity

Calculation of the void fraction has received much less attention than the calculation of heat transfer or pressure drop, although all three of these phenomena are undoubtedly inter-related. The most often referred method for void fraction calculation is that of Lockhard and Martinelli [25] based on their experimental void fraction data reported along with pressure drop results. Lockhard and Martinelli correlated void fraction with the dimensionless parameter, X_{tt}. Their experiment dealt with adiabatic flow; however, in the conclusions of their paper they suggested that their pressure drop correlation could be used for prediction of pressure drop during evaporation and condensation as well. On similar grounds, their void fraction data should be applicable beyond the adiabatic case.

There is another, earlier, method available for void fraction calculation by Martinelli and Nelson [33], derived with the same assumptions for water/steam evaporating flow. The method is similar to the Lockhard-Martinelli method so the Lockhard and Martinelli method was used in this study for calculation of the void fraction in both evaporator and condenser coils.

Correlations for void fraction based on [25] have already been given in section 5.4.8 (equations (90) and (91)).

$$\alpha = (1 + X_{tt}^{0.8}) - 0.378 \qquad \text{for } X_{tt} \leq 10 \tag{99}$$

$$\alpha = 0.823 - 0.157 \ln X_{tt} \qquad \text{for } X_{tt} > 10 \tag{100}$$

Parameter X_{tt}, as defined by equation (64), is a function of flow quality, specific volume, and viscosities of the liquid and vapor, and is not sensitive to the mass flux which in turn affects the slip ratio.

Experimental data of Staub and Zuber [37] for evaporating refrigerant R-22 indicate that void fraction increases with increased mass flow rate. Comparison of their data with void fraction predicted by the Martinelli-Nelson method showed a discrepancy which may lead to underestimation of the two-phase flow mean density by as much as 300 percent. (Note that a small difference in void fraction results in a large error in mean density prediction as density of the vapor and liquid are of different orders of magnitude.) The results of Staub and Zuber also indicated that approximate agreement with the Martinelli-Nelson method could be obtained at high mass fluxes, more than five times higher than those observed in heat pump evaporators.

In discussing the accuracy of a refrigerant mass prediction method, it should be noted that it also depends upon an accurate measurement of the internal volume of the system. Internal volume can be easy calculated for straight pipes. For valves, bends, etc., it can be only approximated.

Mass inventory of a heat pump system, as explained in section 5.1.2, is intended to be used for iteration of refrigerant superheat at the compressor can inlet. The discussions above indicated that mass inventory calculations may have errors from two different sources. These sources are: inaccurate density prediction in the two-phase region, and inaccuracte internal volume measurement. However, these inaccuracies are not of great importance and can be ignored, since the program does not really need prediction of the absolute value of refrigerant mass in the system, but rather requires sensitivity in relative mass predictions in a heat pump with change of operating conditions. This requirement should be satisfied by the Lockhard-Martinelli method and very precise knowledge of the internal volume should not be that important. Since refrigerant vapor superheat at the compressor can inlet is known for a heat pump operating in the cooling mode at design conditions (outdoor temperature 90°F, indoor dry bulb temperature 80°F, and wet bulb 67°F) and does not have to be iterated upon, refrigerant mass in the system can be calculated at this operating condition. This calculated mass of refrigerant may then be used as input data for refrigerant vapor superheat iteration at other outdoor or indoor air conditions at which heat pump simulation results are required.

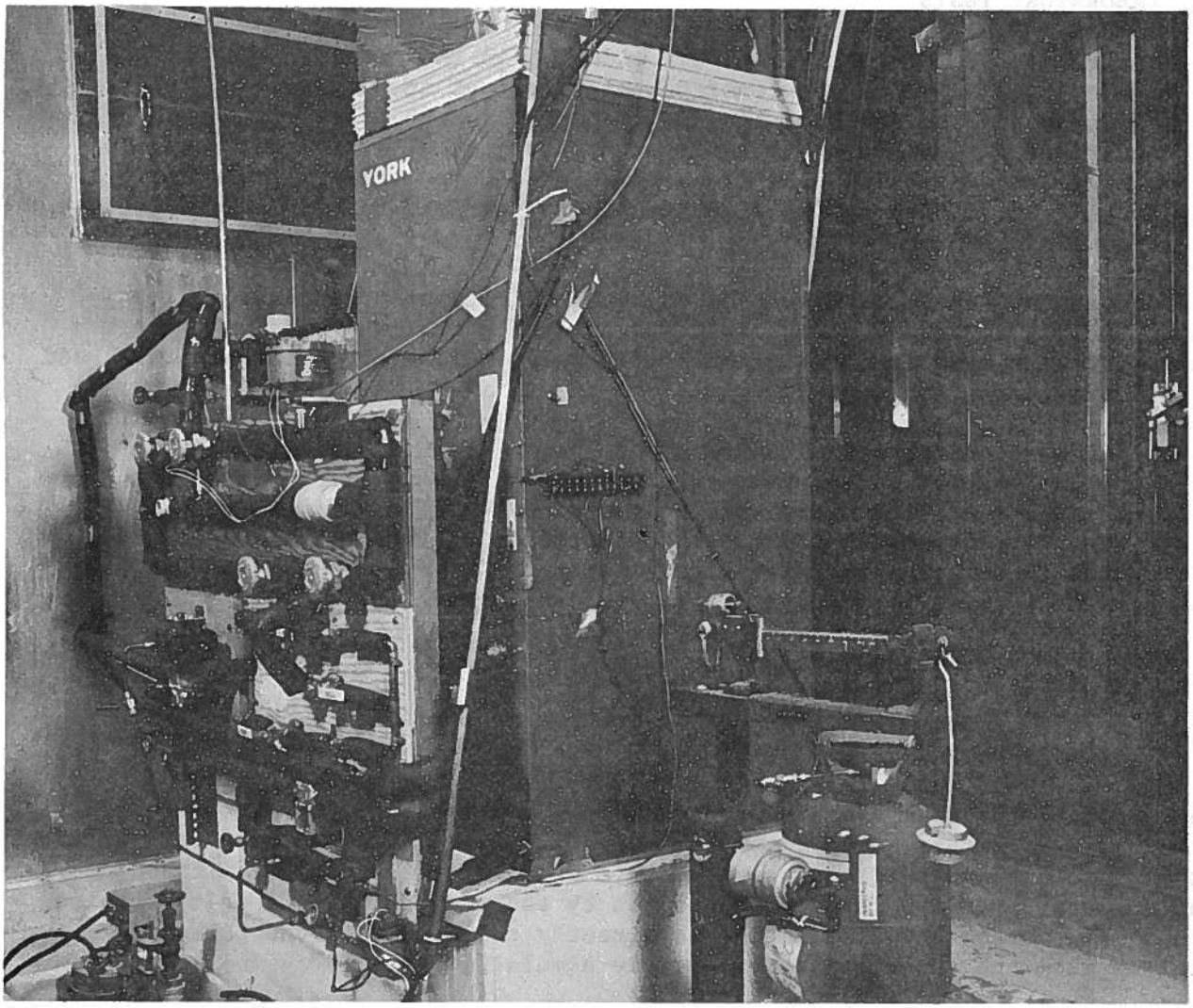

6. MODEL VERIFICATION

A verification of the computer model has been done by comparison of computer predictions with performance data obtained from laboratory tests conducted in NBS environmental chambers. Four heat pumps were available for computer model evaluation. They are denoted here-in as systems 1, 2, 3, and 4. System 1, system 2, and system 3 consisted of the same compressor, outdoor coil, connecting tubing, and expansion device. The only variable element was an indoor section (containing an indoor fan and coil). In the case of system 2, the indoor unit was an original match for the rest of the components. For system 1 and for system 3, the indoor sections were undersized and oversized, respectively. System 4 was a matched indoor/outdoor system of another manufacturer.

6.1 LABORATORY TESTS

An identical series of four tests was conducted in the cooling mode on each of the four systems. The series consisted of a test at an outdoor temperature of 105°F and tests A, B, and C of the NBS recommended test procedure [39]. Thermal conditions during the above tests covered practically the whole range of the cooling mode operating conditions for a heat pump working in the field. Additionally, heat pump system 2 was tested in the heating mode at temperature conditions recommended by [40].

Cooling and heating tests results are presented in table 2 and table 3, respectively. Symbols used in these and following tables in this section are consistent with symbols used in the main program MAIN (refer to appendix I) and have the following meaning:

COP - coefficient of performance
ELUSE - energy consumption rate
P3 - refrigerant pressure at compressor inlet
P8 - refrigerant pressure at compressor outlet
RHOA - relative humidity of outdoor air
RHRA - relative humidity of indoor air
RMASS - refrigerant mass flow rate
TOA - temperature of outdoor air
TRA - temperature of indoor air
TSUP3 - superheat at compressor inlet
QLOAD - heat pump capacity

The capacity reported in table 2 is the one measured by the refrigerant enthalpy method [41]. In this method, the unit capacity is derived from the refrigerant enthalpy change and refrigerant volumetric flow rate measurements with adjustment for heat added to the indoor section by the indoor fan. Capacity obtained by the refrigerant enthalpy method is directly comparable to the capacity obtained from the vapor compression cycle simulation.

During heating mode tests, no liquid subcooling existed in the liquid line of the heat pump. Vapor bubbles existing in the flow made it impossible to measure volumetric flow rate of refrigerant. In this case, system capacity was determined by the air-side enthalpy difference method [41].

6.2 COMPUTER SIMULATION RUNS

Each laboratory test performed was simulated using the computer program HPSIM. Since laboratory tests were performed first, the computer simulations could be made with the same thermal operating conditions that actually existed in the laboratory during the tests.

The first run executed for each system was at design operating conditions (test 2) with refrigerant superheat at the compressor inlet equal to that of laboratory test. The refrigerant charge calculated during this run was used later as input data for other runs requiring superheat iteration.

Table 2. Laboratory Test Results of Heat Pumps in the Cooling Mode

SYSTEM	TEST	TOA	TRA	RHRA	QLOAD	ELUSE	COP	RMASS	P3	TSUP3	P8
-	-	°F	°F	-	Btu/h	Watt	-	lb/h	psia	°F	psia
1	1.1	104.9	79.8	.52	33229	5093	1.912	572	86.6	2.2	286.0
1	1.2	95.2	79.8	.52	36135	4854	2.180	560	82.7	11.0	254.3
1	1.3	82.0	79.6	.52	38542	4564	2.474	545	77.6	23.4	215.9
1	1.4	82.1	79.5	.19	33203	4511	2.157	534	73.0	1.0	210.5
2	2.1	104.9	80.0	.52	34841	5212	1.959	589	88.9	2.3	292.2
2	2.2	94.9	80.0	.52	37548	4938	2.228	578	85.0	13.8	259.5
2	2.3	82.1	80.0	.52	40105	4629	2.538	555	79.3	30.9	220.2
2	2.4	82.1	79.8	.20	37156	4583	2.375	550	76.3	9.4	216.6
3	3.1	105.2	79.9	.51	37963	5542	2.007	640	95.5	1.2	305.2
3	3.2	95.2	79.8	.52	40946	5276	2.274	622	90.9	12.8	270.3
3	3.3	81.9	79.9	.51	42842	4930	2.546	602	85.1	21.9	230.8
3	3.4	82.2	79.9	.21	38551	4867	2.321	591	80.2	1.1	224.9
4	4.1	104.9	80.0	.51	31595	4613	2.007	499	89.3	20.0	316.7
4	4.2	95.0	80.0	.51	32640	4351	2.198	483	84.8	25.0	280.1
4	4.3	82.2	80.0	.51	33656	3982	2.476	449	76.6	32.5	236.2
4	4.4	82.1	80.0	.18	31437	3971	2.320	445	75.2	25.9	233.6

Table 3. Laboratory Test Results of System 2 in the Heating Mode

SYSTEM	TEST	TOA	RHOA	TRA	QLOAD	ELUSE	COP	P3	TSUP3	P8
-	-	°F	-	°F	Btu/h	Watt	-	psia	°F	psia
2	2.5	46.6	.73	70.2	42648	4763	2.624	71.4	0.0	239.9
2	2.6	35.0	.82	69.9	35553	4471	2.330	60.4	0.0	218.2
2	2.7	17.1	.70	70.0	24958	3956	1.848	45.6	0.0	187.9

Cooling simulation results are presented in table 4. Heating simulation results are presented in table 5. A comparison of results is given in table 6. This table shows that the maximum discrepancy found between laboratory test results and computer simulation results was:

capacity - 3.4 percent
energy consumption rate - 7.3 percent
COP - 5.5 percent

The largest deviation of refrigerant conditions was:

refrigerant mass flow - 5.2 percent
refrigerant suction pressure - 3.8 psi
refrigerant superheat at suction - 8.4°F
refrigerant discharge pressure - 23 psi

Agreement between results was generally very good. The only serious difference was in the case of refrigerant discharge pressure where the discrepancy was found to be as much as 23 psi, which corresponds to about 7.5°F of difference in refrigerant saturation temperature in the condenser. This disagreement took place, however, only in the heating mode of operation when the indoor coil was the condenser. Discharge pressure results for cooling operation agreed much better.

In the course of the analyses of this 23 psi pressure difference the following conclusions were made:

- there was a good agreement between refrigerant suction pressure results and capacity results for cooling mode operation, which indicates that the indoor coil is simulated well while operating as an evaporator.

- there was a significant difference in the heat transfer rates in the performed tests in the indoor and outdoor coil working as a condenser. Data indicated that the heat flux was twice as large in the indoor coil than in the outdoor coil, which has considerably more surface area and volume. Additionally, the refrigerant mass flow rate during the heating mode was smaller than during the cooling mode making the refrigerant quality variation even greater in the indoor coil.

If it is assumed that these differences are due to deficiencies in the simulation program in its present form, then it is concluded that the condensing heat transfer coefficient correlation used in HPSIM provides a lower value for the indoor coil than actually exists and is responsible for the high refrigerant discharge pressure obtained in the computer simulation runs.

6.3 VERIFICATION OF THE MASS INVENTORY SIMULATION

Verification of the mass inventory method can be done on different levels. One of the ways is to compare the refrigerant charge in a system tested in a laboratory to the charge computed during a simulation run. This was done for system 1. The system simulation resulted in a charge of 6.1 lb. while the actual heat

Table 4. Cooling Test Simulation Results

SYSTEM	TEST	TOA	TRA	RHRA	QLOAD	ELUSE	COP	RMASS	P3	TSUP3	P8
-	-	°F	°F	-	Btu/h	Watt	-	lb/h	psia	°F	psia
1	1.1	104.9	79.8	.52	33750	5248	1.884	557	86.9	2.0	288.0
1	1.2	95.2	79.8	.52	35580	5000	2.085	545	82.6	11.0	255.4
1	1.3	82.0	79.6	.52	37510	4650	2.364	525	76.6	25.0	214.9
1	1.4	82.1	79.5	.19	33690	4572	2.159	506	73.4	1.0	212.8
2	2.1	104.9	80.0	.52	36010	5401	1.954	586	90.6	5.0	291.8
2	2.2	94.9	80.0	.52	37890	5129	2.165	574	86.1	13.8	258.2
2	2.3	82.1	80.0	.52	39950	4782	2.448	551	79.9	28.0	218.5
2	2.4	82.1	79.8	.20	36570	4740	2.261	544	77.7	1.0	217.4
3	3.1	105.1	79.9	.51	37810	5690	1.947	627	95.3	1.0	298.8
3	3.2	95.2	79.8	.52	40400	5422	2.184	615	91.1	12.8	265.0
3	3.3	81.9	79.9	.51	42940	5067	2.483	598	85.1	2.2	222.3
3	3.4	82.2	79.9	.21	38680	4990	2.271	577	81.6	1.1	222.0
4	4.1	104.9	80.0	.51	32040	4644	2.022	514	90.5	19.8	326.9
4	4.2	95.0	80.0	.51	33070	4379	2.213	498	86.9	25.0	291.7
4	4.3	82.2	80.0	.51	33970	4009	2.482	466	80.4	33.2	248.0
4	4.4	82.1	80.0	.18	32020	3952	2.374	456	77.1	21.3	244.0

Table 5. Heating Test Simulation Results

SYSTEM	TEST	TOA	RHOA	TRA	QLOAD	ELUSE	COP	P3	TSUP3	P8
-	-	°F	-	°F	Btu/h	Watt	-	psia	°F	psia
2	2.5	46.6	.73	70.2	42170	4776	2.587	70.3	0.0	262.9
2	2.6	35.0	.82	69.9	35600	4363	2.391	59.8	0.0	239.5
2	2.7	17.1	.70	70.0	24400	3668	1.949	43.6	0.0	203.0

Table 6. Discrepancy between Laboratory Test Results and Computer Simulation Results

TEST	QLOAD	ELUSE	COP	RMASS	P3	TSUP3	P8
-	%	%	%	%	psi	°F	psi
1.1	1.6	3.0	-1.5	-2.6	0.3	0.2	2.0
1.2	-1.5	3.0	-4.4	-2.6	-0.1	0.0	1.1
1.3	-2.7	1.9	-4.4	-3.8	-1.0	1.6	1.0
1.4	1.5	1.4	0.1	-5.2	0.4	0.0	2.3
2.1	3.4	3.6	0.3	-0.5	1.7	2.7	-0.4
2.2	0.9	3.9	-2.9	-0.6	1.1	0.0	1.3
2.3	-0.4	3.3	-3.5	-0.7	0.6	2.9	-1.7
2.4	-1.6	3.4	-4.8	-1.1	1.4	8.4	-0.8
2.5	-1.1	0.3	-1.4	-	-1.1	0.0	23.0
2.6	0.1	-2.4	2.6	-	-0.6	0.0	21.3
2.7	-2.2	-7.3	5.5	-	-2.0	0.0	15.1
3.1	-0.4	2.7	-3.0	-0.2	-0.2	0.2	-6.4
3.2	-1.3	2.8	-4.0	-1.1	0.2	0.0	-5.3
3.3	0.2	2.8	-2.5	-0.6	0.0	0.1	-6.7
3.4	0.3	2.5	-2.2	-2.3	1.4	0.0	-2.9
4.1	1.4	0.7	0.7	3.0	1.2	-0.2	10.2
4.2	1.3	0.6	0.7	3.1	2.1	0.0	11.6
4.3	0.9	0.7	0.2	3.8	3.8	0.7	11.8
4.4	1.9	-0.3	2.2	2.5	1.9	4.6	10.4

pump was charged with 8.3 lb of refrigerant. For the same system, the outdoor coil was weighed during cooling mode operation giving 5.4 lb of refrigerant while the computed charge for this coil was 4.8 lb. Due to the test installation, it was not possible to weight the indoor coil; however, estimates based on the differences in the above data indicate that almost three times more refrigerant existed in an indoor coil (working as evaporator) than that calculated. A discrepancy of the same order of magnitude for the Martinelle-Nelson method was reported by Staub and Zuber [37]. Though better agreement between a laboratory and calculated charge would promote more confidence in the Lockhard-Martinelli method, it should be recognized that, as explained in section 5.6, the absolute value of the computed charge is not critical since the program iterates a new system status with change in operating conditions based on refrigerant mass inventory performed at design conditions. What is most important for modeling purpose is that the mass inventory based on the Lockhard-Martinelli method provides a means for calculation of change of the refrigerant vapor superheat at the compressor can inlet sufficiently well for accurate heat pump performance prediction.

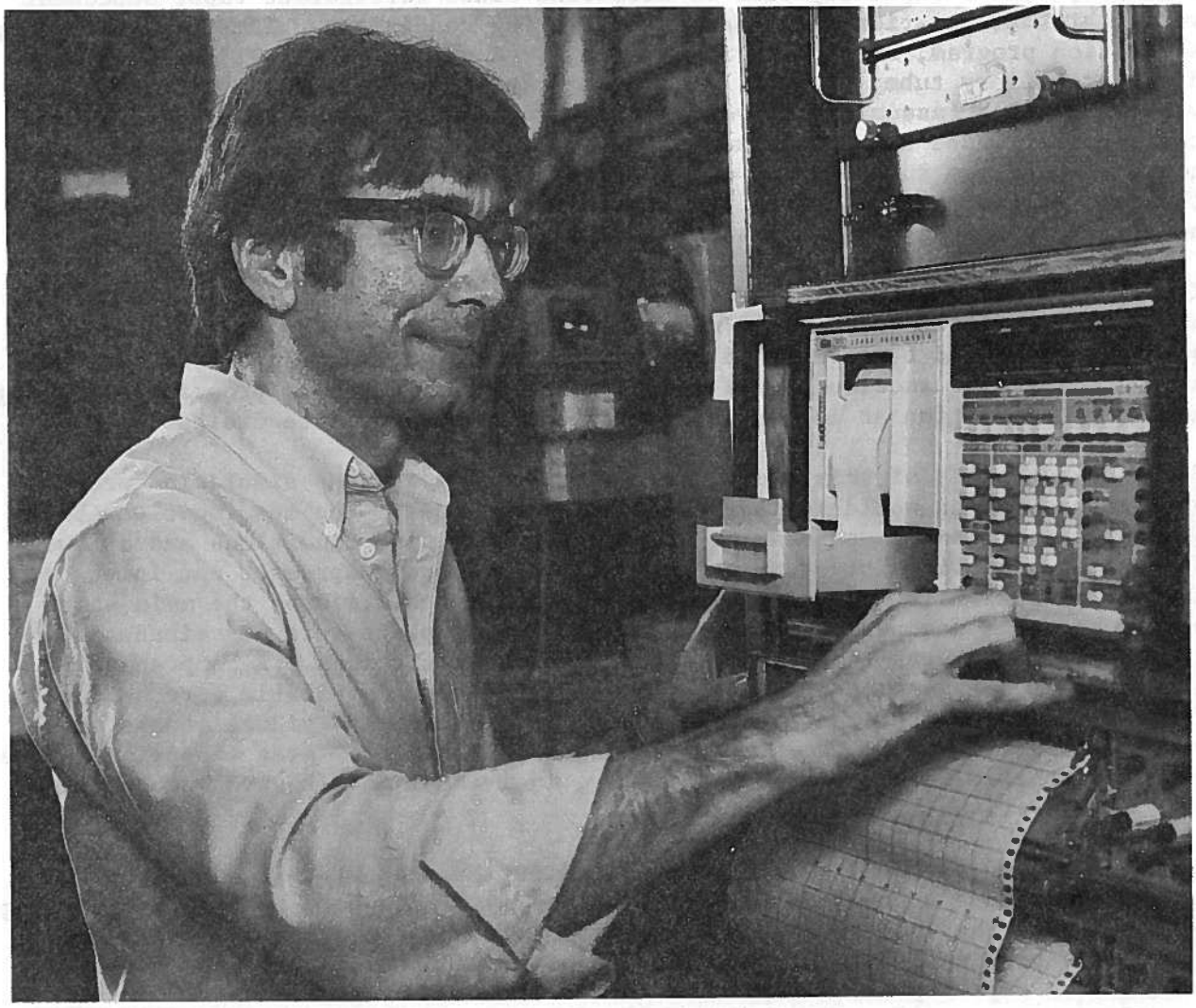

7. SUMMARY AND CONCLUSIONS

The main goal of this study was to formulate an analytical model of an air-source heat pump equipped with a constant flow area expansion device (capillary tube) that could provide accurate heat pump performance predictions.

In the first step of this study, operation of a heat pump was analyzed and previous work in steady-state vapor compression cycle modeling was reviewed. Three mathematical models of a heat pump were found in the literature and their applicability and limitations were studied. Two of the models could only simulate systems equipped with a thermostatic expansion valve (TXV) which maintains constant refrigerant vapor superheat at an evaporator outlet. Operation of a

heat pump with a capillary tube is different since refrigerant vapor superheat varies at that location with changing operating conditions. The third heat pump simulation program, originally formulated for a system with TXV, could accommodate a capillary tube; however, without the ability to calculate refrigerant vapor superheat (assuming its value is always known). Also it was found, that the capillary tube model utilized in this program was adequate only when a subcooled liquid was entering the capillary tube entrance and would not simulate the case of two-phase entering the tube which happens particularly during the heating mode. None of the existing models used operating conditions as input.

Thus, two major conclusions were drawn. First that a new capillary tube model had to be developed which would not carry any modeling restrictions. Second, some method should be formulated for calculation of refrigerant vapor superheat at the compressor suction side. It was also concluded that a program performing heat pump simulation at imposed operating conditions would be desirable.

In the second step of this study, new logic for a heat pump simulation program was proposed which would satisfy the identified needs. The new logic was based on analysis of heat pump behavior at changing operating conditions and allowed for calculation of refrigerant vapor superheat at the compressor can inlet by the refrigerant mass inventory simulation method. Analysis of the main heat pump components was performed and phenomena taking place were described analytically by fundamental equations or applicable correlations. A comprehensive literature search was done and the best correlations[5/] available were selected for the model. These equations were used to formulate individual models of particular heat pump components, including a constant flow area expansion device not available in the literature. Finally, individual models were incorporated into an overall heat pump model, HPSIM.

Verification of the model was conducted against laboratory test data of three heat pump systems in the cooling mode and one system in both heating and cooling mode covering the whole range of heat pump operating conditions. The maximum difference between laboratory results and model predictions was found to be 3.4 percent for capacity and 5.5 percent for coefficient of performance.

The model HPSIM developed in this study is the only model in the open literature that is capable of simulating a heat pump with a constant flow area expansion device at imposed operating conditions without restrictions on refrigerant state at any system location. (A possible exception is the assumption that refrigerant saturated vapor is leaving an accumulator when liquid is collected on its bottom. However, this assumption is felt to be quite reasonable and does not cause modeling difficulties.) The model having a demonstrated accuracy of performance prediction, allows for a wide variety of model applications. As shown in the verification process, the model was used to evaluate the performance of systems with mismatched components. Also it may be used to test how certain modifications of components (e.g., coil tube diameter, fin thickness, fin spacing, coil face area, capillary tube diameter or length, etc.)

5/ Those which appeared to have experimental verification in the conditions most similar to those found during operation of a heat pump.

affect overall performance of a heat pump filled with different refrigerants. This latter application has led to advanced work which will require modification to the refrigerant thermodynamic and transport property equations to include mixtures.

The program HPSIM occupies 31000 decimal words of core memory of a UNIVAC 1108 computer. Computing time depends on size of coils and refrigerant state input guesses. On average, computing time should not exceed 200 seconds. It is felt that the program can be helpful in testing, design, and development of heat pump systems by providing relief from some expensive laboratory tests and by providing consistently reliable results.

8. REFERENCES

1. Hiller, C.C. and Glickman, L.R., Improving Heat Pump Performance via Capacity Control - Analysis and Test, Report No. 24525-96, Heat Transfer Laboratory, Massachusetts Institute of Technology, Cambridge, Masschusetts, 1976.

2. Ellison, R.D. and Creswick, F.A., A Computer Simulation of Steady-State Performance of Air-to-Air Heat Pumps, ORNL/CON-16, Oak Ridge National Laboratory, Oak Ridge, Tennessee, 1978.

3. Chi, J., A Comuter Model HTPUMP for Simulation of Heat Pump Steady-State Performance, National Bureau of Standards, Internal Report, Washington, D.C., 1979.

4. American Society of Heating, Refrigerating, and Air-Conditioning Engineers, ASHRAE Guide and Data Book, Equipment Volume, New York, 1979.

5. Proceedings of the 1976 Purdue Compressor Technology Conference, Purdue Research Foundation, 1978.

6. Proceedings of the 1978 Purdue Compressor Technology Conference, Purdue Research Foundation, 1978.

7. Proceedings of the 1980 Purdue Compressor Technology Conference, Purdue Research Foundation, 1980.

8. Schultz, J.M., The Polytropic Efficiency of Centrifugal Compressors, ASME Transactions, Journal of Engineering for Power, Vol. 84, January 1962.

9. Hirsch, S.R., On the Relation of Compressor Theory to Performance, ASHRAE Journal, July 1973.

10. Rohsenow, W.M. and Choi, H., Heat, Mass and Momentum Transfer, Prentice-Hall, Inc., New Jersey, 1961.

11. Bolstad, M.M. and Jordan, R.C., Theory and Use of the Capillary Tube Expansion Device, Refrigeration Engineering, Vol. 56, No. 6, pg. 519, December 1948.

12. Mikol, E.P., Adiabatic Single and Two-Phase Flow in Small Bore Tubes, ASHRAE Journal, Vol. 5, No. 11, November 1963.

13. Moody, L.F., Friction Factors for Pipe Flows, ASME Transactions, Vol. 66, No. 8, pg. 671, November 1944.

14. Cooper, L., Chu, C.K., and Brosken, W.R., Simple Selection Method for Capillaries Derived from Physical Flow Conditions, Refrigeration Engineering, Vo. 65, No. 7, pg. 37, July 1957.

15. Rezk, A.M.A., Investigation on Flow of R-12 through Capillary Tubes, Paper presented on XV International Congress of Refrigeration, Venezia, September 23-29, 1979.

16. Gouse, S.W. Jr. and Brown, G.A., A Survey of the Velocity of Sound in Two-Phase Mixtures, ASME Paper 64-WA/FE-35, October 1964.

17. Kays, W.M., Loss Coefficient for Abrupt Changes in Flow Cross Section With Low Reynolds Number Flow in Single and Multiple-Tube Systems, ASME Transactions, Vol. 72, No. 8, pg. 1067, November 1950.

18. Whitesel, H.A., Capillary Two-Phase Flow, Refrigerating Engineering, Vol. 65, No. 4, pg. 49, April 1957.

19. Whitesel, H.A., Capillary Two-Phase Flow, Part II, Refrigeration Engineering, Vol. 65, No. 9, pg. 35, September 1957.

20. Erth, R.A., Two-Phase Flow in Refrigeration Capillary Tubes: Analysis and Prediction, Ph.D. Thesis, Purdue University, January 1970.

21. Hopkins, N.E., Rating the Restrictor Tube, Refrigeration Engineering, Vol. 58, No. 11, pg. 1087, November 1950.

22. Carrier, W.H., Anderson, S.W., The Resistance to Heat Flow Through Finned Tubing, ASHVE Transactions, Vol. 50, 1944.

23. Threlkeld, J.L., Thermal Environmental Engineering, Prentice-Hall, Inc., New Jersey, 1970.

24. Traviss, D.P., Baron, A.B., and Rohensow, W.M., Forced-Convection Condensation Inside Tubes, Technical Report No. 72591-74, Massachusetts Institute of Technology, Cambridge, Massachusetts, 1971.

25. Lockhard, R.W., Martinelli, R.C., Chemical Engineering Progress, Vol. 45, pg. 39, 1949.

26. Anderson, S.W., Rich, D.G., and Geary, D.F., Evaporation of Refrigerant 22 in a Horizontal 3/4-in. OD Tube, ASHRAE Transactions, Vol. 72, 1966.

27. Pierre, B., Stromningsmotstand vid Kikande Koldmedier, Kylteknisk Tidskrift, No. 6, December 1957.

28. Briggs, D.E. and Young, E.H., Convection Heat Transfer and Pressure Drop of Air Flowing Across Triangular Pitch Banks of Finned Tubes, 5th AICHE/ ASME National Heat Transfer Conference, Houston, Texas, 1962.

29. Jones, T.V. and Russell, C.B.B., Heat Transfer Distribution on Annular Fins, AIAA-ASME Thermophysics Heat Transfer Conference, Palo Alto, California, May 1978, ASME Paper No. 78-HT-30.

30. Gardner, K.A., Efficiency of Extended Surface, ASME Transactions, Vol. 67, 1945.

31. Wallis, G.B., One-Dimensional Two-Phase Flow, McGraw-Hill, 1969.

32. Pierre, B., Flow Resistance with Boiling Refrigerants, ASHRAE Journal, September 1964.

33. Martinelli, R.C. and Nelson, D.B., Prediction of Pressure Drop During Forced Circulation Boiling of Water, ASME Transactions, No. 6.

34. Traviss, D.P. and Rohsenow, W.M., FLow Regimes in Horizontal Two-Phase Flow with Condensation, ASHRAE Transactions, Vol. 79, Part 2, pg. 31, 1973.

35. Soliman, H.M. and Azer, N.Z., Flow Patterns During Condensation Innside a Horizontal Tube, ASHRAE Transactions, Vol. 77, Part 1, pg. 210, 1971.

36. Travis, D.P. and Rohensow, W.M., The Influence of Return Bends on Downstream Pressure Drop and Condensation Heat Transfer in Tubes, Heat Transfer Laboratory, Massachusetts Institute of Technology, Cambridge, Massachusetts, 1971.

37. Staub, F.W. and Zuber, N., Void Fraction Profiles, Flow Mechanisms, and Heat Transfer Coefficients for Refrigerant 22 Evaporating in a Vertical Tube, ASHRAE Transactions, Vol. 72, 1966.

38. McAdams, W.H., Heat Transmission, McGraw-Hill, Inc., New York, New York.

39. Kelly, G.E. and Parken, W.H., Method of Testing, Rating and Estimating the Seasonal Performance of Central Air-Conditioners and Heat Pumps Operating in the Cooling Mode, NBSIR 77-1271, National Bureau of Standards, Washington, D.C., April 1978.

40. Parken, W.H., Kelly, G.E., and Didion, D.A., Method of Testing, Rating and Estimating the Heating Seasonal Performance of Heat Pumps, NBSIR 80-2002, National Bureau of Standards, Washington, D.C., April 1980.

41. American Society of Heating, Refrigerating, and Air-Conditioning Engineers, Inc., ASHRAE Standard 37-69, Methods of Testing for Rating Unitary Air Conditioning and Heat Pump Equipment, New York, New York, April 1969.

42. Hsu, Y. and Graham, R.W., Transport Processes in Boiling and Two-Phase Systems, McGraw-Hill, 1976.

43. Martin, J.J. and Hou, Y.C., Development of a New Equation of State for Gases, A.I.CH.E. Journal, Vol. 1, pp. 142-151, 1955.

44. Martin, J.J., Correlations and Equations Used in Calculating Thermodynamic Properties of Freon Refrigerants, Thermodynamics and Transport Properties of Gases, Liquids, and Solids, ASME, New York, 1959.

45. McHarness, R.C., Eiseman, B.J., and Martin, J.J., The New Thermodynamic Properties of "Freon-12," Refrigerating Engineering, Vol. 63, September 1955.

46. Freon Products Bulletin T-22, Freon" Products Division, E.I. du Pont de Nemours & Company, Wilmington, Delaware, 1966.

47. Downing, R.C., Refrigerating Equations, ASHRAE Transactions, Vol. 80, Part 2, 1974.

48. Kartsounes, G.T. and Erth, R.A., Computer Calculation of the Thermodynamic Properties of Refrigerants 12, 22, and 502, ASHRAE Transactions, Vol. 77, 1971.

49. Lewis, G.N. and Randall, M., Thermodynamics, McGraw-Hill, Inc., New York, New York, 1961.

50. ASHRAE Thermophysical Properties of Refrigerants, New York, New York, 1976.

51. Kletskii, A.V., Thermophysical Properties of Freon-22, Committee of Standards, Moscow, USSR, 1970.

52. Reid, R.C. and Sherwood, T.K., The Properties of Gases and Liquids, McGraw-Hill, Inc., New York, New York, 1966.

53. Biguris, G. and Wenzel, L.A., Industrial Engineering Chemical Fundamentals, Vol. 9, No. 1, 1970.

54. International Critical Tables, McGraw-Hill Book Co., pg. 216, New York, 1929.

55. Fischer, S.K. and Rice, C.K., A Steady-State Computer Design Model for Air-to-Air Heat Pumps, ORNL/CON-80, Oak Ridge National Laboratory, Oak Ridge, Tennessee, 1981.

56. Ellison, R.D., Creswick, F.A., Fisher, S.K., and Jackson, W.L., A Computer Model for Air-Cooled Refrigerant Condensers with Specified Refrigerant Circulating, ASHRAE Transactions, Vol. 87, 1981.

APPENDIX A. CALCULATION OF THE THERMODYNAMIC AND TRANSPORT PROPERTIES OF REFRIGERANTS R-12 and R-22

Thermodynamic property equations for refrigerants have been presented in numerous publications. The equation of state was developed by Martin and Hou [43]. A review of correlations and equations has been given by Martin [44]. Constants for these relations were published in [45] and [46] for R-12 and R-22, respectively. Downing [47] assembled refrigerant thermodynamic property equations along with constants for R-12, R-22, and ten other refrigerants.

Equations presented by Martin [2] have been supported by Du Pont and have become the accepted thermodynamic properties of refrigerants. They have been used by other authors in references [1], [2], [3], [48] and by several heat pump manufacturers.

The four basic refrigerant property equations used in the calculations are:

1. Vapor pressure at saturation
2. liquid density at saturation
3. pressure - volume - temperature behavior
4. specific heat of vapor

Refrigerant constants for these equations can be found in table A1. Other symbols are explained with each equation.

The saturation vapor pressure as a function of temperature is:

$$\ln(P) = AG + \frac{BG}{T} + CG \cdot \ln(T) + DG \cdot T + \frac{EG(FG - T)}{T} \ln(FG - T) \qquad (A1)$$

where P = vapor saturation pressure (psia)
T = vapor saturation temperature (R)

The saturated liquid density equation is:

$$\rho_L = AL + BL\left(1 - \frac{T}{TC}\right)^{BPL} + CL\left(1 - \frac{T}{TC}\right)^{CPL} + DL\left(1 - \frac{T}{TC}\right)^{DPL} + EL\left(1 - \frac{T}{TC}\right)^{EPL} \qquad (A2)$$

where ρ_L = saturated liquid density (lb/ft^3)
T = temperature of saturated liquid (R)

The constant volume specific heat at zero pressure equation is:

$$C\overset{*}{v} = AC + BC \cdot T + CC \cdot T^2 + DC \cdot T^3 + \frac{EC}{T^2} \qquad (A3)$$

where C_v^* = constant volume specific heat at zero pressure (Btu/lb • F)
T = gas temperature (R)

The equation of state is:

$$P = \frac{A1 \cdot T}{(v - B1)} + \frac{A2 + B2 \cdot T + C2 \cdot \exp(-AK \cdot T \cdot TC)}{(v - B1)^2}$$
$$+ \frac{A3 + B3 \cdot T + C3 \cdot \exp(-AK \cdot T/TC)}{(v - B1)^3} + \frac{A4 + B4 \cdot T + C4 \cdot \exp(-AK \cdot T/TC)}{(v - B1)^4}$$
$$+ \frac{A5 + B5 \cdot T + C5 \cdot \exp(-AK \cdot T/TC)}{(v - B1)^5}$$
$$+ \frac{[C6 + B6 \cdot T + C6 \cdot \exp(-A1 \cdot T/TC)]\exp(-2ALPHA \cdot v)}{[C1 + \exp(-ALPHA)]} \qquad (A4)$$

where P = vapor pressure (psia)
T = vapor temperature (R)
v = vapor specific volume (ft^3/lb)
TC = refrigerant critical temperature (R)

Using these four equations and other exact thermodynamic relations, a complete set of vapor refrigerant thermodynamic properties can be determined under any conditions.

The exact thermodynamic relations required are:

$$Cv = C_v^* + \int T \cdot \left(\frac{\partial^2 P}{\partial T^2}\right)_v dv \qquad (A5)$$

$$Cp = Cv - T \frac{\left(\frac{\partial P}{\partial T}\right)_v^2}{\left(\frac{\partial P}{\partial v}\right)_T} \qquad (A6)$$

$$s = \int \frac{C_v^*}{T} dT + \int \left(\frac{\partial P}{\partial T}\right)_v dv + Y \qquad (A7)$$

$$i = \int C_v^* \cdot dT + P \cdot v + \int \left[T\left(\frac{\partial H}{\partial T}\right)_v - P\right]dv + X \qquad (A8)$$

where the new symbols mean

Cv = vapor specific heat at constant volume
Cp = vapor specific heat at constant pressure
i = vapor enthalpy
s = vapor entropy
X,Y = constant (see table A1)

The derivation of equations (A5), (A6), (A7), and (A8) may be found in reference [49].

Besides the above equations, algorithms have to be used to calculate the specific heat at constant pressure of liquid, as well as the viscosity and conductivity of the liquid and vapor. There are many correlations available (see reference [1], [2], [3], [50], [51]) to calculate these refrigerant properties. It was decided to use those proposed by Chi [3], developed in the form of the 5th power polynomial, because they are accurate within $\pm$ 0.5 percent and easy to handle in one subroutine:

$$PROP = \sum_{j=1}^{6} A(I,J) \cdot T^{J-1} \qquad (A9)$$

where A(I,J) = twelve coefficients for calculated property (six for $T \leq 100°F$, J = 1 to 6 and six for $T > 100°F$, J = 7 to 12)
I = 1 for liquid viscosity (lb/h•ft)
I = 2 for vapor viscosity (lb/(h•ft))
I = 3 for liquid conductivity (Btu/(h•ft•F))
I = 4 for vapor conductivity (Btu/(h•ft•F))
I = 5 for liquid specific heat at constant pressure (Btu/(lb•F))
T = saturated temperature (F)
PROP = calculated property at saturated temperature

The coefficients to be used in equation (A9) are given in table A2. Equation (A9) allows for the computation of the refrigerant property values at saturation temperature. For those in the superheated state, there is a need to account for the effect of temperature on viscosity and conductivity. This can be done by using the power law, since viscosity and conductivity may be said to be proportional to T^n. The exponent, n, varies with temperature and is assumed in this document to equal 0.5 as called for by the kinetic theory of gases [52].

In conclusion, eight functions and subroutines are used in the HPSIM heat pump simulation program to determine the refrigerant thermodynamic and transport properties. The equations described in this appendix are applied with constants presented in tables A1 and A2. The listing of these subprograms are given along with other subprograms, in appendix J. Input and output data are explained in the form of comment statements in each routine. For a quick reference, a list and application of refrigerant property routines is also given in table A3.

Table A1. Coefficients and Physical Constants for Freon-12 and Freon-22 to be used in Equations (A1) through (A8)

Coefficients and Physical Constants	FREON-12	FREON-22
TC	6.9330000E+02	6.6450000E+02
PC	5.9690000E+02	7.2191000E+02
VC	2.8700000E+02	3.0525000E-02
AG	9.1835883E+01	6.7598246E+01
BG	-7.9131381E+03	-8.8538843E+03
CG	-1.2471522E+01	-7.8610310E+00
DG	1.0892245E-02	5.0448235E-03
EG	0.	4.4574600E-01
FG	0.	6.8610000E+02
AL	3.4840000E+01	3.2760000E+01
BL	1.8601368E+01	5.4634409E+01
CL	2.1983963E+01	3.6748920E+01
DL	5.3341175E+01	-2.2292560E+01
EL	-3.1509939E+00	2.0473289E+01
BPL	1.	3.3333333E-01
CPL	5.0000000E-01	6.6666667E-01
DPL	3.3333333E-01	1.
EPL	2.	1.3333333E+00
A1	8.8734000E-02	1.2409800E-01
B1	6.5093890E-03	2.0000000E-03
C1	0.	0.
A2	-3.4097270E+00	-4.3535470E+00
B2	1.5943480E-03	2.4072520E-02

Table A1. (Continued)

Coefficients and Physical Constants	FREON-12	FREON-22
C2	-5.6762767E+01	-4.4066868E+01
A3	6.0239450E-02	-1.7464000E-02
B3	-1.8796180E-05	7.6278900E-05
C3	1.3113990E+00	1.4837630E+00
A4	-5.4873700E-04	2.3101420E-03
B4	0.	-3.6057230E-06
C4	0.	0.
A5	0.	-3.7240440E-05
B5	3.4688340E-09	5.3554650E-08
C5	-2.5439070E-05	-1.8450510E-04
A6	0.	1.3633870E+08
B6	0.	-1.6726130E+05
C6	0.	0.
ALPHA	0.	5.4820000E+02
AK	5.4750000E+00	4.2000000E+00
AC	8.0945000E-03	2.8128360E-02
BC	3.3266200E-04	2.2554080E-04
CC	-2.4138960E-07	-6.5096070E-08
DC	6.7236300E-11	0.
EC	0.	0.
FC	0.	2.5634100E+02
X	3.9556551E+01	6.2400900E+01
Y	-1.6537940E-02	-4.5333500E-02

Table A2. Coefficients for Freon-12 and Freon-22 to be Used in Equation (A9)

Coefficients	Freon-12	Freon-22
A(1,1)	0.75800E+00	0.64600E+00
A(1,2)	0.44230E-02	0.29194E-02
A(1,3)	0.22659E-04	0.12164E-04
A(1,4)	-0.80937E-07	-0.74985E-07
A(1,5)	0.48640E-09	0.83951E-09
A(1,6)	-0.38993E-11	-0.37512E-11
A(1,7)	0.16672E+01	0.69684E+01
A(1,8)	0.37691E-01	0.24319E+00
A(1,9)	0.48998E-03	0.35924E-02
A(1,10)	-0.32598E-05	-0.26187E-04
A(1,11)	0.10701E-07	0.93884E-07
A(1,12)	0.14069E-10	0.13301E-09
A(2,1)	0.26200E-01	0.26600E-01
A(2,2)	0.58000E-04	0.63804E-04
A(2,3)	0.0	0.10761E-06
A(2,4)	0.0	0.32061E-08
A(2,5)	0.0	0.43463E-10
A(2,6)	0.0	0.13175E-12
A(2,7)	0.10065E+01	0.66330E+00
A(2,8)	0.37971E-01	0.25757E-01
A(2,9)	0.53504E-03	0.37913E-03
A(2,10)	0.36443E-05	0.27734E-03
A(2,11)	0.12032E-07	0.10053E-07
A(2,12)	0.15478E-10	0.14474E-10
A(3,1)	0.49000E-01	0.63000E-01
A(3,2)	0.11950E-03	0.15820E-03
A(3,3)	0.36320E-07	0.12289E-06
A(3,4)	0.52080E-09	0.17453E-08
A(3,5)	0.31690E-11	0.52685E-11
A(3,6)	0.31689E-13	0.10856E-13
A(3,7)	0.33483E+00	0.46705E+00
A(3,8)	0.10635E-01	0.19421E-01
A(3,9)	0.14902E-03	0.28507E-03
A(3,10)	0.10214E-05	0.20429E-05
A(3,11)	0.34038E-08	0.71963E-08
A(3,12)	0.44300E-11	0.99460E-11
A(4,1)	0.43000E-02	0.48000E-02
A(4,2)	0.17000E-04	0.19881E-04
A(4,3)	0.0	0.24815E-08
A(4,4)	0.0	0.28518E-09
A(4,5)	0.0	0.62001E-11
A(4,6)	0.0	0.31001E-13
A(4,7)	0.12814E+00	0.51539E+00

Table A2. (Continued)

Coefficients	Freon-12	Freon-22
A(4,8)	0.48691E-02	0.18936E-05
A(4,9)	0.68452E-04	0.26762E-03
A(4,10)	0.46711E-06	0.18936E-05
A(4,11)	0.15484E-08	0.65891E-08
A(4,12)	0.20038E-11	0.90041E-11
A(5,1)	0.21700E+00	0.27100E+00
A(5,2)	0.14160E-03	0.24054E-03
A(5,3)	0.64705E-06	0.38936E-07
A(5,4)	0.55390E-08	0.23481E-07
A(5,5)	0.13779E-10	0.97345E-10
A(5,6)	0.17912E-12	0.44953E-12
A(5,7)	0.15409E+01	0.49002E+00
A(5,8)	0.64802E-01	0.83123E-02
A(5,9)	0.91255E-03	0.13105E-03
A(5,10)	0.62141E-05	0.96844E-06
A(5,11)	0.20422E-07	0.36462E-08
A(5,12)	0.26255E-10	0.52089E-11

Table A3. Refrigerant Property Functions and Subroutines

Property Function or Subroutine	Application
CPCV	Calculate specific heat at constant volume and at constant pressure, specific heat ratio, and sonic velocity of refrigerant vapor from temperature and pressure.
ITRPR	Iterate refrigerant vapor thermodynamic properties from given pressure and specific volume or enthalpy or entropy.
SATP	Calculate refrigerant saturation pressure from given temperature.
SATPR	Calculate dynamic viscosity, thermal conductivity of liquid and vapor, and refrigerant liquid specific heat at saturation from given temperature.
SATT	Calculate refrigerant saturation temperature from given pressure.
SATVF	Calculate specific volume of saturated liquid refrigerant from given temperature.
VPSV	Calculate specific volume of vapor from given temperature and pressure.
VPVHS	Calculate refrigerant vapor thermodynamic properties from given temperature and pressure.

APPENDIX B. CALCULATION OF PROPERTIES OF MOIST AIR

For the selection of moist air property equations, it was assumed that air dry bulb temperature, T, relative humidity, and pressure would be known and the properties that would be the output were: humidity ratio, specific heat at constant pressure, gas constant, dynamic viscosity, and thermal conductivity. Presented here are the psychometric equations in their fundamental form. They are derived assuming moist air to be a mixture of two independent perfect gases, so that the perfect gas equation of state and Dalton's rule can be applied. The transport properties, dynamic viscosity, and thermodynamic conductivity of air are assumed to be negligibly affected by the moisture content. Correlations for these two properties were based on dry air data.

Relations of this appendix were applied in air properties subroutine AIRPR.

The humidity ratio is determined by:

$$w = 0.622\ PSAT/(PATM - \phi \cdot PSAT) \tag{B1}$$

where PATM = atmospheric pressure
PSAT = saturation pressure of water vapor at temperature T
w = humidity ratio (lb water/lb dry air)
ϕ = relative humidity (-)

The saturated water vapor pressure, PSAT (psi), is calculated by the polynominal approximation:

For $T > 32°F$

$$PSAT = \exp(19.504 - 10.431z - 0.2755z^2 + 0.03940z^3)$$

For $32 \leq$ to $< 180°F$

$$PSAT = \exp(13.4353 - 5.0988z - 1.6896z^2 + 0.17829z^3)$$

For $T \geq 180°F$

$$PSAT = \exp(16.8255 - 14.213z + 7.5568z^2 - 4.01506z^3 + 0.17692z^4)$$

where $$z = \frac{1000}{460 + T} \tag{B2}$$

The specific heat at constant pressure is:

$$Cp = (Cp_{dry} + 0.444)/(1 + w) \tag{B3}$$

where Cp = specific heat at constant pressure of moist air (Btu/(lb moist air • F))
Cp_{dry} = specific heat at constant pressure of dry air (Btu/(lb • F))
w = humidity ratio (lb water/lb dry air)

The specific heat at constant pressure of dry air is approximated by the following polynominal:

$$Cp_{dry} = 0.2478786 - 0.4204563 \cdot 10^{-4} \cdot TR + 0.567857 \cdot 10^{-7} \cdot TR^2 - 0.14936056\ TR^3 \quad \text{(B4)}$$

where TR = T + 460°F is the dry bulb air temperature on the Rankine scale

The gas constant is:

$$R = (53.34 + 85.76 \cdot w)/(1 + w) \quad \text{(B5)}$$

where R = moist air gas constant $(\frac{lbf \cdot ft}{lb \cdot R})$

w = humidity ratio (lb water/lb dry air)

The dynamic viscosity and thermal conductivity values are obtained from the respective equations:

$$\mu = 5.5029 \cdot 10^{-3} + 8.7157 \cdot 10^{-5}\ TR - 2.9464 \cdot 10^{-8} TR^2 + 6.25 \cdot 10^{-12} TR^3 \quad \text{(B6)}$$

$$k = -2.853 \cdot 10^{-4} + 3.268 \cdot 10^{-5}\ TR - 8.253 \cdot 10^{-9} TR^2 + 1.239 \cdot 10^{-12} TR^3 \quad \text{(B7)}$$

where k = moist air thermal conductivity (Btu/(h•F•ft))
TR = 460 + T = dry bulb air temperature on the Rankine scale (R)

APPENDIX C. CALCULATION OF WATER AND FROST PROPERTIES

The equations presented below are for calculation of the properties of water and frost deposited on a heat pump evaporator outer surface. These properties, for specific conditions, are either solely a function of temperature or can be assumed to be constant. The equations below are used in the water and frost properties subroutine WATPR.

The following fourth degree polynomial expression is used for calculating water density, conductivity, dynamic viscosity and latent heat of condensation:

$$PROP = \sum_{I=1}^{5} A(I) \cdot T^{I-1} \qquad (C1)$$

where A(I) = five constants per calculated property
PROP = calculated property
T = water temperature (F)

Constants A(I) for each property are given in table C1. The specific heat of water at constant pressure is assumed to be independent of temperature and to have a constant valu of $Cp = 1 \frac{Btu}{lb \cdot F}$.

The density of frost, as proposed in [53], is calculated by the following equation:

$$\rho_f = \exp(b1 + b2 \cdot (TW - TP)) \qquad (C2)$$

where $b1 = 11.9521 + 0.02422\ TPR + 35.5498\ WA - 9.1742 \cdot 10^{-7}\ VA + 3.1138 \cdot 10^{-9}\ VA \cdot TPR - 0.03838$
$b2 = 13.1606 - 0.02133\ TPR - 81.955\ WA/32.018 - TP$
TP = tube temperature (F)
TPR = TP + 460. tube temperature (R)
TW = water (frost) temperature (F)
WA = air humidity ratio
VA = air velocity (ft/sec)
ρ_f = density of frost (lb/ft^3)

The frost conductivity, as proposed in [54], is calculated by the equation:

$$k_f = 0.012138 + 3.8909\ 10^{-3} \cdot \rho_f + 5.1409\ 10^{-6} \cdot \rho_f^3 \qquad (C3)$$

where k_f = frost conductivity ($Btu/(h \cdot F \cdot ft)$)
ρ_f = frost density (lb/ft^3)

Frost heat of sublimation, h_{SUBL}, and frost specific heat, C_f, are assumed to have the following constant values:

$h_{SUBL} = 1219.0$ Btu/lb
$C_f = 0.46$ Btu/(lb•F)

Table C1. Water Property Evaluation Constants which are Used in Equation (C1)

Calculated Property A(I)	Density lb/ft^3	Dynamic viscosity lb/(h•ft)	Thermal conductivity Btu/(h•F•ft)	Latent heat of condensation Btu/lb
A(1)	0.11647 E+03	0.79422 E+03	-0.27694	0.31514 E+04
A(2)	-0.40054	0.47589 E+01	0.45215 E-03	0.13714 E+02
A(3)	0.10815 E-02	0.10622 E-01	0.49008 E-05	0.35945 E-01
A(4)	0.12387 E-05	0.10416 E-04	0.88613 E-08	0.43525 E-04
A(5)	0.49002 E-09	0.37690 E-08	0.41387 E-11	0.19695 E-07

APPENDIX D. COMPRESSOR SIMULATION SUBROUTINE PERCOM

Reference is made to figure 4 where the configuration of the main heat pump components is shown. It was decided to cover in one subroutine called PERCOM all refrigerant processes from point 1 to point 10. The refrigerant path covered by this subroutine consists of:

- flow through a suction tube 1-2 and discharge tube 9-10
- flow through a reversing valve on suction side 2-3 and discharge side 8-9
- flow through a compressor 3-8

Input data to PERCOM is detailed in comment statements inserted in the program. Basically it consists of:

- connecting tube parameters
- four-way valve parameters
- compressor parameters
- ambient air conditions
- refrigerant state at the compressor can inlet (point 3)
- refrigerant pressure at discharge (point 6)

Compressor and four-way valve parameters have to be found from a laboratory test. For a four-way valve, these parameters are heat transfer and pressure drop parameters and can be calculated with aid of the program VALPAR. In the case of a compressor, parameters to be found are:

η_e = electric motor efficiency versus load
RPM = electric motor speed (RPM) versus load
η_m = compressor mechanical efficiency
C_e = compressor effective clearance
η_p = compressor polytropic efficiency
$CQ_{4,5}$, $CQ_{6,7}$, $CQ_{7,8}$, $CQ_{3,C}$, $CQ_{C,A}$ = heat transfer parameters
$CP_{3,4}$, $CP_{4,5}$, $CP_{6,7}$, $CP_{7,8}$ = pressure drop parameters

One of the parameters, the compressor mechanical efficiency, η_m, is assumed here to be constant and equal to 0.96. The rest of the parameters can be calculated by means of subroutine COMPAR. Efficiency, η_e, and RPM as functions of mechanical load are both part of typical electric motor characteristics for its class, (see figures 10 and 12). Coefficients describing these curves are required as an input to COMPAR. In the course of these calculations, new coefficients are computed which retain the shape of the characteristics curves, although a change in absolute values of these coefficients does occur according to test data supplied. The rest of the parameters (compressor effective clearance, compressor polytropic efficiency, five heat transfer parameters, and four pressure drop parameters) are calculated by COMPAR using test data and relations presented in section 5.2.2. Subroutine COMPAR is called by the main program MAIN. Logic of PERCOM may be followed by looking at the program listing with inserted comment statements. Based on a known refrigerant state at the can inlet (point 3), refrigerant parameters at the suction valve (point 5) are guessed and since compression pressure is given, the compression can be

computed. Using the refrigerant mass flow rate from this computation and applying equations given in section 5.2.2, enthalpy and pressure balances are conducted. If balance is not reached, the guess of the refrigerant state at the suction valve, point 5, is adjusted. Calculations are repeated until balances are satisfied.

Once refrigerant states at compressor stations 3 to 8 and the mass flow rate are known, other refrigerant paths are computed. Simulation of a four-way valve and pipes are done by routines VALVE4 and PIPEPI respectively.

Output from subroutine PERCOM is detailed in the program comment statements and consists of refrigerant thermodynamic properties for points 1 to 10, refrigerant mass flow rate, compressor RPM, energy consumption rate, electric motor efficiency, compression efficiency, and volumetric efficiency.

APPENDIX E. CALCULATION OF CRITICAL PRESSURE FOR TWO-PHASE FANNO FLOW

In this appendix, the procedure is explained for calculation of critical pressure of a flow if mass flow rate and stagnation enthalpy are given. The procedure focuses on the fact that Fanno flow assumes maximum entropy at the flow critical pressure. Hence, the point of maximum entropy on the Fanno line is being sought and once determined, the choking pressure is found.

The entropy of two-phase flow is calculated by the equation:

$$s = s_L + x(s_V - s_L) \tag{E1}$$

where s = entropy
x = quality
subscripts L and V refer to liquid and vapor phase, respectively.

Since the entropy of saturated liquid and of saturated vapor, s_L and s_V, are known for a given pressure, the entropy of two-phase flow can be found if the quality is known.

The quality for Fanno flow can be found using the energy equation:

$$i_o = i + \frac{G^2}{2} \cdot v^2 \tag{E2}$$

where G = mass flux
i = enthalpy
i_o = stagnation enthalpy
v = specific volume

Two-phase specific enthalpy and specific volume are:

$$i = i_L + x(i_V - i_L) \tag{E3}$$

$$v = v_L + x(v_V - v_L) \tag{E4}$$

Substituting and rearranging, the following quadratic equation can be obtained:

$$x^2 + x \cdot b + c = 0 \tag{E5}$$

where $$b = \frac{2(v_V - v_L) \cdot v_L \cdot G^2 + i_V - i_L}{G^2(v_V - v_L)^2}$$

$$c = \frac{2(i_L - i_o)}{G^2} + v_L^2 \frac{1}{(v_V - v_L)^2}$$

Equations (E5) allows calculation on the quality for given Fanno flow (mass flux and stagnation enthalpy known) at a particular pressure. This quality can then

be used to find entropy by equation (E1). Thus the maximum entropy and the critical pressure of the flow can be found numerically.

Search for the maximum entropy along the Fanno flow path was tried by two different iteration methods. The Newton-Raphson method appeared to be unstable for single-precision calculations. Stability of this method could be assured by performing calculations in the double precision mode. Such calculations consume twice as much computing time as single-precision calculations and would require keeping some refrigerant property subroutines as double precision routines. It was felt to be more reasonable to use the binary search method. The binary search method is not as efficient as the Newton-Raphson method; however, it provides a stable solution in single-precision calculations for maximum entropy.

APPENDIX F. CAPILLARY TUBE SIMULATION SUBROUTINE EXDEV

The purpose of the capillary tube simulation routine is to calculate the refrigerant mass flow rate when capillary dimensions, refrigerant inlet state, and pressure in the evaporator are given. Depending on the above input, there are several possible capillary tube operation modes. For example, the refrigerant can be either a single or a two-phase state prior to the tube entrance. If there is a two-phase mixture at the inlet (a highly undesirable but possible condition under very low load operating conditions), two-phase flow will exist along the whole tube length.

For a subcooled liquid at the inlet, there are three flow alternatives:

- liquid flow only along the whole tube length
- liquid flow in the front portion of the tube and two-phase flow in the further portion of the tube
- two-phase flow only along the whole tube length

Each of the above flow situations can exist with or without choking condition at the tube exit. The capillary tube simulation routine EXDEV developed in this study can distinguish among all of the above operational modes. During the course of the calculations, the refrigerant critical pressure is found by routine PCHOKE using a binary search iteration method. Then equations (38), (43), and (48) are used to compute the refrigerant mass flow rate. The density-pressure integral in equation (48) is evaluated by routine TSIMP based on a Simpson's rule. An iteration solution is required to obtain the final simulation result since choking pressure, friction factor, fractions of tube length with liquid and two-phase flow, and the velocity head used to correct enthalpy are functions of refrigerant mass flow rate which has to be found. The Newton-Raphson method is used in the iteration for the final EXDEV solution. The logic of the routine EXDEV is presented in figure F1. The input and output data are listed in comment statements in this routine.

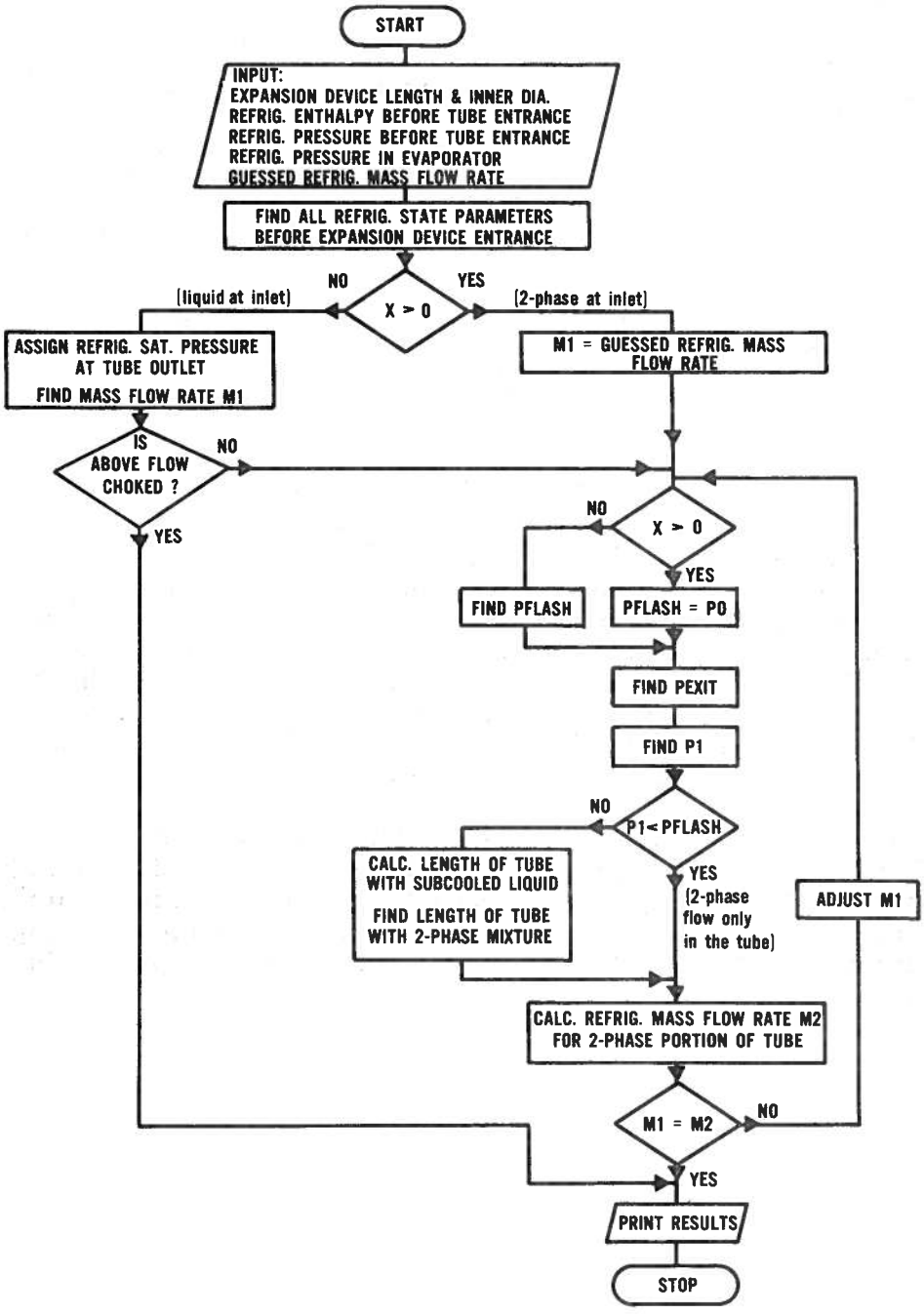

Figure F1. Logic of constant flow area expansion device simulation program EXDEV

APPENDIX G. EVAPORATOR AND CONDENSER SIMULATION SUBROUTINES EVPHXM AND CNDNEW

The tube-by-tube approach to coil simulation has been explained in section 5.4 where applicable heat, mass, and momentum transfer equations have also been presented. Though the evaporator and condenser simulation programs require somewhat different heat transfer relations, their logic is the same as shown in figure G1.

The input to coil simulation program is coil design data, refrigerant flow distribution sequence, and air and refrigerant inlet conditions. During the first bank of tubes' performance calculations, the air parameters upstream of each tube row are estimated. The program then computes the heat transfer rate and pressure drop tube-by-tube from the inlet to the exit of the coil. Mean refrigerant properties in each tube are used to calculate heat transfer rates and pressure drops applying equations described in section 5.4. An iterative procedure is used for each tube since only refrigerant conditions at tube inlet are known when the calculations start, and initially the average refrigerant properties in a tube have to be assumed to be those at the inlet conditions. Upstream air temperature and humidity ratio may not be accurately known at the time tube performance is being calculated, so a second iterative loop is used to update air-side data after each round. It should be realized that, while in the condenser case, update of air-side data means update of air temperature and humidity ratio; for the evaporator it also includes liquid (frost) layer thickness. When refrigerant enthalpy values at the coil exit obtained from two consecutive loops are within the imposed tolerance, the calculations of coil performance are completed and results printed.

Both the evaporator coil simulation model EVPMXM and condenser coil simulation model CNDNEW comply with the logic and equations previously described[6/]. Input and output data for these programs are detailed in comment statements at the beginning of each subroutine. Other inserted comment statements along with the flow chart (figure G1) facilitate the understanding of both program's organization.

6/ For reasons of organization of the overall heat pump simulation program, EVPHXM performs evaporator calculations backwards from the evaporator exit to the inlet.

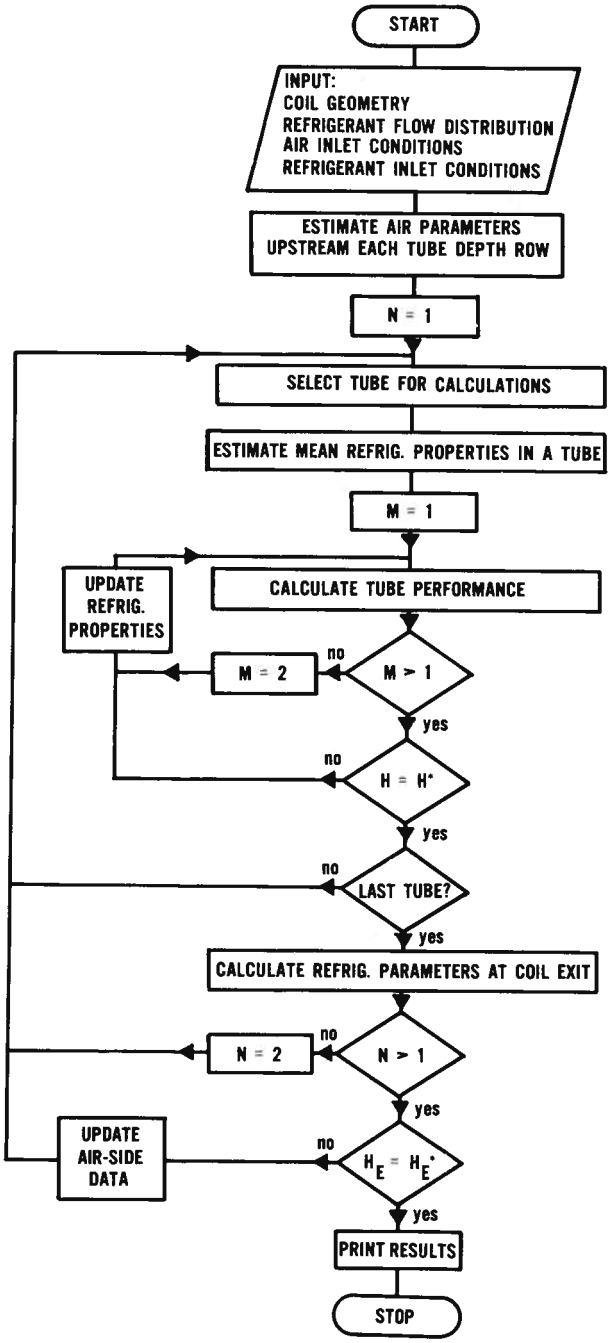

Figure G1. Flow chart for coil simulation program

APPENDIX H. THE LOGIC FOR THE MAIN PROGRAM, MAIN

The principle of the logic for the heat pump model has been explained in section 5.1.2. It is based on three balances:

- enthalpy balance
- pressure balance
- mass balance

The enthalpy balance and pressure (mass flow rate) balance are interdependent and have to be found in a simultaneous iteration process. Their solution provides refrigerant properties in the system which are required for mass inventory calculations. The balances are performed in the manner as shown in figure H1, which presents the logic developed during this study and contained in the main program MAIN.

The objective of the logic is to iterate refrigerant states at key locations of a heat pump for given outdoor and indoor conditions. The addresses of the key locations used in the program MAIN are consistent with those marked in figures 4 and H1:

1 - evaporator exit, suction pipe inlet
2 - suction pipe outlet, low pressure 4-way valve inlet
3 - low pressure 4-way valve exit, compressor can inlet
4 - inside compressor can
5 - compressor cylinder at suction
6 - compressor cylinder at discharge
7 - discharge manifold
8 - compressor can exit, high pressure 4-way valve inlet
9 - high pressure 4-way valve exit, discharge pipe inlet
10 - discharge pipe outlet, condenser inlet
11 - condenser outlet, liquid line inlet
12 - liquid outlet, expansion device outlet
13 - evaporator inlet

The thermodynamic processes shown in figure H1 and figure 5 are covered by five subroutines: PERCOM, CNDNEW, LQLINE, EXDEV and EVPHXM. The iteration process starts with a guessed refrigerant pressure and vapor superheat at the compressor can inlet and with guessed compressor discharge pressure (points 3 and 6). From these data, the compressor performance simulation subroutine PERCOM computes the refrigerant mass flow rate through the compressor and refrigerant parameters from point 1 to 10. The condenser and liquid line subroutines CNDNEW and LQLINE are called next to perform calculations which yield refrigerant states at point 11 and 12. Subsequently, the expansion device simulation program EXDEV computes refrigerant mass flow rate through the flow restrictor. At this point, the mass flow rate through the compressor, RMASS, and mass flow rate through the expansion device, XMASS, are compared and mass flow balance is sought. This is done by resuming calculations by PERCOM, CNDNEW, LQLINE, and EXDEV, holding constant refrigerant parameters at the compressor can inlet (point 3) and adjusting refrigerant saturation

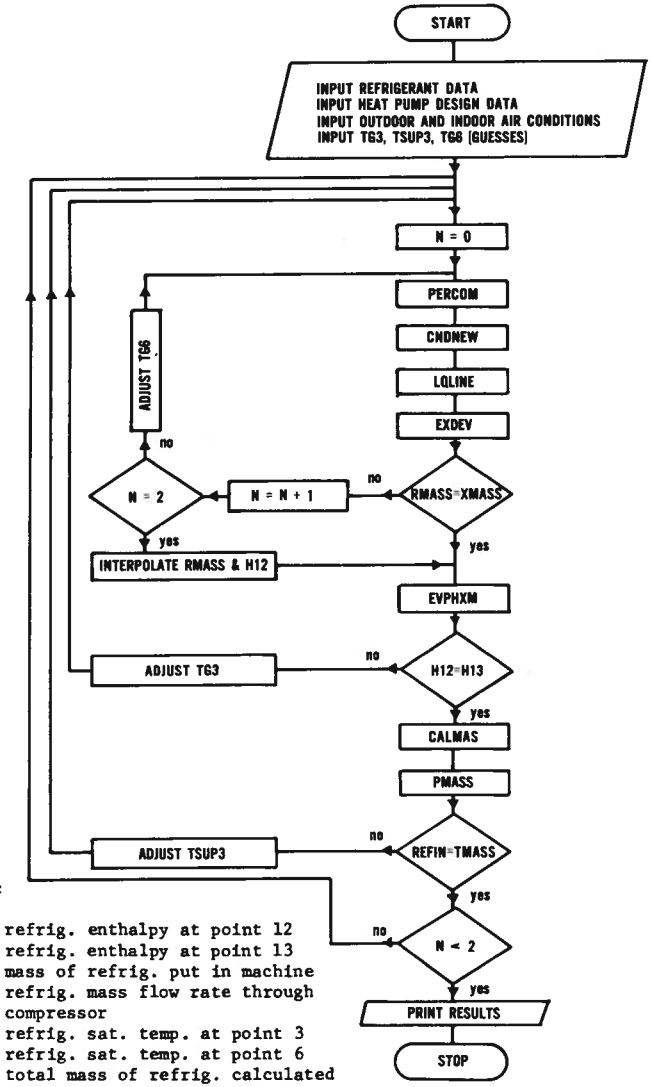

Symbols:

H12 - refrig. enthalpy at point 12
H13 - refrig. enthalpy at point 13
REFIN - mass of refrig. put in machine
RMASS - refrig. mass flow rate through compressor
TG3 - refrig. sat. temp. at point 3
TG6 - refrig. sat. temp. at point 6
TMASS - total mass of refrig. calculated by inventory
TSUP3 - refrig. superheat at point 3
XMASS - refrig. mass flow rate through expansion device

PERCOM - calculates performance of compressor with 4-way valve and tubings connecting compressor with both coils
Input: refrig. state at point 3 and pressure at point 6
Output: RMASS and refrig. state at points 1 through 10

CNDNEW - calculates performance of condenser
Input: RMASS and refrig. state at point 10
Output: refrig. state at point 11

LQLINE - calculates pressure drop in a liquid line
Input: RMASS and refrig. state at point 11
Output: refrig. state at point 12

EXDEV - calculates performance of expansion device
Input: refrig. state at point 12 and pressure at point 13
Output: XMASS

EVPHXM - calculates performance of evaporator
Input: RMASS and refrig. state at point 1
Output: refrig. state at point 13

CALMAS - calculates mass of refrig. in a coil
Input: refrig. state at each coil tube end
Output: mass of refrig. in a coil

PMASS - calculates mass of refrig. in a pipe
Input: refrig. state at tube ends
Output: mass of refrig. in a pipe

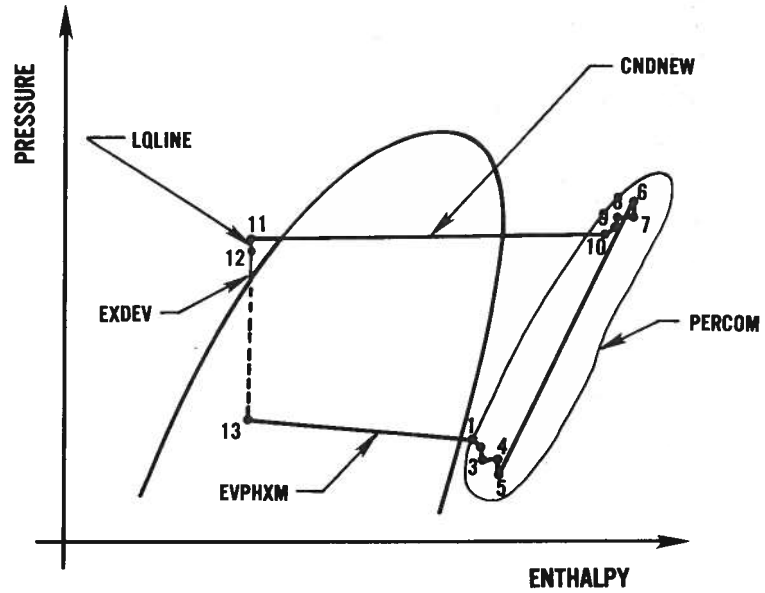

Figure H1. Heat pump simulation program HPSIM flow chart

temperature at discharge (point 6) until an appropriate saturation temperature at point 6 is found at which RMASS and XMASS are equal.

The evaporator performance simulation routine, EVPHXM, was chosen in this logic to be run after the mass flow balance between the compressor and expansion device has been found. (EVPHXM requires the most computing time of all the subroutines.) The subroutine EVPHXM computes evaporator performance in a backward scheme from the actual flow direction with the refrigerant state at point 1 and mass flow rate as input, yielding the refrigerant state at point 13 as output. As the thermodynamic processes in the liquid line and flow restrictor are adiabatic, enthalpy at point 12, H12, should be equal to that at evaporator inlet, H13. If they are not equal, the refrigerant state at point 3 (i.e., saturation temperature) is adjusted and all calculations have to be repeated from the beginning. (The other parameter defining the refrigerant state at point 3, the refrigerant superheat, is left unchanged.)

Once an enthalpy balance and mass flow balance are established, two out of three refrigerant parameters guessed at the beginning are temporarily obtained. To verify the third guessed parameter, i.e., the refrigerant vapor superheat at the compressor can inlet, the refrigerant mass inventory in the system is used. Each time it is performed, it provides a result based on refrigerant states in the system found after solving enthalpy and pressure balances with the assumed vapor superheat at point 3. If the amount of refrigerant obtained from mass inventory calculations is smaller than the refrigerant put into the system, the superheat guess has to be decreased and all calculations have to be repeated from the beginning. If the superheat is equal to zero and the mass inventory result is still smaller than refrigerant mass input, it means that some of the refrigerant is stored in the form of liquid in the accumulator and saturated vapor is entering the compressor. This situation or the equality between the mass inventory results at design and actual operating conditions marks an end of the iteration process and the results are printed.

In the course of the computing process, the main program gathers information about the heat pump components' performance, updated at each iteration loop, and applies them to anticipate changes of some parameters caused by a change in some state property. This allows for the iteration process to converge faster with each iteration loop. The Newton-Raphson iteration procedure is used in the solution of the main program.

APPENDIX I. PROGRAM USER'S GUIDE

HPSIM is written in Fortran IV and makes use of standard Fortran mathematical functions. It is built around the main program, MAIN, and 41 subprograms for heat pump component simulation, and heat transfer, fluid mechanics, and fluid property calculation. Relations used in the heat pump component simulation subprograms, and fluid mechanics and heat transfer routines are described in the main text of this report. Equations used in the refrigerant, moist air, water, and frost property routines are described in appendices A, B, and C.

All subprograms and routines used in heat pump simulation program are listed in alphabetic order in table I1, with a short statement of their application. The program HPSIM occupies 31000 decimal words of core memory of Univac 1108 computer.

I.1 INPUT DATA CODING

There are five categories of input values for the HPSIM runs, namely:

- heat pump data;
- refrigerant physical constants;
- run controlling data;
- indoor/outdoor air conditions;
- refrigerant parameters (guesses).

Refrigerant physical constants and heat pump design data are read into the program from a disk file. File 7 and file 8 are used in reading statements which input these data for the refrigerant properties and heat pump design data, respectively. The physical constants for refrigerants 12 and 22 in proper input format are given in tables I2 and I3. The heat pump design data input code is presented in table I4. Included are the Fortran symbols with their explanation. One example of heat pump input data in original format is given in table I5.

Run control data, indoor/outdoor air conditions, design data, and refrigerant property guesses are input at the terminal. They are clearly solicited by the program and responses have to be given as follows:

1. Request PERFORMANCE(1) or COMPRESSOR PARAMETERS(2), IPTP =

   Response: 1 for heat pump performance evaluation

   or 2 for compressor parameters evaluation

2. Request: ANSWER 1 FOR YES OR 0 FOR NO
   DO YOU WANY ANY INPUT DATA PRINTED? LPF =

   Response: 0 for no input data print

   or 1 for input data printout (request for specification of desired data will follow)

3. Request: NSYS = 1 FOR HEATING, NSYS = 2 FOR COOLING
LONG = 1 IF REFRIGERANT CHARGE BALANCE REQUIRED, OTHERWISE PUT LONG = 0

Response: as explained in the request

4. Request: TG3, TSUP3, TG6

Response: TG3 = saturation temperature of refrigerant vapor at compressor can inlet (F)

TSUP 3 = refrigerant vapor superheat at compressor can inlet (F)

TG6 = saturation temperature of refrigerant vapor in compressor cylinder after compression (all guesses, subject to iteraction)

5. Request: POA, TOA, RHOA, PRA, TRA, RHRA = ?

Response: POA = outside air pressure (psia)

TOA = outside air temperature (F)

RHOA = outside air relative humidity (decimal fraction)

PRA = indoor air pressure (psia)

TRA = indoor air temperature (F)

RHRA = indoor air relative humidity (decimal fraction)

6. Request: I = 999 for DISCONTINUATION?

Response: 999 to terminate HPSIM runs, otherwise enter any other number, then system will repeat requesting data from 1 to 5 for the next HPSIM run.

All input data symbols follow general Fortran practice. Variables beginning with I to N are integers, and all other letters represent real numbers. Free field input format is used for all input variables.

I.2 OUTPUT DATA CODING

Output data consists of refrigerant thermodynamic states at 13 heat pump key locations, identified on figure 4, along with results describing the heat pump performance. Symbols used for output data have the following meaning:

T,P,H,S,X - refrigerant temperature (F), pressure (psia), enthalpy (Btu/lb), entropy, (Btu/(lb • F), quality (-)

Table I1. Programs Used in a Heat Pump Simulation Model HPSIM

PROGRAM	PURPOSE
AIRHT	Calculate air-side finned tube heat transfer coefficient
AIRPR	Calculate moist air properties
CALMAS	Calculate mass of refrigerant in a coil
CNDHTC	Calculate condensation heat transfer coefficient inside a tube
CNDNEW	Simulate condenser performance
COMPAR	Calculate compressor performance parameters
CPCV	Calculate specific heat of vapor refrigerant
DISFLW	Determine refrigerant flow distribution in a coil
DYNADP	Calculate dynamic pressure drop for single-phase flow
DYNDP2	Calculate dynamic pressure drop for two-phase flow
EVPDP	Calculate frictional evaporation pressure drop
EVPHT1	Calculate evaporation heat transfer coefficent
EVPHXM	Simulate evaporator performance
EXDEV	Simulate expansion device performance
FEEDP	Calculate correction factor for 2-phase pressure drop
FINEFF	Calculate fin efficiency
FLASH	Calculate flashing temperature and pressure for Fanno flow
ITRPR	Iterate refrigerant vapor thermodynamic properties from given pressure and other than temperature property
LQLINE	Calculate pressure drop in a liquid line
MAIN	Read input data, iterate heat pump simulation solution, print results
OVLHTC	Calculate overall heat transfer coefficient for dry finned tube

PROGRAM	PURPOSE
PCHOKE	Calculate critical pressure for two-phase Fanno flow
PERCOM	Simulate compressor performance
PIPEPI	Simulate pipe performance
PMASS	Calculate refrigerant mass in a tube
RHOM	Calculate two-phase mixture density on Fanno flow path
SATP	Calculate refrigerant saturation pressure
SATPR	Calculate refrigerant properties at saturation
SATT	Calculate refrigerant saturation temperature
SATVF	Calculate specific volume of saturated refrigerant liquid
SFANNO	Calculate two-phase mixture entropy for Fanno flow
SPHDP	Calculate frictional single-phase pressure drop in a tube
SPHDP1	Calculate frictional single-phase pressure drop in a tube
SPHTC	Calculate single-phase heat transfer coefficient
TSIMP	Integrate using Simpson's rule
UPWAO	Calculate overall conductance for wet finned tube
VALPAR	Calculate reversing valve performance parameters
VALVE4	Simulate reversing valve performance
VPSV	Calculate refrigerant vapor specific volume
VPVHS	Calculate refrigerant parameters at and above saturation
WATPR	Calculate water and frost properties
XTTCAL	Calculate Lockhard-Martinelli parameter

Table I2. Date File DATA12 Containing Physical Constants for Refrigerant 12 in the Input Format to Program HPSIM

```
Q$Q$Q$*DATA12(1)
      1         FREON-12
      2       6.9330000E+02,5.9690000E+02,2.8700000E-02
      3       4.5967000E+02,1.8505300E-01,2.7182818E+00
      4       9.1835883E+01,-7.9131381E+03,-1.2471522E+01
      5       1.0892245E-02,0.,0.
      6       120.,312.
      7       3.4840000E+01,1.8691368E+01,2.1983963E+01
      8       5.3341175E+01,-3.1509939E+00,1.
      9       5.0000000E+01,3.3333333E-01,2.
     10       8.8734000E-02,6.5093890E-03,0.
     11       -3.4097270E+00,1.5943480E-03,-5.6762767E+01
     12       6.0239450E-02,-1.8796180E-05,1.3113990E+00
     13       -5.4873700E-04,0.,0.
     14       0.,3.4688340E-09,-2.5439070E-05
     15       0.,0.,0.
     16       0.,5.4750000E+00
     17       8.0945000E-03,3.3266200E-04,-2.4138960E-07
     18       6.7236300E-11,0.,0.
     19       3.9556551E+01,-1.6537940E-02
     20       0.75800E+00,-0.44230E-02,0.22659E-04
     21       -0.80937E-07,0.48640E-09,-0.38993E-11
     22       0.16672E+01,-0.37691E-01,0.48998E-03
     23       -0.32598E-05,0.10701E-07,-0.14069E-10
     24       0.26200E-01,0.58000E-04,0.0
     25       0.,0.,0.
     26       -0.10065E+01,0.37971E-01,-0.53505E-03
     27       0.36446E-05,-0.12032E-07,0.15478E-10
     28       0.49000E-01,-0.11950E-03,0.36320E-07
     29       0.52080E-09,-0.31690E-11,-0.31689E-13
     30       0.33483E+00,-0.10635E-01,0.14902E-03
     31       -0.10214E-05,0.34028E-08,-0.44300E-11
     32       0.43000E-02,0.17000E-04,0.0
     33       0.,0.,0.
     34       -0.12814E+00,0.48691E-02,-0.68452E-04
     35       0.46711E-06,-0.15484E-08,0.20038E-11
     36       0.21700E+00,0.14160E-03,0.64705E-06
     37       0.55390E-08,-0.13779E-10,-0.17912E-12
     38       -0.15410E+01,0.64802E-01,-0.91255E-03
     39       0.62141E-05,-0.20422E-07,0.26255E-10
```

Table I3. Data File DATA22 Containing Physical Constants for Refrigerant 22 in the Input Format to Program HPSIM

```
Q$Q$Q$*DATA22(1)
     1          FREON-22
     2       6.6450000E+02,7.2191000E+02,3.0525000E-02
     3       4.5967000E+02,1.8505300E-01,2.7182818E+00
     4       6.7598246E+01,-8.8538843E+03,-7.8610310E+00
     5       5.0448235E-03,4.4574700E-01,6.8610000E+02
     6       140.,240.
     7       3.2760000E+01,5.4634409E+01,3.6748920E+01
     8       -2.2292560E+01,2.0473289E+01,3.3333333E-01
     9       6.6666667E-01,1.,1.3333333E+00
    10       1.2409800E-01,2.0000000E-03,0.
    11       -4.3535470E+00,2.4072520E-03,-4.4066868E+01
    12       -1.7464000E-02,7.6278900E-05,1.4837630E+00
    13       2.3101420E-03,-3.6057230E-06,0.
    14       -3.7240440E-05,5.3554650E-08,-1.8450510E-04
    15       1.3633870E+08,-1.6726120E+05,0.
    16       5.4820000E+02,4.2000000E+00
    17       2.8128360E-02,2.2554080E-04,-6.5096070E-08
    18       0.,0.,2.5734100E+02
    19       6.2400900E+01,-4.5333500E-02
    20       0.64600E+00,-0.29194E-02,0.12164E-04
    21       -0.74985E-07,0.83951E-09,-0.37512E-11
    22       0.69684E01,-0.24319E00,0.35924E-02
    23       -0.26187E-04,0.93884E-07,-0.13301E-09
    24       0.26600E-01,0.63804E-04,0.10761E-06
    25       -0.32061E-08,0.43463E-10,-0.13175E-12
    26       -0.66330E00,0.25757E-01,-0.37913E-03
    27       0.27734E-05,-0.10053E-07,0.14474E-10
    28       0.63000E-01,-0.15820E-03,-0.12289E-06
    29       0.17453E-08,-0.52685E-11,-0.10857E-13
    30       -0.46705E00,0.19421E-01,-0.28507E-03
    31       0.20429E-05,-0.71963E-08,0.99460E-11
    32       0.48000E-02,0.19881E-04,0.24815E-08
    33       0.28518E-09,-0.62001E-11,0.31001E-13
    34       0.51539E00,-0.18601E-01,0.26762E-03
    35       -0.18936E-05,0.65891E-08,-0.90041E-11
    36       0.27100E+00,0.24054E-03,0.38936E-07
    37       0.23481E-07,-0.97345E-10,0.44953E-12
    38       0.49002E00,-0.83123E-02,0.13105E-03
    39       -0.96884E-06,0.36462E-08,-0.52089E-11
```

Table I4. Heat Pump Input Data Code to Program HPSIM

All input data are in FORTRAN free field input format with data values on the same line separated by commas.

Line 1. ATITLE

ATITLE = title, maximum 80 characters

line 2: ELEFUL, SWPVOL, ETAPLY, CLREFF

ELEFUL = compressor motor energy input rate at max. rated load (kW)

SWPVOL = compressor swept volume per revolution (in^3)

ETALPY = compressor polytropic efficiency (-)

CLREFF = compressor clearance volume as fraction of stroke volume (-)

Line 3: EMETA(I), I = 1,5

EMETA(I) = compressor motor efficiency in fraction at fraction of full load specified by EMPOT(I), I = 1,5 (-)

Line 4: EMETA(I) I = 6,11
EMETA(I) = compressor motor efficiency in fraction at fraction of full load specified by EMOPT(I), I = 6,11 (-)

Line 5: EMOPT(I), I = 1,5

EMOPT(I) = compressor motor full load fraction (-)

Line 6: EMOPT(I), I = 6,11

EMPOT(I) = compressor motor full load fraction (-)

Line 7: EMRPM(I), I = 1,6

EMRPM(I) = coefficient for compressor motor RPM calculations (-)

Line 8: CPC34, CPC45, CPC67, CPC78

CPC34 = pressure drop parameter at compressor can inlet ($(lbf \cdot h^2)/(lb \cdot in^2 \cdot ft^3)$)

CPC45 = pressure drop parameter at compressor suction valve ($(lbf \cdot h^2)/(lb \cdot in^2 \cdot ft^3)$)

CPC67 = pressure drop parameter at compressor delivery valve ($(lbf \cdot h^2)/(lb \cdot in^2 \cdot ft^3)$)

CPC78 = pressure drop parameter at compressure can exit ($(lbf \cdot h^{2.2})/(lb \cdot in^2 \cdot ft^{2.8})$)

Line 9: CQC4C, CQCCOA, CQC45, CQC67, CQC78

CQC4C = parameter for compressor can wall - refrigerant vapor heat transfer ($ft^{0.2}$)

CQCCOA = parameter for compressor can - ambient air heat transfer ($Btu/h \cdot F^{1.333}$)

CQC45 = suction valve heat transfer parameter ($ft^{0.2}$)

CQC67 = delivery valve heat transfer parameter ($ft^{0.2}$)

CQC78 = heat transfer parameter at can exit ($ft^{0.2}$)

Line 10: CQ, CPDR

CQ = parameter for 4-way valve heat transfer ($ft^{0.2}$)

CPDR = pressure drop parameter for 4-way valve ($(lbf \cdot h^2)/(lb \cdot in^2 \cdot ft^3)$)

Line 11: ACCH, ACCD, VCAN, REFIN

ACCH = accumulator height (in)

ACCD = accumulator inner diameter (in)

VCAN = volume of compressor can filled by refrigerant (in^3)

REFIN = refrigerant charge (lb)

Line 12: NDEP(1), NROW(1)

NDEP(1) = number of indoor coil tube depth rows (-)

NROW(1) = rumber of tubes per indoor coil depth row (-)

Line 13: DI(1), DO(1), DT(1), RPCH(1), DPCH(1), WIDTH(1)

DI(1) = inner diameter of indoor coil tubes (in)

DO(1) = outer diameter of indoor coil tubes (in)

DT(1) = indoor coil fin tip diameter (in)

RPCH(1) = pitch between tubes of the same depth in indoor coil (in)

DPCH(1) = depth pitch for indoor coil tubes (in)

WIDTH(1) = indoor coil width (equal tube length) (in)

Line 14: FPCH(1), FTK(1), FMK(1), TMK(1), AMAS(1)

FPCH(1) = indoor coil fin pitch (in)

FTK(1) = indoor coil fin thickness (in)

FMK(1) = indoor coil fin material thermal conductivity (Btu/(ft • h • F))

TMK(1) = indoor coil tube material thermal conductivity (Btu/(ft • h • F))

AMAS(1) = air mass flow rate through indoor coil (lb/h)

Line 15: CONST(1), CPOW(1), ANGLE(1)

CONST(1) = constant for air side heat transfer correlation for indoor coil equal to 0.134 (-)

CPOW(1) = constant for air side heat transfer correlation for indoor coil equal to 0.681 (-)

ANGLE(1) = angle between indoor coil face and air streamlines (rad)

Line 16: EIDFAN

EIDFAN = indoor fan energy input rate (kW)

Line 17: NREPTI

NREPTI = number of repeating sections in indoor coil (-)

Line 18: NTUBE(1,I) I = 1,5

NTUBE(1,1) = number of tubes in first row in each section of indoor coil (-)

NTUBE(1,2) = number of tubes in second row in each section of indoor coil (-)

NTUBE(1,3) = number of tubes in third row in each section of indoor coil (-)

NTUBE(1,4) = number of tubes in fourth row in each section of indoor coil (-)

NTUBE(1,5) = number of tubes in fifth row in each section of indoor coil (-)

Line 19: IFROM(1,I), I = 1,10

IFROM(1,1) = number of tube of indoor coil from which tube 1 receives refrigerant when indoor coil works as evaporator (-)

IFROM(1,2) = number of tube of indoor coil from which tube 2 receives refrigerant when indoor coil works as evaporator (-)

IFROM(1,3) =

IFROM(1,9) =

IFROM(1,10) = number of tube of indoor coil from which tube 10 receives refrigerant when indoor coil works as evaporator (-)

Line 20: IFROM(1,I), I = 11,20

IFROM(1,I) = number of tube indoor coil from which tube I receives refrigerant when indoor coil works as evaporator (-)

Line 21: IFROM(1,I), I = 21,30

Line 22: IFROM(1,I), I = 31,40

Line 23: IFROM(1,I), I = 41,50

Line 24: IFROM(1,I), I = 51,60

Line 25: IFROM(1,I), I = 61,70

Line 26: IFROM(1,I), I = 71,80

Line 27: IFROM(1,I), I = 81,90

Line 28: IFROM(1,I), I = 91,100

Line 29: IFROM(1,I), I = 101,110

Line 30: IFROM(1,I), I = 111,120

Line 31: IFROM(1,I), I = 121,130

IFROM(1,I) = number of indoor coil from which tube I receives refrigerant when indoor coil works as evaporator (-)

Line 32: NDEP(2), NROW(2)

NDEP(2) = number of outdoor coil tube row depths (-)

NROW(2) = number of tubes per outdoor coil depth row (-)

Line 33: DI(2), DO(2), DT(2), RPCH(2), DPCH(2), WIDTH(2)

DI(2) = inner diameter of outdoor coil tubes (in)

DO(2) = outer diameter of outdoor coil tubes (in)

DT(2) = outdoor coil fin tip diameter (in)

RPCH(2) = pitch between tubes of the same depth in outdoor coil (in)

DPCH(2) = depth pitch for outdoor coil tubes (in)

WITDTH(2) = outdoor coil width (equal tube length) (in)

Line 34: FPCH(2), FTK(2), FMK(2), TMK(2), AMAS(2)

FPCH(2) = outdoor coil fin pitch (in)

FTK(2) = outdoor coil fin thickness (in)

FMK(2) = outdoor coil fin material thermal conductivity (Btu/(ft • h • F))

TMK(2) = outdoor coil tube material thermal conductivity (Btu/(ft • h • F))

AMAS(2) = air mass flow rate through outdoor coil (lb/h)

Line 35: CONST(2), CPOW(2), ANGLE(2)

CONST(2) = constant for air side heat transfer correlation for outdoor coil equal to 0.134 (-)

CPOW(2) = constant for air side heat transfer correlation for outdoor coil equal to 0.681 (-)

ANGLE(2) = angle between outdoor coil face and air streamlines (rad)

Line 36: EIDFAN

EIDFAN = outdoor fan energy input rate (kW)

LINE 37: NREPTO

NREPTO = number of repeating sections in outdoor coil (-)

Line 54: RL, RD, RK1, RD1, RK2, RD2

RL = length of compressor-indoor coil tubing (in)

RD = inner diameter of compressor-indoor coil tubing (in)

RK1 = thermal conductivity of compressor-indoor coil tubing material (Btu/(ft • h • F))

RD1 = outdoor diameter of compressor-indoor coil tubing (in)

RK2 = thermal conductivity of compressor-indoor coil tubing insulation (Btu/(ft • h • F))

RD2 = outer diameter of compressor-outdoor coil tubing insulation (Btu/(ft • h • F))

Line 55: RYL, RYD

RYL = liquid line length (in)

RYD = liquid line diameter (in)

Note on coil input data:

As a coil depth it is understood direction perpendicular to a coil surface facing incoming air. Line 13 and 33: for fin tip diameter DT(I) refer to figure 21. Lines 19-31 and 39-51; tubes are numbered consecutively from the first tube in the first row (facing incoming air) to the last tube in the last row. Enter 0 (zero), if considered tube receives refrigerant from coil inlet port; enter 999, if the tube is nonexistant.

Table I5. Example of Heat Pump Data in the Input Format to Program HPSIM

```
Q$Q$Q$*SYST42(1)
      1       **** SYSTEM 2 ****
      2       5.,5.228,0.744,0.1743
      3       0.1996,0.3355,0.5446,0.6540,0.6958
      4       0.7233,0.7414,0.7519,0.7595,0.7623,0.7633
      5       0.05,0.1,0.2,0.3,0.4
      6       0.5,0.6,0.7,0.8,0.9,1.0
      7       3578.,23.53,-831.4,3542.,-6140.,3234.
      8       4.773E-7,1.353E-5,2.755E-4,9.436E-5
      9       37.16,105.7,0.2312,0.2213,3.170
     10       0.905,1.637E-05
     11       10.,4.,100.,0.
     12       3.29
     13       .315,.375,1.055,1.,0.875,18.
     14       .0769,.0055,118.,118.,5800.
     15       .134,.681,.642
     16       .640
     17       1
     18       29,30,29,0,0
     19       2,32,4,0,34,5,6,7,8,9
     20       10,11,12,13,16,17,18,19,20,21
     21       22,23,24,25,55,0,26,27,58,31
     22       1,3,3,33,34,35,36,37,38,39
     23       40,41,42,14,15,47,48,49,50,51
     24       52,53,54,25,56,57,27,28,29,30
     25       60,61,62,63,64,65,66,67,68,69
     26       70,71,43,44,45,46,78,79,80,81
     27       82,83,84,85,86,87,88,59,999,999
     28       999,999,999,999,999,999,999,999,999,999
     29       999,999,999,999,999,999,999,999,999,999
     30       999,999,999,999,999,999,999,999,999,999
     31       999,999,999,999,999,999,999,999,999,999
     32       2,36
     33       0.315,0.375,1.128,1.,1.,64.
     34       0.0625,0.0055,118.,118.,16600.
     35       .134,.681,.671
     36       .510
     37       6
     38       6,6,0,0,0
     39       2,3,4,5,6,0,1,7,8,9
     40       10,11,999,999,999,999,999,999,999,999
     41       999,999,999,999,999,999,999,999,999,999
     42       999,999,999,999,999,999,999,999,999,999
     43       999,999,999,999,999,999,999,999,999,999
     44       999,999,999,999,999,999,999,999,999,999
     45       999,999,999,999,999,999,999,999,999,999
     46       999,999,999,999,999,999,999,999,999,999
     47       999,999,999,999,999,999,999,999,999,999
     48       999,999,999,999,999,999,999,999,999,999
     49       999,999,999,999,999,999,999,999,999,999
     50       999,999,999,999,999,999,999,999,999,999
     51       999,999,999,999,999,999,999,999,999,999
     52       0.078,0.5,1,0.073,0.5,1
     53       50.,0.68,223.,0.750,0.05,1.75
     54       100.,0.68,223.,0.750,0.05,1.75
     55       180.,0.311
   END PRT
```

```
INDOOR FAN KW=  6.400-001

NO. OF REPEATING SECTIONS:  1

NTUB(1):
  29   30   29    0    0

IFROM(1):
   2   32    4    0   34    5    6    7    8    9
  10   11   12   13   16   17   18   19   20   21
  22   23   24   25   55    0   26   27   58   31
   1    3    3   33   34   35   36   37   38   39
  40   41   42   14   15   47   48   49   50   51
  52   53   54   25   56   57   27   28   29   30
  60   61   62   63   64   65   66   67   68   69
  70   71   43   44   45   46   78   79   80   81
  82   83   84   85   86   87   88   59  999  999
 999  999  999  999  999  999  999  999  999  999
 999  999  999  999  999  999  999  999  999  999
 999  999  999  999  999  999  999  999  999  999
 999  999  999  999  999  999  999  999  999  999


OUTDOOR COIL DATA:

NDEP(2)      NROW(2)
 2           36

DI(2)        DO(2)        DT(2)        RPCH(2)      DPCH(2)      WIDTH(2)
3.150-001    3.750-001    1.128+000    1.000+000    1.000+000    6.400+001

FPCH(2)      FTK(2)       FMK(2)       TMK(2)       AMAS(2)
6.250-002    5.500-003    1.180+002    1.180+002    1.660+004

CONST(2)     CPOW(2)      ANGLE(2)
1.340-001    6.810-001    6.710-001

OUTDOOR FAN KW=  5.100-001

NO. OF REPEATING SECTIONS:  6

NTUB(2):
   6    6    0    0    0

IFROM(2):
   2    3    4    5    6    0    1    7    8    9
  10   11  999  999  999  999  999  999  999  999
 999  999  999  999  999  999  999  999  999  999
 999  999  999  999  999  999  999  999  999  999
 999  999  999  999  999  999  999  999  999  999
 999  999  999  999  999  999  999  999  999  999
 999  999  999  999  999  999  999  999  999  999
 999  999  999  999  999  999  999  999  999  999
 999  999  999  999  999  999  999  999  999  999
 999  999  999  999  999  999  999  999  999  999
 999  999  999  999  999  999  999  999  999  999
 999  999  999  999  999  999  999  999  999  999
 999  999  999  999  999  999  999  999  999  999
```

```
116
117     EXP. DEVICE:          ID      LENGTH     #
118
119     AT INDOOR COIL      .0780       .50      1
120     AT OUTDOOR COIL     .0730       .50      1
121
122
123     TUBING CONNECTING COMPRESSOR @ IND. COIL:
124
125     RL          RD          RK1         RD1         RK2         RD2         RK3
126     1.000+002   6.800-001   2.230+002   7.500-001   5.000-002   1.750+000
127
128
129     TUBING CONNECTING COMPRESSOR @ OUT. COIL:
130
131     YL          YD          YK1         YD1         YK2         YD2         YK3
132     5.000+001   6.800-001   2.230+002   7.500-001   5.000-002   1.750+000
133
134
135     LIQUID LINE:
136
137     RYL         RYD
138     1.800+002   3.110-001
139
140
141
142     NSYS=1 FOR HEATING, NSYS=2 FOR COOLING
143     LONG=1 IF REF. CHARGE BALANCE REQUESTED, OTHERWISE PUT LONG=0
144     NSYS,LONG=?
145     2,0
146     TG3,TSUP3,TG6=?
147     45.,13.8,127.
148
149     POA,TOA,RHOA,PRA,TRA,RHRA=?
150     14.7,94.9,0.4,14.7,80.,0.51
151
152     INPUT DATA TO PERCOM:
153
154     TG3         TSUP3       TG6         TRA         TOA
155     4.500+001   1.380+001   1.270+002   8.000+001   9.490+001
156
157     COMPRESSOR ITERATION:
158
159     EI          ETAE        ETAC        ETAV        CPRPM       RMASS
160     4.165+000   7.434-001   9.556-001   7.151-001   3.506+003   6.070+002
161
162     I   T           P           H           X
163     1   5.047+001   9.492+001   1.093+002   1.000+000
164     2   4.985+001   9.436+001   1.092+002   1.000+000
165     3   5.880+001   9.069+001   1.110+002
166     4   1.045+002   9.056+001   1.191+002
167     5   1.079+002   8.682+001   1.199+002
168     6   2.321+002   3.000+002   1.366+002
169     7   2.249+002   2.724+002   1.359+002
170     8   2.062+002   2.711+002   1.321+002
171     9   1.972+002   2.695+002   1.302+002
172    10   1.964+002   2.694+002   1.301+002
173
```

```
290       LIQUID LINE:
291
292       INPUT  -   PIN =2.597+002     TIN =9.729+001     XIN = .000
293       OUTPUT -   POUT=2.581+002     TOUT=9.729+001     XOUT= .000
294
295
296       EXPANSION DEVICE:
297
298       INPUT  -    P12  =2.581+002    H12 =3.826+001    P13 =9.730+001
299       OUTPUT -    POUT =2.004+002    XMASS =6.633+002
300
301       INPUT DATA TO PERCOM:
302
303       TG3         TSUP3       TG6         TRA         TOA
304       4.300+001   1.380+001   1.240+002   8.000+001   9.490+001
305
306       COMPRESSOR ITERATION:
307
308       EI          ETAE        ETAC        ETAV        CPRPM       RMASS
309       4.031+000   7.409-001   9.562-001   7.144-001   3.515+003   5.864+002
310
311       I  T           P           H           X
312       1  4.839+001   9.171+001   1.091+002   1.000+000
313       2  4.772+001   9.116+001   1.090+002   1.000+000
314       3  5.680+001   8.763+001   1.108+002
315       4  1.038+002   8.750+001   1.191+002
316       5  1.073+002   8.389+001   1.199+002
317       6  2.306+002   2.890+002   1.366+002
318       7  2.234+002   2.622+002   1.359+002
319       8  2.047+002   2.608+002   1.321+002
320       9  1.956+002   2.593+002   1.302+002
321      10  1.948+002   2.592+002   1.301+002
322
323       INPUT DATA TO CNDNEW:
324
325       T           P           TAIR
326       1.948+002   2.592+002   9.490+001
327
328       CONDENSER ITERATION:
329
330       AT AIR T=  9.490+001
331
332       T           P           H           X
333       1.948+002   2.592+002   1.301+002   1.000+000
334       9.894+001   2.558+002   3.882+001    .000
335
336       LIQUID LINE:
337
338       INPUT  -   PIN =2.558+002     TIN =9.894+001     XIN = .000
339       OUTPUT -   POUT=2.541+002     TOUT=9.894+001     XOUT= .000
340
341
342       EXPANSION DEVICE:
343
344       INPUT  -    P12  =2.541+002    H12 =3.882+001    P13 =9.733+001
345       OUTPUT -    POUT =2.056+002    XMASS =6.064+002
346
347       INPUT DATA TO EVPHXM:
```

```
348
349     T           P           H           TAIR        RH          RMASS
350     4.839+001   9.171+001   1.091+002   8.000+001   5.100-001   5.873+002
351
352     EVAPORATOR ITERATION:
353
354     T           P           H           X
355     4.839+001   9.171+001   1.091+002   1.000+000
356     4.880+001   9.673+001   4.332+001   2.283-001
357
358     INPUT DATA TO PERCOM:
359
360     TG3         TSUP3       TG6         TRA         TOA
361     4.199+001   1.380+001   1.227+002   8.000+001   9.490+001
362
363     COMPRESSOR ITERATION:
364
365     EI          ETAE        ETAC        ETAV        CPRPM       RMASS
366     3.973+000   7.391-001   9.565-001   7.135-001   3.518+003   5.756+002
367
368     I  T           P           H           X
369     1  4.731+001   9.011+001   1.090+002   1.000+000
370     2  4.661+001   8.958+001   1.089+002   1.000+000
371     3  5.579+001   8.611+001   1.108+002
372     4  1.036+002   8.599+001   1.192+002
373     5  1.070+002   8.244+001   1.199+002
374     6  2.301+002   2.841+002   1.366+002
375     7  2.230+002   2.577+002   1.359+002
376     8  2.043+002   2.565+002   1.321+002
377     9  1.951+002   2.550+002   1.303+002
378    10  1.943+002   2.548+002   1.301+002
379
380     INPUT DATA TO CNDNEW:
381
382     T           P           TAIR
383     1.943+002   2.548+002   9.490+001
384
385     CONDENSER ITERATION:
386
387     AT AIR T=  9.490+001
388
389     T           P           H           X
390     1.943+002   2.548+002   1.301+002   1.000+000
391     1.012+002   2.513+002   3.957+001    .000
392
393     LIQUID LINE:
394
395     INPUT  -    PIN =2.513+002      TIN =1.012+002      XIN =  .000
396     OUTPUT -    POUT=2.497+002      TOUT=1.012+002      XOUT=  .000
397
398
399     EXPANSION DEVICE:
400
401     INPUT  -     P12  =2.497+002     H12 =3.957+001     P13 =9.513+001
402     OUTPUT -     POUT =2.127+002     XMASS =5.281+002
403
404     INPUT DATA TO PERCOM:
405
```

```
 406      TG3          TSUP3        TG6          TRA          TOA
 407      4.199+001    1.380+001    1.233+002    8.000+001    9.490+001
 408
 409      COMPRESSOR ITERATION:
 410
 411      EI           ETAE         ETAC         ETAV         CPRPM        RMASS
 412      3.984+000    7.394-001    9.562-001    7.111-001    3.517+003    5.735+002
 413
 414      I  T            P            H            X
 415      1  4.721+001    9.009+001    1.090+002    1.000+000
 416      2  4.651+001    8.955+001    1.089+002    1.000+000
 417      3  5.579+001    8.611+001    1.108+002
 418      4  1.037+002    8.599+001    1.192+002
 419      5  1.072+002    8.247+001    1.200+002
 420      6  2.312+002    2.865+002    1.368+002
 421      7  2.241+002    2.606+002    1.361+002
 422      8  2.053+002    2.593+002    1.322+002
 423      9  1.960+002    2.579+002    1.304+002
 424     10  1.952+002    2.578+002    1.302+002
 425
 426      INPUT DATA TO CNDNEW:
 427
 428      T            P            TAIR
 429      1.952+002    2.578+002    9.490+001
 430
 431      CONDENSER ITERATION:
 432
 433      AT AIR T=  9.490+001
 434
 435      T            P            H            X
 436      1.952+002    2.578+002    1.302+002    1.000+000
 437      9.892+001    2.544+002    3.882+001     .000
 438
 439      LIQUID LINE:
 440
 441      INPUT  -   PIN =2.544+002      TIN =9.892+001      XIN = .000
 442      OUTPUT -   POUT=2.528+002      TOUT=9.892+001      XOUT= .000
 443
 444
 445      EXPANSION DEVICE:
 446
 447      INPUT  -    P12  =2.528+002    H12 =3.882+001    P13 =9.510+001
 448      OUTPUT -    POUT =2.056+002    XMASS =5.983+002
 449
 450      INPUT DATA TO EVPHXM:
 451
 452      T            P            H            TAIR         RH           RMASS
 453      4.721+001    9.009+001    1.090+002    8.000+001    5.100-001    5.742+002
 454
 455      EVAPORATOR ITERATION:
 456
 457      T            P            H            X
 458      4.721+001    9.009+001    1.090+002    1.000+000
 459      4.760+001    9.479+001    3.917+001    1.630-001
 460
 461      INPUT DATA TO PERCOM:
 462
 463      TG3          TSUP3        TG6          TRA          TOA
```

```
464       4.199+001  1.380+001  1.231+002  8.000+001  9.490+001
465
466       COMPRESSOR ITERATION:
467
468       EI         ETAE       ETAC       ETAV       CPRPM      RMASS
469       3.984+000  7.394-001  9.563-001  7.119-001  3.517+003  5.741+002
470
471       I  T          P          H          X
472       1  4.724+001  9.009+001  1.090+002  1.000+000
473       2  4.654+001  8.956+001  1.089+002  1.000+000
474       3  5.579+001  8.611+001  1.108+002
475       4  1.037+002  8.599+001  1.192+002
476       5  1.072+002  8.246+001  1.200+002
477       6  2.309+002  2.857+002  1.367+002
478       7  2.238+002  2.596+002  1.360+002
479       8  2.050+002  2.584+002  1.322+002
480       9  1.957+002  2.569+002  1.304+002
481      10  1.950+002  2.568+002  1.302+002
482
483       INPUT DATA TO CNDNEW:
484
485       T          P          TAIR
486       1.950+002  2.568+002  9.490+001
487
488       CONDENSER ITERATION:
489
490       AT AIR T=  9.490+001
491
492       T          P          H          X
493       1.950+002  2.568+002  1.302+002  1.000+000
494       9.958+001  2.534+002  3.904+001   .000
495
496       LIQUID LINE:
497
498       INPUT  -   PIN =2.534+002     TIN =9.958+001     XIN = .000
499       OUTPUT -   POUT=2.518+002     TOUT=9.958+001     XOUT= .000
500
501
502       EXPANSION DEVICE:
503
504       INPUT  -    P12  =2.518+002   H12 =3.904+001    P13 =9.511+001
505       OUTPUT -    POUT =2.077+002   XMASS =5.777+002
506
507       INPUT DATA TO PERCOM:
508
509       TG3        TSUP3      TG6        TRA        TOA
510       4.199+001  1.380+001  1.231+002  8.000+001  9.490+001
511
512       COMPRESSOR ITERATION:
513
514       EI         ETAE       ETAC       ETAV       CPRPM      RMASS
515       3.979+000  7.393-001  9.563-001  7.120-001  3.518+003  5.744+002
516
517       I  T          P          H          X
518       1  4.725+001  9.010+001  1.090+002  1.000+000
519       2  4.655+001  8.956+001  1.089+002  1.000+000
520       3  5.579+001  8.611+001  1.108+002
521       4  1.036+002  8.599+001  1.192+002
```

```
 5  1.071+002  8.246+001  1.199+002
 6  2.308+002  2.855+002  1.367+002
 7  2.237+002  2.595+002  1.360+002
 8  2.049+002  2.582+002  1.322+002
 9  1.956+002  2.567+002  1.303+002
10  1.948+002  2.566+002  1.302+002

 INPUT DATA TO CNDNEW:

 T          P          TAIR
 1.948+002  2.566+002  9.490+001

 CONDENSER ITERATION:

 AT AIR T=  9.490+001

 T          P          H          X
 1.948+002  2.566+002  1.302+002  1.000+000
 9.970+001  2.532+002  3.908+001   .000

 LIQUID LINE:

 INPUT  -   PIN =2.532+002     TIN =9.970+001     XIN = .000
 OUTPUT -   POUT=2.516+002     TOUT=9.970+001     XOUT= .000


 EXPANSION DEVICE:

 INPUT  -    P12  =2.516+002    H12 =3.908+001    P13 =9.512+001
 OUTPUT -    POUT =2.080+002    XMASS =5.741+002

 INPUT DATA TO EVPHXM:

 T          P          H          TAIR       RH         RMASS
 4.725+001  9.010+001  1.090+002  8.000+001  5.100-001  5.744+002

 EVAPORATOR ITERATION:

 T          P          H          X
 4.725+001  9.010+001  1.090+002  1.000+000
 4.761+001  9.481+001  3.921+001  1.835-001

 MASSCOND =4.962+000

 MASSEVAP =6.557-001

 REFIN =  0.000+000     TMASS =  6.442+000

 ********************************************************
 *** SYSTEM 2 ****

 TOA        RHOA       TRA        RHRA
 9.490+001  4.000-001  8.000+001  5.100-001

 CFMIND     CFMOUT
 1.323+003  3.899+003
```

```
580       RESULTS:
581
582       I  T           P           H           S           X
583       1  4.725+001   9.010+001   1.090+002   2.199-001   1.000+000
584       2  4.655+001   8.956+001   1.089+002   2.199-001   1.000+000
585       3  5.579+001   8.611+001   1.108+002   2.243-001   1.000+000
586       4  1.036+002   8.599+001   1.192+002   2.400-001   1.000+000
587       5  1.071+002   8.246+001   1.199+002   2.422-001   1.000+000
588       6  2.308+002   2.855+002   1.367+002   2.433-001   1.000+000
589       7  2.237+002   2.595+002   1.360+002   2.442-001   1.000+000
590       8  2.049+002   2.582+002   1.322+002   2.386-001   1.000+000
591       9  1.956+002   2.567+002   1.303+002   2.359-001   1.000+000
592      10  1.948+002   2.566+002   1.302+002   2.357-001   1.000+000
593      11  9.970+001   2.532+002   3.908+001   7.932-002    .000
594      12  9.970+001   2.516+002   3.908+001   7.896-002    .000
595      13  4.761+001   9.481+001   3.921+001   8.146-002   1.835-001
596
597       TG3         TSUP3       TG6         RMASS       TMASS
598       4.199+001   1.380+001   1.231+002   5.744+002   6.442+000
599
600       QLOAD       ELUSE       COP
601       3.789+004   5.129+000   2.165+000
602
603
604
605       I=999 FOR DISCONTINUATION
606       999
  END PRT

@BRKPT PRINT$
```

NBS-114A (REV. 2-8C)

U.S. DEPT. OF COMM. BIBLIOGRAPHIC DATA SHEET (See instructions)	1. PUBLICATION OR REPORT NO. NBS BSS 155	2. Performing Organ. Report No.	3. Publication Date May 1983

4. TITLE AND SUBTITLE

COMPUTER MODELING OF THE VAPOR COMPRESSION CYCLE WITH CONSTANT FLOW AREA EXPANSION DEVICE

5. AUTHOR(S)

Piotr Domanski and David Didion

6. PERFORMING ORGANIZATION *(If joint or other than NBS, see instructions)*

NATIONAL BUREAU OF STANDARDS
DEPARTMENT OF COMMERCE
WASHINGTON, D.C. 20234

7. Contract/Grant No.

8. Type of Report & Period Covered

Final

9. SPONSORING ORGANIZATION NAME AND COMPLETE ADDRESS *(Street, City, State, ZIP)*

Department of Energy
1000 Independence Avenue, S.W.
Washington, D C 20585

10. SUPPLEMENTARY NOTES

Library of Congress Catalog Card Number: 83-600524

☐ Document describes a computer program; SF-185, FIPS Software Summary, is attached.

11. ABSTRACT *(A 200-word or less factual summary of most significant information. If document includes a significant bibliography or literature survey, mention it here)*

An analysis of the vapor compression cycle and the main components of an air source heat pump during steady-state operation has been performed with emphasis on fundamental phenomena taking place between key locations in the refrigerant system. The basis of the general heat pump model formulation is the logic which links the analytical models of heat pump components together in a format requiring an iterative solution of refrigerant pressure, enthalpy and mass balances.

The modeling effort emphasis was on the local thermodynamic phenomena which were described by fundamental heat transfer equations and equation of state relationships among material properties. In the compressor model several refrigerant locations were identified and the processes taking place between these locations accounted for all significant heat and pressure losses. Evaporator and condenser models were developed on a tube-by-tube basis where performance of each coil tube is computed separately by considering the cross-flow heat transfer with the external air stream and the appropriate heat and mass transfer relationships. A capillary tube model was formulated with the aid of Fanno flow theory.

The developed heat pump model has been validated by checking computer results against laboratory test data for full and part load operation for the cooling/dehumidifying mode as well as the heating mode under frosting conditions.

12. KEY WORDS *(Six to twelve entries; alphabetical order; capitalize only proper names; and separate key words by semicolons)*

Air conditioner; capillary tube; coil; condenser; compressor; evaporator; expansion device; heat pump; modeling; vapor compression cycle

13. AVAILABILITY

☒ Unlimited

☐ For Official Distribution. Do Not Release to NTIS

☒ Order From Superintendent of Documents, U.S. Government Printing Office, Washington, D.C. 20402.

☐ Order From National Technical Information Service (NTIS), Springfield, VA. 22161

14. NO. OF PRINTED PAGES

162

15. Price

USCOMM-DC 6043-P80

*U.S. GOVERNMENT PRINTING OFFICE: 1983-0-380-997/5057